



Calcium looping for CCS-ready combustion of solid fuels

Doctoral Thesis in Chemical Engineering

*Dipartimento di Ingegneria Chimica, dei Materiali e della
Produzione Industriale*

Università degli Studi di Napoli Federico II

Antonio Coppola

Scientific Committee:

Prof. Piero Salatino

Dr. Riccardo Chirone

Dr. Fabrizio Scala

*A mio padre,
del quale sono fiero ed orgoglioso.*

Antonio

A coloro che soffrono, lottano, sognano, credono, sperano

Ringraziamenti

Non è possibile portare a termine una tesi di dottorato se non con il supporto di diverse persone a cui sono particolarmente riconoscente.

Innanzitutto, voglio ringraziare il Prof. Piero Salatino che mi ha accolto nel suo gruppo di ricerca, trasmettendomi la sua passione per la scienza e il suo rigore scientifico.

Un ringraziamento speciale va al dott. Fabrizio Scala ed al dott. Riccardo Chirone, che hanno fatto parte del comitato scientifico, offrendomi in questi tre anni di attività tutta la loro esperienza e le loro straordinarie conoscenze, oltre ad un grande sostegno.

Inoltre, voglio ringraziare il dott. Fabio Montagnaro, il dott. Roberto Solimene, la dott.ssa Osvalda Senneca, il Sig. Luciano Cortese: senza il vostro aiuto questo lavoro non sarebbe mai stato ultimato.

Index

Abstract.....	1
1. Introduction.....	5
1.1. Global warming: an overview	5
1.2. Carbon capture technologies	13
1.3. The Calcium Looping Cycle.....	19
1.4. Sorbent deactivation	24
1.5. Sorbent deactivation induced by sulphation	30
1.6. Synthetic and natural alternative sorbents.....	32
1.7. Sorbent reactivation and pretreatment	34
1.8. Calcium-Looping reactor configuration.....	38
1.9. Attrition phenomena	39
2. Objectives and contribution to knowledge of the present work	44
3. Experimental.....	46
3.1. Materials and experimental set-up.....	46
3.2. Procedures	47
3.2.1. Procedure for the calcium looping tests	47
3.2.2. Evaluation of attrition/fragmentation phenomena	50
3.2.3. Evaluation of the CO ₂ capture capacity.....	52
3.2.4. Evaluation of the calcium conversion degree to sulphate	53
3.3. Effect of temperature and CO ₂ partial pressure during calcination	55
3.4. Effect of SO ₂ during carbonation	56
3.5. Oxy-firing conditions and the effect of SO ₂ using limestone as sorbent	57
3.6. Oxy-firing conditions and the effect of SO ₂ using dolomite as sorbent.....	59
3.7. Reactivation by hydration.....	59
4. Results and discussion	62
4.1. Effect of temperature and CO ₂ partial pressure during calcination	62
4.1.1. CO ₂ Capture Capacity.....	62
4.1.2. Particle Size Distribution.....	63
4.1.3. Elutriation Rate	66
4.2. Effect of SO ₂ during carbonation	70
4.2.1. Calcium conversion to sulphate	70

4.2.2. CO ₂ capture capacity.....	72
4.2.3. Particle size distribution.....	73
4.2.4. Elutriation rate.....	75
4.3. Oxy-firing conditions and the effect of SO ₂	76
4.3.1. CO ₂ capture capacity.....	76
4.3.2. Particle size distribution.....	79
4.3.3. Elutriation rate.....	81
4.4. Oxy-firing conditions and the effect of SO ₂ using dolomite as sorbent.....	87
4.4.1. CO ₂ capture capacity.....	87
4.4.2. Particle size distribution.....	90
4.4.3. Elutriation rate.....	92
4.5. Reactivation by hydration.....	95
4.5.1. Microstructural characterization of reactivated sorbent.....	95
4.5.2. CO ₂ capture capacity.....	98
4.5.3. Particle size distribution.....	99
4.5.4. Elutriation rate.....	101
5. Conclusions.....	104
5.1. Effect of temperature and CO ₂ partial pressure during calcination.....	104
5.2. Effect of SO ₂ during carbonation.....	105
5.3. Oxy-firing conditions and the effect of SO ₂	106
5.4. Oxy-firing conditions and the effect of SO ₂ using dolomite as sorbent.....	107
5.5. Sorbent reactivation.....	108
References.....	110

Abstract

The present thesis describes the research activities undertaken by the candidate in the frame of his Doctoral program. It addresses key aspect of the Calcium looping process for carbon capture and sequestration which are proven to affect its feasibility and competitiveness.

The introduction reports an overview of the current global warming issues associated with emissions of greenhouse gases of anthropogenic nature, emphasized by the perspective of a persistent strong dependence of the energy demand on fossil fuels which are the most important source of CO₂ emissions. Hence, the portfolio of currently available and perspective *Carbon Capture and Storage* technologies (CCS), aimed at mitigating carbon dioxide emissions, is surveyed. Carbon dioxide capture processes are critically presented with a clue on their main operational characteristics, strengths and drawbacks.

The *calcium looping cycle* is a promising CO₂ capture technology which is characterized by a comparatively low energy penalty. For this reason, it has gained prominence among competing carbon capture technologies. The potential of this technology for short- to medium-term application has stimulated the interest of the candidate for this topic and has provided the motivation for the present study, which has been undertaken in the frame of research programs active at the Dipartimento di Ingegneria Chimica, dei Materiali e della Produzione Industriale of Università degli Studi di Napoli Federico II and of the Istituto di Ricerche sulla Combustione of Consiglio Nazionale delle Ricerche. The process is described in detail, with consideration of the underlying chemistry and physics as well as of the aspects pertaining to chemical reaction engineering. The latter is largely based on the exploitation of

the dual interconnected fluidized beds concept, which is currently considered the best suited reactor configuration for industrial application. A key aspect of the process is represented by the mechanism and extent of sorbent attrition phenomena associated with fluidized bed processing, which has been thoroughly scrutinized in the present investigation.

This study addresses specific aspects of the calcium looping technology, and is based on a comprehensive experimental campaign carried out with the aid of purposely designed lab-scale fluidized bed facilities. In particular, the performance of six natural limestones, in terms of CO₂ capture capacity and attrition tendency, has been investigated and quantified under different operating conditions. The effect of the presence of SO₂ in the flue gases on the performance of limestones as sorbent candidates in Ca-looping has been assessed, again, with consideration of both sorption performance and attrition tendency. The possibility to use an alternative natural sorbent, namely dolomite, has been assessed. Finally, the potential of processes aimed at the regeneration of the sorption capacity of spent limestone has been investigated with a specific focus on reactivation promoted by water hydration.

Results show that, under mild calcination conditions, sorbent attrition is extensive only during early cycling. The attrition rate progressively declines over repeated cycles, also during the calcination stage when the softer CaO is produced. It is inferred that combined chemically and thermally induced sintering of the sorbent affects the particle structure increasing its mechanical strength toward abrasive wear. The CO₂ capture capacity of the sorbent decays over iterated cycles toward an asymptotic level. This feature, which has already been documented in the literature, is possibly related to the very same structural modifications that are responsible for the improvement of abrasive strength over iterated cycles. Bed temperature and CO₂ concentration both appear to influence the sorbent behaviour by affecting the parallel course of

calcination/carbonation and sintering. In particular, a combination of high bed temperature and high CO₂ partial pressures during calcination, representative of process conditions relevant to oxy-firing in the calciner, significantly enhances particle sintering.

An important aspect that deserves investigation is the effect of the presence of SO₂ in the flue gases on the performance of the Ca-looping cycle. It is well established that SO₂ competes with CO₂ for the sorbent. This aspect has been investigated in the present study with reference to process conditions representative of the industrial process. Experimental results confirm the detrimental effect of SO₂ on CO₂ uptake. However the decrease of the CO₂ sorption capacity varies with the SO₂ content in the flue gas according to a less-than-linear dependence: small concentrations of SO₂ induce a pronounced decrease of the CO₂ capture capacity, but only marginal decrements of CO₂ uptake are observed as SO₂ concentration is further increased.

Regardless of the operating conditions, in-bed particle fragmentation of limestones is always limited, and the attrition rate turns out to be only moderately affected by the presence of SO₂.

The CO₂ sorption capacity of the dolomite is much larger than that of the limestones, in spite of the lower calcium content of this sorbent, under comparable process conditions. The large magnesium content in the dolomite hinders particle sintering and preserves the reactivity of Ca over prolonged cycling. However, the presence of SO₂ significantly depresses the sorbent CO₂ capture capacity. Moreover, contrary to the limestones, the dolomite is subject to extensive attrition.

Experimental results on the regeneration of the sorption capacity of spent limestone by water hydration has proven the potential of this technique. Microstructural changes in the sorbent properties induced by hydration suggest

to hydrate limestone for short times (in the order of a few minutes) to get a substantially complete chemical hydration process, avoiding longer hydration times that would only imply “cramming” phenomena, lower enhancement in the active porosity, increased attrition tendency and reduced reactivation.

1. Introduction

1.1. Global warming: an overview

The rising temperatures of the atmosphere and of the ocean, the increase of the sea level, the melting of the permanent ice in the Arctic and Antarctic regions are unequivocal signs that the global climate is changing (Figure 1.1). In particular, the global temperature has increased by 0.74°C over the last 100 years, with an rate of temperature that has been nearly twice (0.13°C per 10 years) during the last 50 years when compared with that recorded in the previous century.

Since the start of the industrial era (about 1750) the human activities have contributed to the climate change through the emission of greenhouse gases (GHG, see Figure 1.2) and aerosols in the atmosphere. GHG and particles accumulate in the atmosphere altering the Earth's energy balance between incoming solar radiation and outgoing infrared radiation, in a way that results in global warming.

The main anthropogenic GHGs are: carbon dioxide, methane, nitrous oxide and halocarbons (a group of gases containing fluorine, chlorine and bromine). Notably, water vapour is the most abundant and important greenhouse gas, which however is only slightly influenced by human activities by methane emissions, since this gas is chemically decomposed in the stratosphere producing a small amount of water. As regards the effect of aerosols, the third assessment report of the Intergovernmental Panel on Climate Change (IPCC, 2007) stated that suspended particles are able to affect the Earth's climate in

both a direct and indirect way. The direct effect is the same as that of GHGs and is related to scattering and absorption of radiation coming from the sun, altering the radiative balance of the atmosphere. The indirect effect is due to the propensity of these small particles to modify the radiative properties, the amount and the lifetime of the clouds. In particular, an aerosol particle acts as a cloud condensation nucleus, which is function of size, chemical composition, mixing state and environmental conditions (Penner et al., 2001). Moreover, it is possible to distinguish between two different indirect effects: the ‘first indirect effect’, also known as ‘cloud albedo effect’ or ‘Twomey effect’ (Twomey, 1977, Ramaswamy et al., 2001, Lohmann and Feichter, 2005), is related to the cloud droplet number concentration and hence on the cloud droplet size. The effect induced on liquid water content, cloud height and lifetime of clouds is called ‘second indirect effect’, ‘cloud lifetime effect’ or ‘Albrecht effect’ (Albrecht, 1989, Ramaswamy et al., 2001, Lohmann and Feichter, 2005).

The increase of the CO₂ concentration in the atmosphere is recognized as the main responsible for global warming (IPCC, 2007). The CO₂ concentration in the atmosphere has fluctuated around 280±20ppm for 10,000 years until 1750. During the industrial age, such value has undergone an appreciable increase reaching a mean value of 367ppm in the 1999 and 379ppm in the 2005 (IPCC, 2007) (Figure 1.2).

The Intergovernmental Panel on Climate Change has estimated, by means of mathematical models, that the global temperature and the average sea level will likely undergo an increase of 1.1-6.4K and 0.18-0.59m, respectively, in this century (Blamey et al., 2010a).

Power plants firing fossil fuels represent the most important source of anthropogenic CO₂ emissions. The modern society is heavily dependent on

relatively cheap and abundant fossil fuels which supply about 85% of the global energy demand (Li and Fan, 2008).

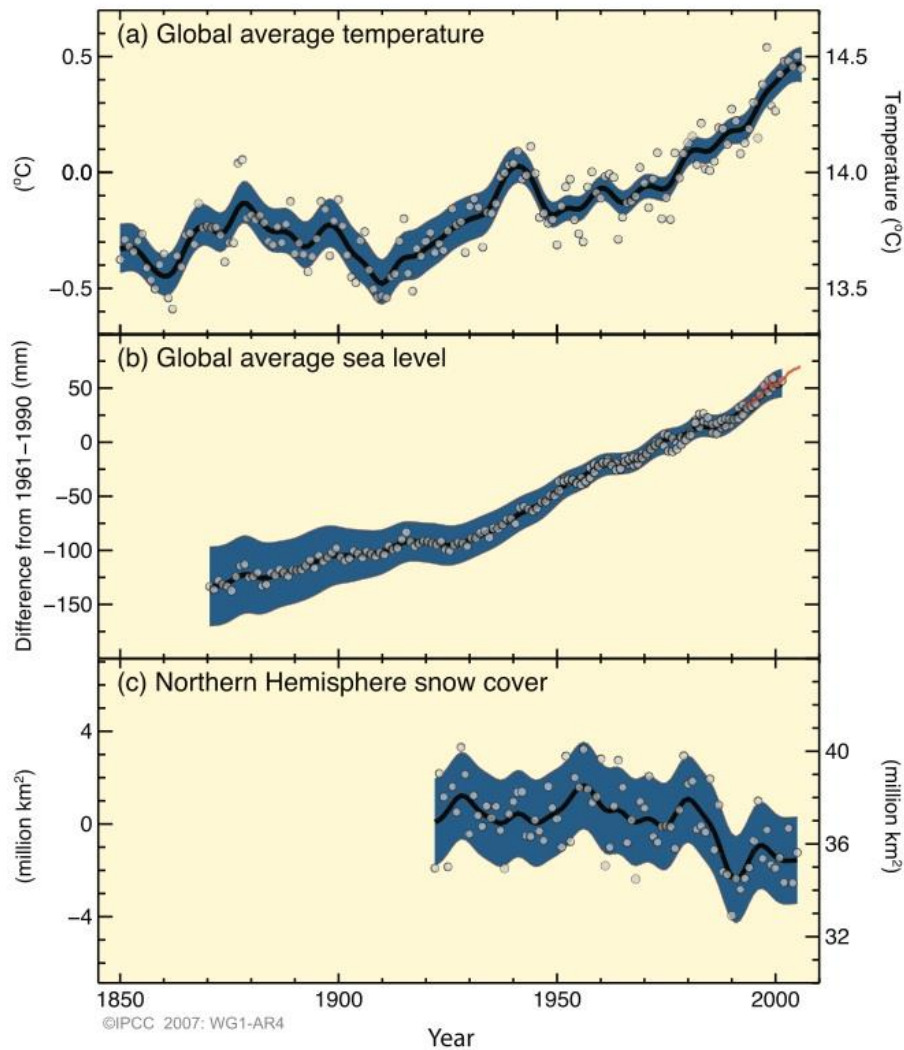


Figure 1.1. Observed changes in (a) global average surface temperature, (b) global average sea level from tide gauge (blue) and satellite (red) data and (c) Northern Hemisphere snow cover for March-April. All changes are relative to corresponding averages for the period 1961–1990. Smoothed curves represent decadal average values while circles show yearly values. The shaded areas are the uncertainty intervals estimated from a comprehensive analysis of known uncertainties (a and b) and from the time series (c) (IPCC, 2007).

The International Energy Agency (IEA) and the European Environment Agency (EEA) have estimated that, in the medium term, fossil fuels will still be the main energy source. Among them, coal will be characterized by the higher demand growth rate, as compared with natural gas and petroleum (IEA, 2008).

Coal produces twice as much CO₂ compared to natural gas, for the same produced energy, resulting in a significant increase of CO₂ emissions. It is estimated that the CO₂ emissions will increase from 29 billion tons per year, in 1997, up to 40 billion tons per year in 2030 (Li and Fan, 2008).

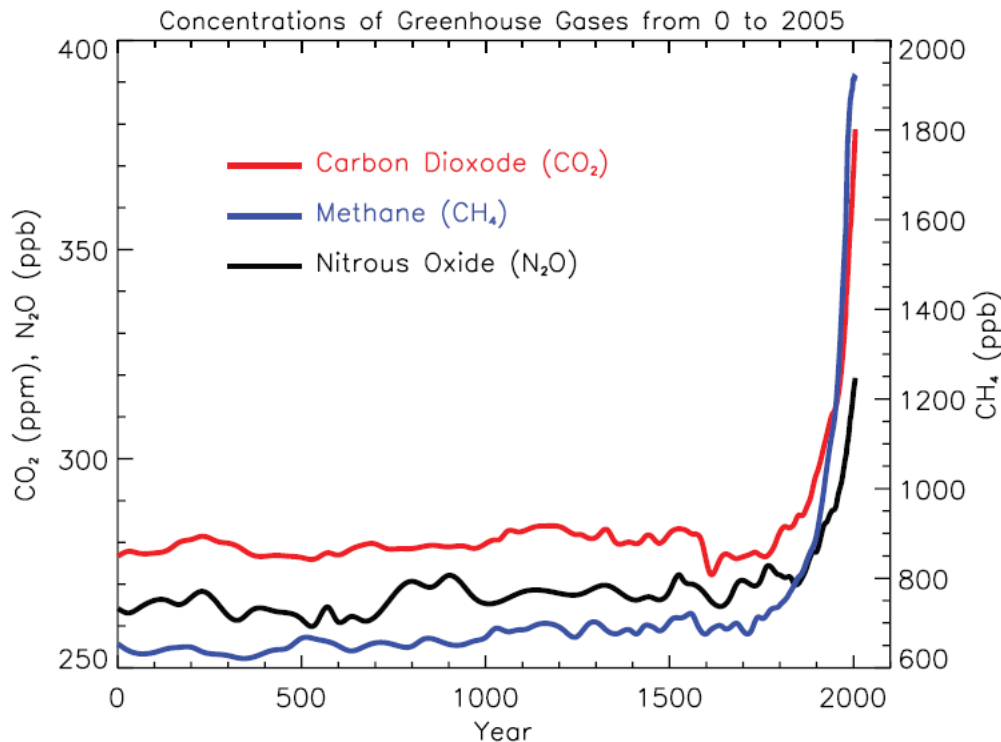


Figure 1.2. Atmospheric concentrations of important long-lived greenhouse gases over the last 2,000 years (IPCC, 2007).

Renewable energy sources represent an option for lowering the greenhouse gas emissions and entail a broad class of technologies such as bioenergy, direct solar energy, geothermal energy, hydropower, ocean energy and wind energy. Though a growing number of renewable energy technologies are reaching technical maturity and are being deployed at significant scale, others are in an earlier phase of technical maturity and commercial deployment or can only meet the needs of specialized niche markets. On a global basis, it is estimated that renewable energy accounted for 12.9% of the total 492 Exajoules

of primary energy supply in 2008. In particular, this percentage value varies substantially by country and region (IPCC, 2011). Moreover, the global energy demand could increase up to 45% in 2030, and this demand cannot be fulfilled by utilization of renewable energies only.

In addition to availability and cost, other factors hinder the exploitation of renewable energy sources. Among these factors, discontinuity or seasonality of their production and issues associated with energy distribution and dispatching play key roles.

In a scenario of continuing generation of anthropogenic CO₂, there is a urgent need to develop technologies to mitigate the climate change by limiting its emissions to the atmosphere. This urgency has stimulated the development of different concepts to remove CO₂ from flue gases generated at power plants, collectively classified as Carbon Capture and Storage (CCS) technologies (IPCC, 2005; Steeneveldt et al., 2006). As far as CO₂ sequestration is concerned, three main methods are been proposed: geological storage, ocean storage and mineral carbonation (IPCC, 2005).

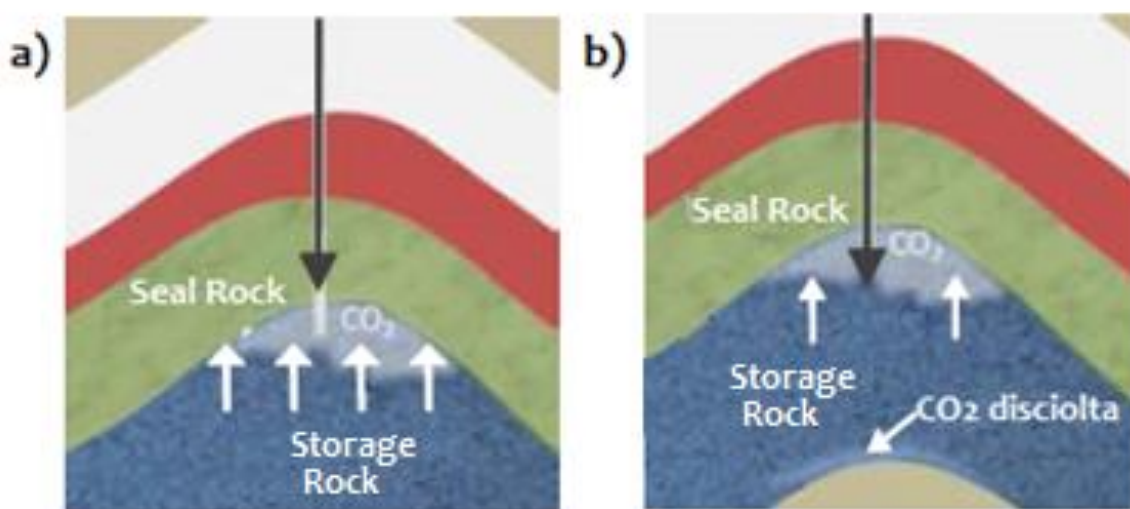


Figure 1.3. Geological CO₂ storage in the subsoil.

The CO₂ geological storage involves a preliminary step of gas compression up to a supercritical state and the subsequent injection of the dense fluid in deep geological formations. This CO₂ storage method is the most accredited because evidence from oil and gas fields indicates that hydrocarbons and other gases and fluids, including CO₂, can remain trapped for millions of years (Magoon and Dow, 1994; Bradshaw et al., 2005). At depths below about 800m the pressure has values which permit to keep the CO₂ in a liquid state with a liquid-like density which provides for an efficient utilization of the underground space, considering that in these conditions CO₂ has a volume 500 times lower than in ambient conditions. Moreover, this technology can take advantage of the accumulated experience on the technique called Enhanced Oil Recovery (EOR) which is used to improve oil extraction injecting CO₂ in the oilfields. Another option is CO₂ injection into deep saline formations which could have a higher storage capacity than oilfields. These formations are widespread and contain enormous quantities of water, which is unsuitable for agriculture or human consumption. Unfortunately, the features of these formations are not well-known and there is a need for further characterization. CO₂ could also be injected into permeable rocks (called reservoir or storage rocks), with elevated storage capacity thanks to their extensive porosity. The low CO₂ density leads to a filling of the upper layers of the storage rock (see Figure 1.3a), but its migration to the surface is hindered by a dense and gastight rock called seal rock, as shown in Figure 1.3b. Geological storage of CO₂ is comprehensively surveyed by Benson (2005).

Ocean storage is accomplished by injecting CO₂ into the sea, at depths exceeding 3,000m, where CO₂ is denser than sea water forming a "CO₂ lake" (IPCC, 2005). Numerical models indicate that deep ocean storage could isolate CO₂ from the atmosphere for several centuries (Hoffert et al., 1979; Kheshgi et al., 1994). This method could require the utilization of a ship or a submerged pipeline for CO₂ transportation. In particular, pipelines, for oil and gas

applications, are reaching ever-greater depths, but not enough for ocean storage. Unfortunately, studies have demonstrated that extensive CO₂ sequestration might give rise to remarkable changes in sea chemistry, in particular could harm marine organisms (Pörtner et al., 2004). Ocean storage presents many open issues which need further understanding.

Mineral carbonation (or mineral sequestration) is accomplished by letting CO₂ react with metal-oxide bearing materials, thus forming the corresponding carbonates and a solid byproduct, silica for example. In nature such a reaction is called silica weathering and occurs on a geological time-scale. The purpose is to fix the CO₂ as carbonates (Seifritz, 1990; Dunsmore, 1992; Lackner et al., 1995), stable compounds which would provide storage capacity on a geological time-scale. Suitable materials could be the natural and abundant silicate rocks, olivine and serpentine materials or alkaline industrial residues, such as slag from steel production or fly ash. In particular, there are two different ways to use silicate rocks for carbonation: in the *ex-situ* method, carbonation occurs in a chemical plant after mining and pre-treating the silicates, while in the *in-situ* method, CO₂ is injected in a silicate-rich geological formation or into alkaline aquifers. From a thermodynamic point of view, inorganic carbonates represent a lower energy state than free CO₂; therefore the carbonation reaction is exothermic and can theoretically yield energy. However, the kinetics of natural mineral carbonation is slow; hence all currently implemented processes require energy intensive preparation of the solid reactants to achieve reasonable conversion rates and/or additives that must be regenerated and recycled using external energy sources. The *in-situ* carbonation is very similar to geological storage, while the *ex-situ* carbonation involves several steps and hence economic/energy penalties such as mining, transportation, grinding, activation (when necessary), disposal of carbonates and byproducts. Industrial residues can be carbonated in the same plant where they are produced. Despite this potential penalty, the interest in this

storage method stems from two important aspects: *i)* the abundance of metal oxide bearing materials; in particular, magnesium and calcium silicate deposits are sufficient to fix the CO₂ that could be produced from the combustion of all fossil fuels resources; *ii)* the possibility to fix CO₂ permanently in stable solids, which can be stored in an environmentally suitable location.

An alternative sequestration method is represented by the industrial use of CO₂ as a gas or a liquid or as a feedstock for production of chemicals (IPCC, 2005). CO₂ is an industrial gas which has a large use for production of several chemicals, such as urea, refrigeration systems, inert agent for food packaging and many other applications. Large amounts of CO₂ are used for Enhanced Oil Recovery in the United States. Much of the CO₂ used commercially derives from synthetic fertilizer and hydrogen plants which use either chemical or physical solvent scrubbing systems. Other sources include the fermentation of sugar to produce ethyl alcohol and the production of sodium carbonate from limestone. In some countries (United States, Italy, Norway and Japan) CO₂ is extracted from natural CO₂ wells. It is also recovered during the production and treatment of raw natural gas which often contains CO₂ as an impurity. Furthermore, a number of processes, for productions of chemicals and polymers, are considering the use of CO₂ to substitute CO, CH₄ and CH₃OH as a source of carbon. Moreover, CO₂ could be used for production of fuels, such as biomass production. By photosynthesis, solar energy can convert water and CO₂ into organic compounds like starch, which can produce fuels like CH₄, CH₃OH, H₂ or biodiesel (Larson, 1993). Despite this potential, the contribution of industrial uses of captured CO₂ to the mitigation of climate change is expected to be small.

Another important aspect of the CCS technology is the transportation of CO₂ from the emission sites to the storage sites, which can occur in three different states: gas, liquid and solid. Commercial transport uses tanks, ships and pipelines for gaseous and liquid CO₂. The gas compression, and hence the

volume reduction, is necessary to avoid large facilities for gas transportation by pipelines. Volume can be further reduced by liquefaction which is a strategy used for transportation of liquefied petroleum gas or liquefied natural gas by ship. These technologies can be transferred to liquid CO₂ transport. Solidification would require much more energy as compared with the other options.

The use of CO₂ pipelines is not new: they now extend over more than 2500 km in the western USA, where they carry 50 MtCO₂ yr⁻¹ from natural sources to enhanced oil recovery plants (IPCC, 2005). Conveyed CO₂ should be dry and containing a small quantities of contaminants (such as H₂S) in order to minimize pipeline corrosion. However, it is possible to design a corrosion resistant pipeline which could operate safely with a gas that contains water and other contaminants. Obviously, a transportation infrastructure, which carries CO₂, requires an extended network of pipelines, which ensures the needed safety, particularly in highly populated zones. From this viewpoint, existing experience has been carried out in zones with low population densities, while the safety issue could become more complex in populated areas.

1.2. Carbon capture technologies

CO₂ capture can be accomplished according to four possible approaches (IPCC, 2005; Figueroa et al., 2008; Kanniche et al., 2010):

- post-combustion;
- pre-combustion;
- oxy-fuel combustion;
- chemical-looping combustion.

Pre-combustion capture is characterized by three steps (Figure 1.4): step 1: the production of synthesis gas; step 2: CO₂ removal; step 3: combustion of hydrogen. The most efficient path to pre-combustion capture is represented by the Integrated Gasification Combined Cycle (IGCC) technology, which combines a gasification process with a gas turbine cycle. The process starts with a partial oxidation of the solid fuel at elevated temperatures (> 800°C), with oxygen (coming from an air separation unit) and steam, producing a raw syngas. The CO in the syngas can be converted to CO₂ and H₂ via the water-gas shift reaction. The produced stream contains an elevated amount of CO₂, which can be removed by chemical or physical processes, and further purified from polluting compounds, such as H₂S, HCl, ammonia and Hg. Finally, the H₂-rich stream is sent to a gas turbine for energy production. After separation, CO₂ is sent to a compression unit and is ready for sequestration (Amann et al., 2009).

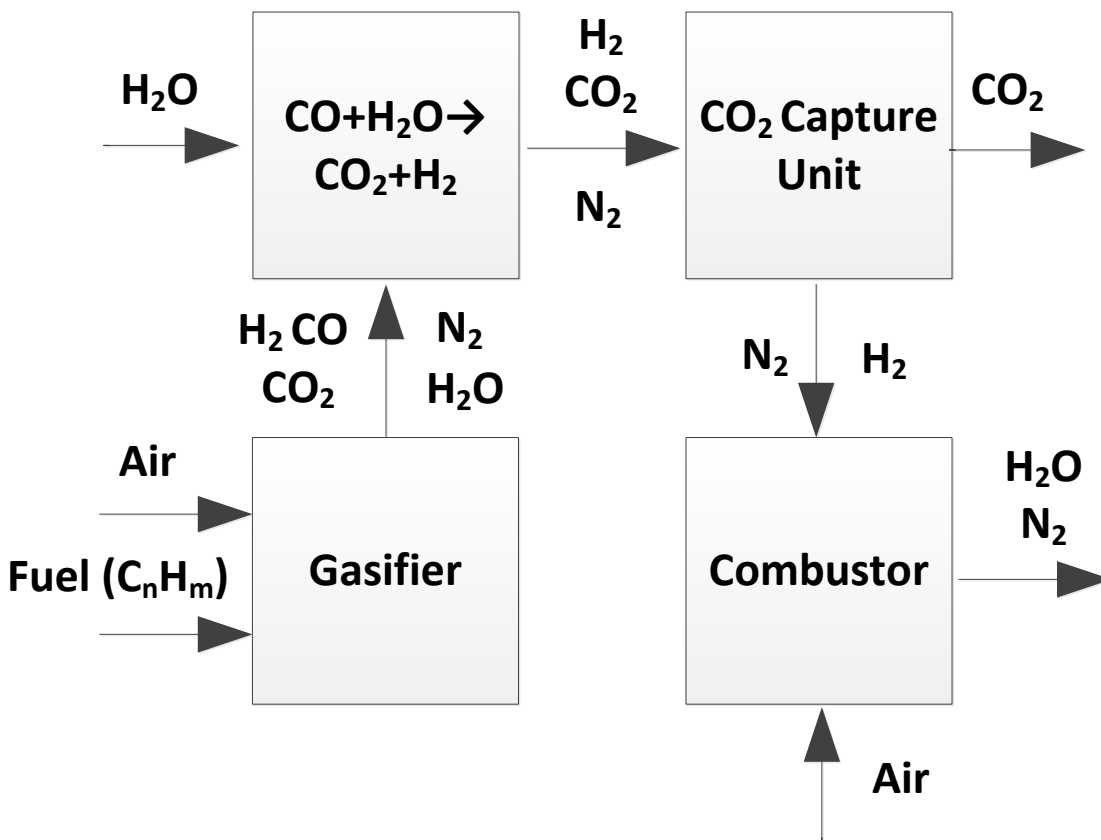


Figure 1.4. Typical scheme of a pre-combustion process

The IGCC process represents a new technological frontier because it permits to overcome the main problem of the gas turbines: to run with clean fuels avoiding erosion and fouling of the internal parts of the system. This feature is due to the easy management of pollutants in the IGCC; the utilization of an air separation unit, and hence the absence of N_2 , involves a higher partial pressure of the pollutants than in traditional power plants, hence a more efficient removal. When compared with direct combustion, drawbacks of IGCC have been represented by larger capital-intensity and lower availability, which can both be overcome by better understanding and optimization of the technology.

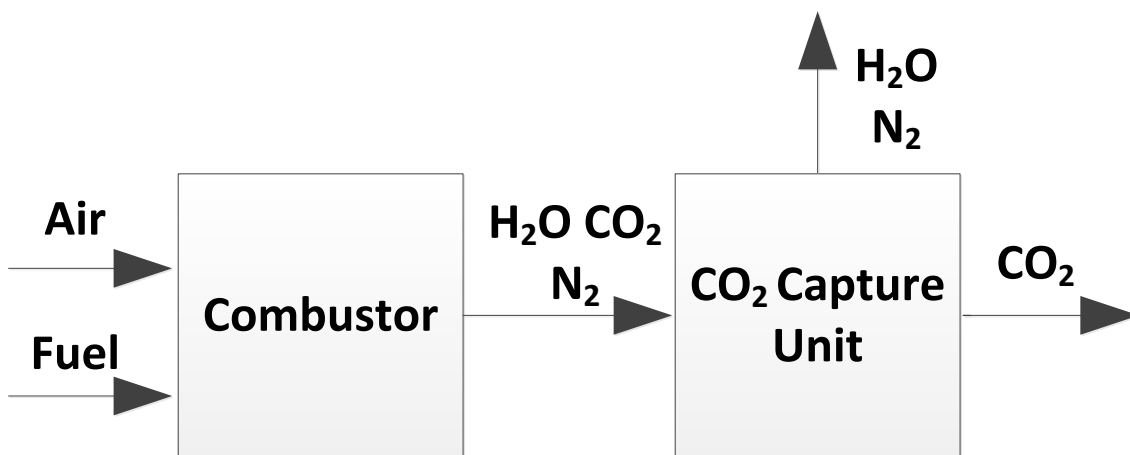


Figure 1.5. Typical scheme of a post-combustion process

Post-combustion capture consists in the treatment of the exhaust gases produced by combustion of fossil fuels (Figure 1.5). Its main advantage is the possibility to easily retrofit existing power plants. This technology is based on CO_2 separation from the flue gas, with a typical CO_2 content of 10-20% by volume, using a variety of processes such as chemical absorption, adsorption, membrane or cryogenic separation. At present, chemical absorption is the most widely used technology. This process employs the reaction of an aqueous alkali solvent with CO_2 . MEA (monoethanolamine), MDEA (methyldiethanolamine) and

DEA (diethanolamine) are currently the main chemical absorbents of interest for CO₂ separation (Aaron and Tsouris, 2005). Amines capture CO₂ from the flue gas at low temperature and release it after heating (stripping), producing an almost pure CO₂ stream. Figure 1.6 shows a typical amine scrubbing system (Rochelle, 2009). CO₂ is captured at ambient temperature by amines which are regenerated by steam at temperatures of 100-120°C, obtaining a pure CO₂ stream after water condensation. Unfortunately, these absorbents have an elevated energy demand for their regeneration and are degraded by the impurities contained in the exhaust gas; hence they are used to treat very clean gas mixtures containing only small quantities of impurities such as dust, SO_x, NO_x, H₂S and oxygen.

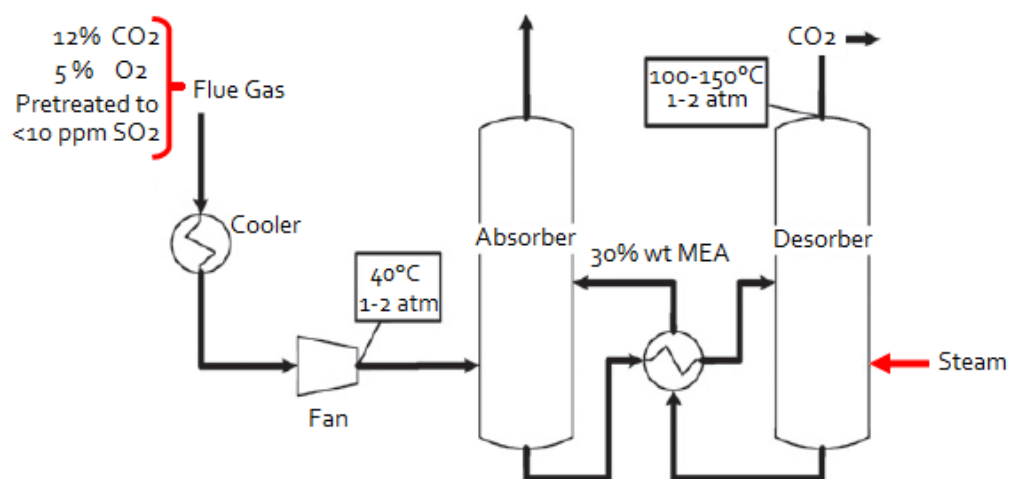


Figure 1.6. Amine scrubbing system for CO₂ capture.

Oxy-fuel combustion (or oxyfiring) is based on combustion of fuels using pure oxygen (up to 97%) as oxidant. Oxy-fuel combustion overcomes the issues associated with the presence of nitrogen in the reaction environment, so that the flue gas will be composed mainly of CO₂ and water (Figure 1.7). The next step is to separate water from CO₂ by condensation, yielding an almost pure CO₂ stream ready for sequestration. Part of the exhaust gas is recycled to the combustion

chamber in order to control the temperature level. Oxyfiring requires an air separation unit to provide nearly pure oxygen for combustion. This process is conceptually very simple. Existing combustion plants can be in principle retrofitted for oxyfiring, though problems might arise due to air intake and leakage. The oxygen production step represents the most significant energy penalty for this technology (Buhre et al., 2005; Toftegaard et al., 2010).

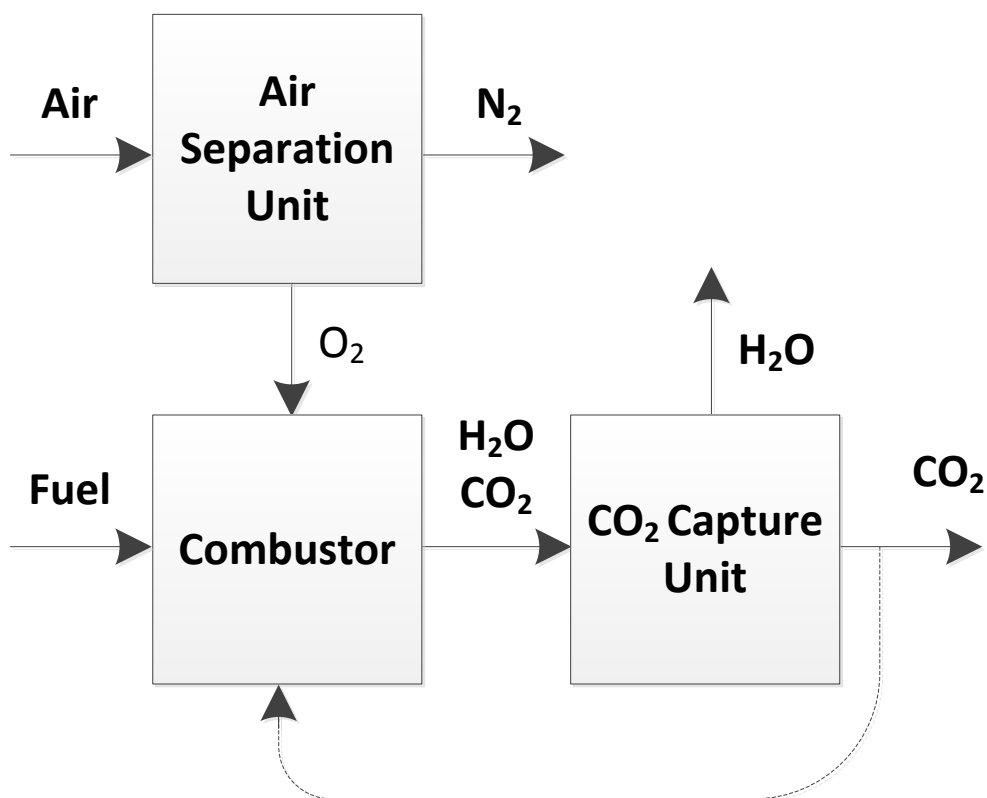
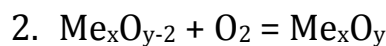


Figure 1.7. Typical scheme of a oxy-fuel combustion process.

Chemical looping combustion (Mattison and Lyngfelt, 2001; Lyngfelt et al., 2008; Wang and Anthony, 2007) is an innovative and very challenging combustion technology with inherent CO₂ sequestration, which has attracted much attention over the last years. The concept is based on the utilization of solid oxygen carriers (OC) which promote fuel oxidation without direct contact with atmospheric oxygen. Typical OCs consist of an active phase, which could be

a suitable metal oxide, supported on an inert material for ensuring chemical, thermal and mechanical stability (Adànez et al., 2004, 2012; Wolf et al., 2005; Johansson, 2007). The process involves two reaction steps:



where C_nH_{2m} is a generic fuel, while Me_xO_y and Me_xO_{y-2} are the metal oxide in the oxidized and reduced form, respectively. The process involves cyclic steps of OC reduction by the fuel and oxidation by atmospheric air, which take place iteratively in the Fuel Reactor (reaction 1) and in the Air Reactor (reaction 2) (Figure 1.8). The oxidation of the carrier is exothermic, whereas the reduction step is endothermic, with the remarkable exceptions of CuO (de Diego et al., 2004) and Mn_2O_3 which are characterized by an exothermic reduction stage. The key issue of this technology is to find suitable OCs (active phase and support) for the process. Several metal oxides have been proposed in the literature to be used as OC (Wolf et al., 2005; Johansson, 2007; Chandel et al., 2009, Lyngfelt et al., 2008, Adànez et al., 2004): candidate carriers are nickel, cobalt, copper, iron and manganese oxides. Alternative CLC concepts are based on the use of sulphate/sulphide cycles (Wang and Anthony, 2008) or on alternated oxygen chemisorption/desorption on carbon (Salatino and Senneca, 2009).

Features required for a good OC are (Adànez et al., 2012):

- high reactivity with the fuel and oxygen in the temperature range of interest for the process;

- high oxygen ratio (moles of oxygen which the carrier is able to exchange per mole of metal oxide);
- low propensity to attrition/fragmentation and agglomeration phenomena;
- inexpensiveness and environmental friendliness.

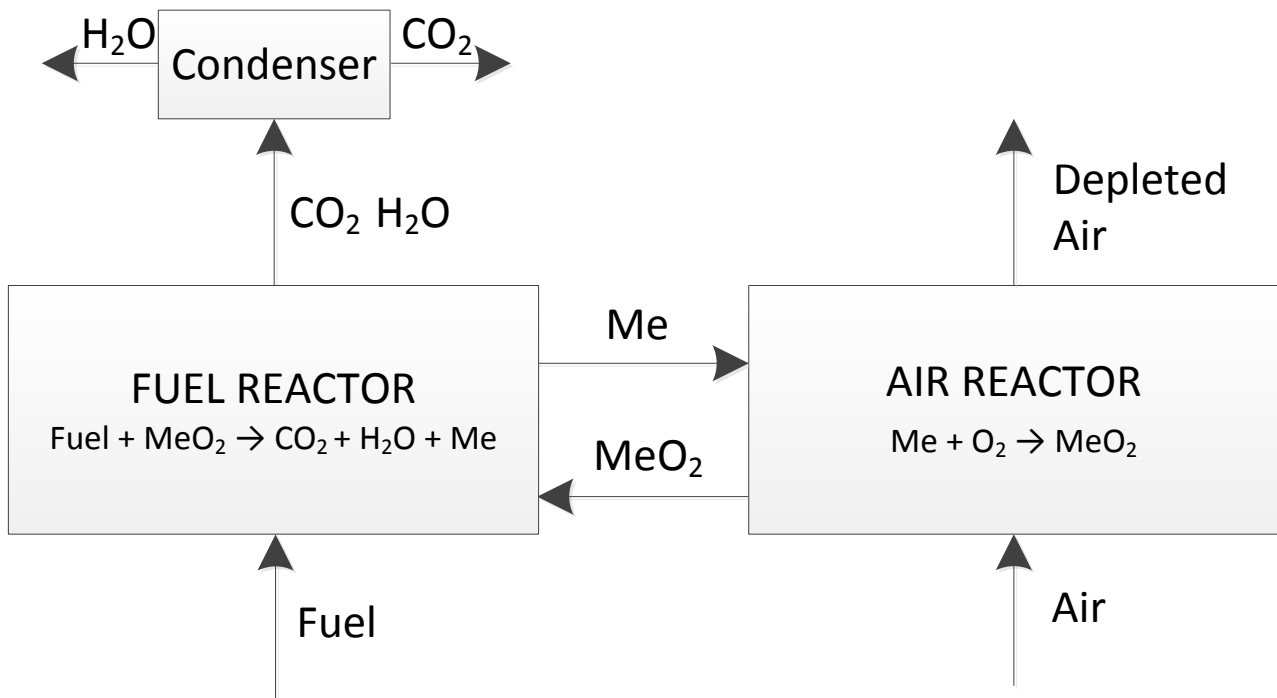
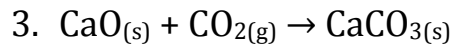


Figure 1.8. Typical scheme of a chemical looping combustion process.

1.3. The Calcium Looping Cycle

The calcium looping cycle is a post combustion process which uses CaO-based sorbents, typically derived from natural limestone, to capture CO_2 from flue gas (Shimuzu et al., 1999; Dean et al., 2011a; Stanmore and Gilot, 2005;

Alonso et al., 2010; Blamey et al., 2010b). The process is based on the reversible carbonation reaction:



Carbonation ($\Delta H_{r,298K} = -182.1\text{kJ/mol}$) proceeds at a satisfactory rate at temperatures in the range 650–700°C (Fennel et al., 2007a; Sun et al., 2007a), while the reverse calcination reaction is carried out at 850–950°C. The calcium oxide sorbent is repeatedly cycled between two reactors (Figure 1.9). In one reactor (the carbonator) carbonation of CaO particles occurs, capturing CO₂ from the flue gas. The sorbent particles are then circulated to another reactor (the calciner) where calcination takes place. The regenerated CaO particles are returned to the carbonator, leaving a concentrated stream of CO₂ ready for sequestration. Because of the deactivation of sorbent material, the process needs a continuous or periodic feeding of fresh sorbent (make-up) and a purge for deactivated (spent) one, as shown in the Figure 1.9.

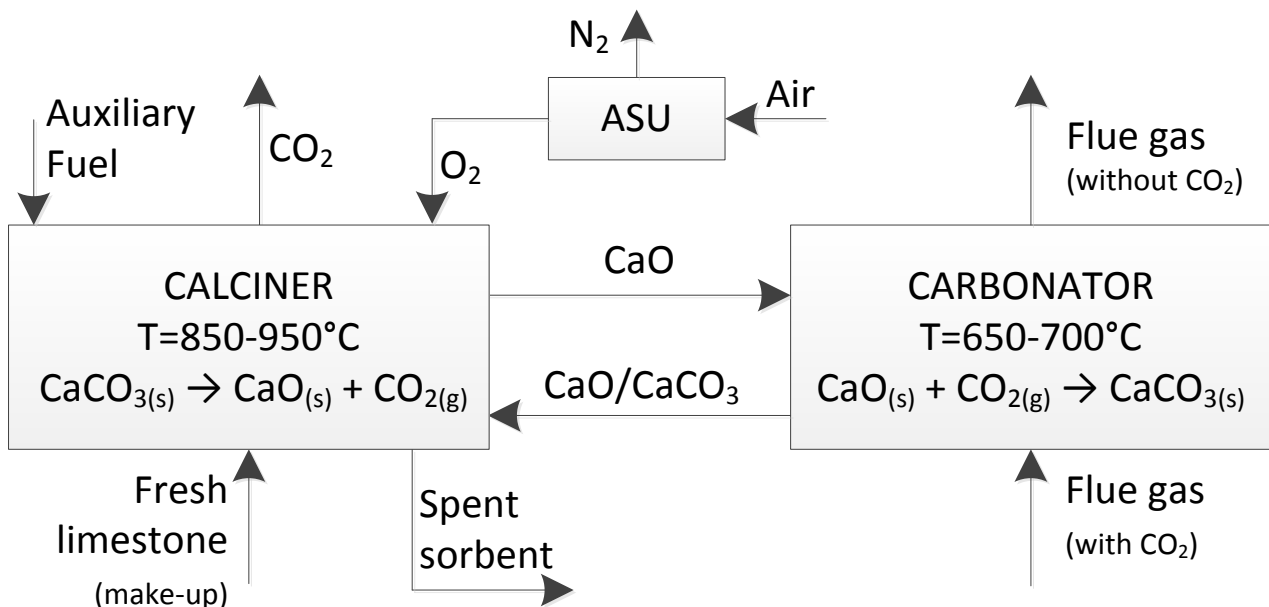


Figure 1.9. Typical scheme of a calcium looping process under oxy-firing condition in the calciner.

The endothermicity of the calcination reaction and the temperature difference between sorbent streams entering and leaving the calciner imply the necessity to provide an energy input to the calciner. Shimizu et al. (1999, 2002) have proposed to oxyfire coal (auxiliary fuel) in the calciner with O_2 provided by an external air separation unit, whose estimated size would be approximately one third of that required for an oxy-fuel power plant. This option involves temperature and CO_2 concentrations in the calciner typical of oxyfiring, which have important consequences on sorbent deactivation, hence on process efficiency.

Calcium looping can also be implemented in a pre-combustion version (Harrison, 2008), known as sorption-enhanced gasification. In this version the carbonator can be operated as a gasifier-carbonator, where gasification of a solid fuel and in situ uptake of the generated CO_2 are accomplished at the same time. This option could have some advantages:

- The CO_2 , produced by gasification, is continuously removed from the reaction environment by the sorbent, so the gasification is driven towards a higher production of H_2 ;
- The carbonation, being an exothermic process, could provide the heat needed for the gasification reaction;
- Calcium carbonate and calcium oxide promote the destruction of tars (Florin and Harris, 2008) which are a severe issue when using hydrogen.

Figure 1.10 (McBride et al., 2002) reports the partial pressure of CO_2 corresponding to the thermodynamic equilibrium of the calcination reaction, as a function of temperature. Several analytical expressions have been proposed to describe this curve. Selected equations are given in Table 1.1.

Table 1.1. Selected equations expressing CO₂ partial pressure at equilibrium for calcination.

4. $P_{CO_2}^{eq} = 1.826 \times 10^7 \times e^{-\frac{19680}{T}} [bar]$	Baker, 1962
5. $P_{CO_2}^{eq} = 4.137 \times 10^7 \times e^{-\frac{20474}{T}} [bar]$	Silcox et al., 1989

Operating conditions in the calciner must be chosen so as to promote calcination and to reach a compromise between achieving acceptable reaction rates and preventing sorbent deactivation (which are both enhanced at high temperature). As far as operation of the carbonator is concerned, a compromise must be found between two factors: fast carbonation rate, promoted at high temperature, and elevated carbonation degree, promoted at low temperature (as shown by the equilibrium conditions for calcination reaction in Figure 1.10).

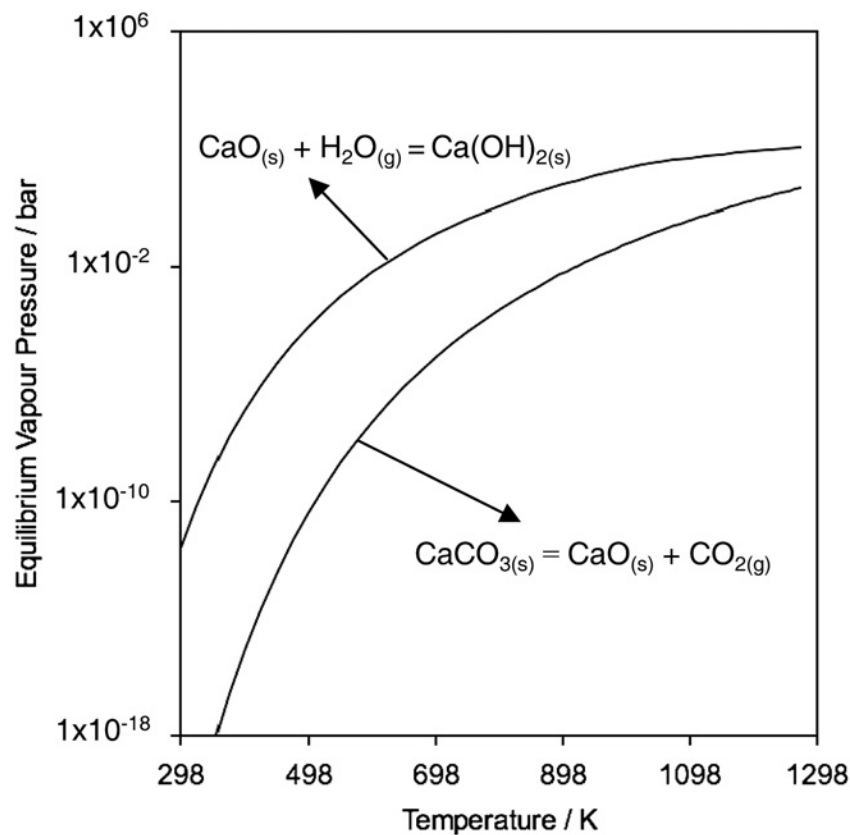


Figure 1.10. Equilibrium partial pressure of gaseous CO₂ and H₂O above CaO as a function of temperature (McBride et al., 2002)

As regards reaction kinetics, the calcination reaction is characterized by a complex kinetic expression, which depends on three factors (Stanmore and Gilot, 2005): CO₂ concentration, which inhibits the reaction; particle size, which can determine both thermal and diffusive limitations; catalysis/inhibition induced by impurities. Blamey et al. (2010a) have shown that there are two CO₂ pressure ranges which have different effect on the calcination rate: for $P_{CO_2} < 10^{-2}P_{CO_2}^{eq}$, where P_{CO_2} denotes the CO₂ partial pressure and $P_{CO_2}^{eq}$ the equilibrium partial pressure of CO₂ at a certain temperature, the calcination rate is practically independent from CO₂ partial pressure; when $P_{CO_2} \approx 10^{-2}P_{CO_2}^{eq}$, a parabolic relationship is observed between calcination rate and CO₂ partial pressure, after which a linear dependence on $(P_{CO_2}^{eq} - P_{CO_2})$ is found. A possible explanation of this behaviour is that calcination is quickly completed at low CO₂ partial pressure. On the contrary, in a reactor at atmospheric pressure with a CO₂ concentration lower than 100%, calcination needs a higher temperature to take place at an appreciable rate (Blamey et al., 2010a).

Carbonation is characterized by an initial fast stage, controlled by chemical reaction, followed by a very slow one, controlled by diffusion phenomena (Blamey et al., 2010a; Bhatia and Perlmutter, 1983). The resulting final carbonation degree is typically much lower than 100%.

One of the most important advantages of this process derives from the utilization of limestone which “...is one of the cheapest industrial chemicals (after water) and is environmentally benign” (E. J. Anthony). Moreover, the process has a lower energy penalty than amine scrubbing: it is in the order of 6-8% for calcium-looping and 9.5-12.5% for amine-based system (Dean et al., 2011a). A further advantage could be represented by the lower capital and operational costs than the traditional amine-based system. A preliminary economic analysis (MacKenzie et al., 2007) shows that the cost for CO₂ capture is about 19.75

US\$/ton CO₂ for the calcium-looping process, which is fairly low if compared with those of the amine system (32.5-80 US\$/ton CO₂, data refer to year 2005). In addition, there is the possibility of an integration of the calcium-looping process with the cement industry (Abanades et al., 2005; Bosoaga et al., 2009), which is the most important CO₂ producer after the energy industry. Indeed, the spent sorbent coming from calcium-looping process may be used as a raw material determining various energetic/environmental benefits. Some studies have demonstrated that spent sorbent produces a clinker with comparable features to commercial cement (Dean et al., 2001b). This integration might reduce CO₂ emissions related to these processes.

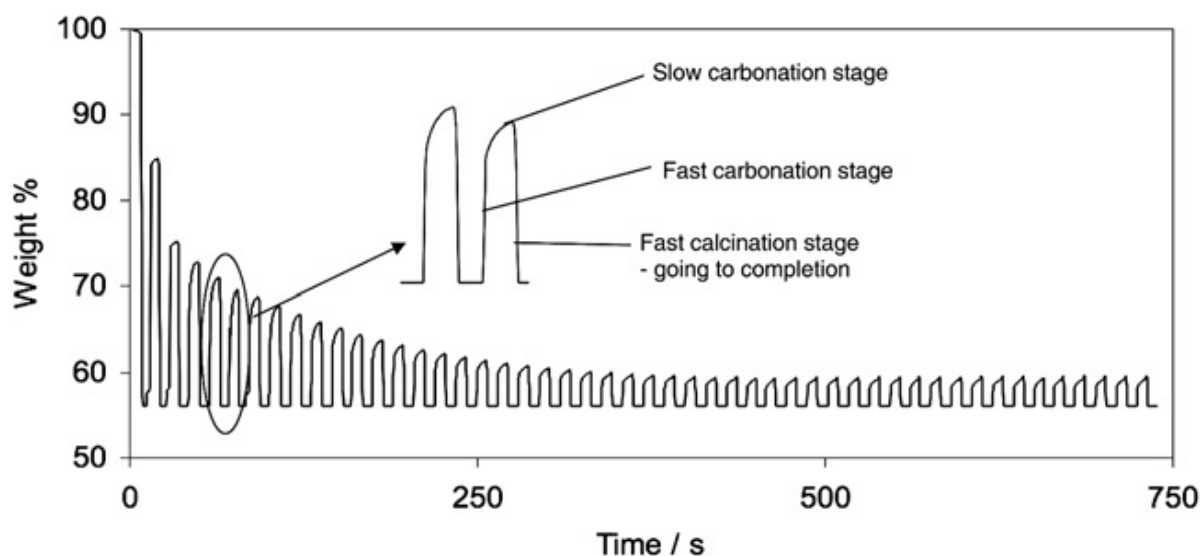


Figure 1.11. Iterated calcination/carbonation cycles of limestone in a TGA (Blamey et al., 2010a)

1.4. Sorbent deactivation

Several studies have been carried out on sorbent deactivation under alternated calcination/carbonation cycles (Blamey et al., 2010a; Curran et al.,

1967; Barker, 1973; Silaban e Harrison, 1995; Abanades, 2002; Abanades e Alvarez, 2003; Grasa e Abanades, 2006). Sorbent deactivation entails a progressive drop in the CO₂ capture capacity, defined as the amount of captured CO₂ per amount of sorbent. Figure 1.11 shows a typical trend of the mass of sorbent (in percentage), under repeated calcination/carbonation cycles. It is clear that the mass increase after each carbonation step is reduced upon iterating cycles, ultimately reaching an asymptotic value of about 8-10% of the initial value (Grasa and Abanades, 2006). Similarly, Figure 1.12 shows such a decrease in terms of the maximum value for CaO conversion degree (indicated as X_{CaO}). “Maximum conversion” is defined as the calcium conversion degree reached after the rapid stage of the carbonation reaction. Figure 1.12a reports X_{CaO} for an elevated number of cycles, highlighting the presence of a residual/asymptotic value equal to about 0.075 (Grasa and Abanades, 2006). Figure 1.12b shows the sharp decay after the first 40 cycles.

The causes of sorbent deactivation lie in two different effects. The first one is related to the reaction pathway between CO₂ and CaO. It is interesting to underline that CaO, obtained by calcination, is more porous (Barker, 1973) and reactive toward CO₂ than natural lime. This is likely due to the presence of a network of small pores formed after calcination (Sun et al., 2007a). It was estimated that carbonation takes place in pores with a maximum dimension of 150nm (Fennel et al., 2007b). Carbonation yields a solid product which has a higher molar volume than CaO, so that a carbonate layer is generated on the external particle surface and on the internal surface of the pores, resulting in pore hindrance and in trapping of un-reacted CaO inside the particles. Some of these pores remain closed even after calcination, entailing a permanent decrease of reactive surface.

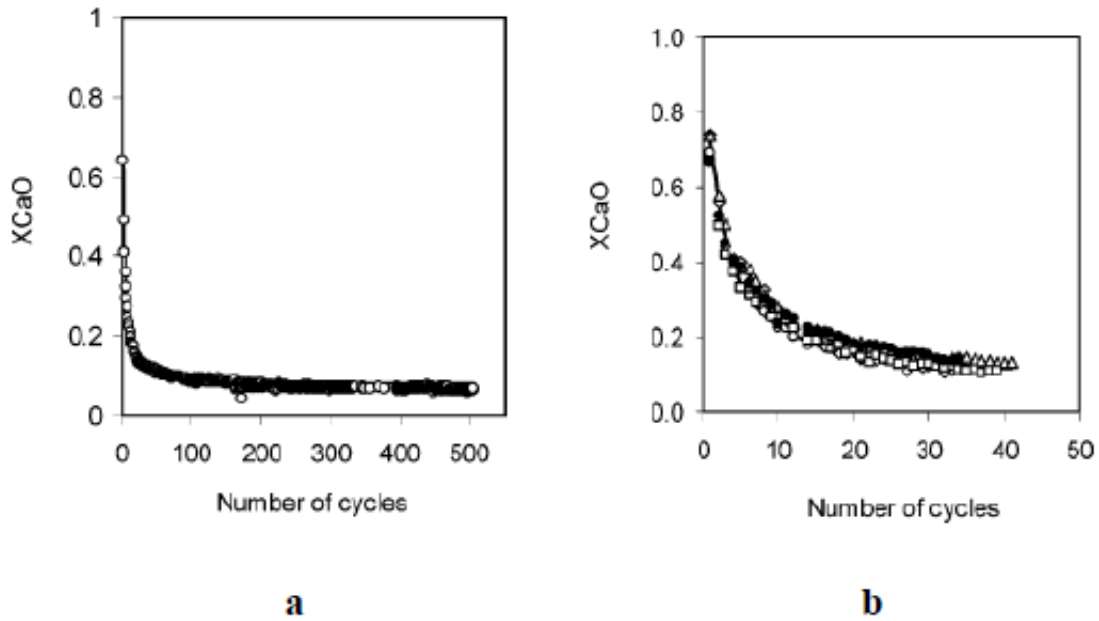


Figure 1.12. Sorbent conversion vs number of cycles for the experiment (Grasa e Abanades, 2006).

The main cause of the CO₂ capacity decay has been identified in sorbent sintering and in the associated changes of pore size, which depends on the process temperature and on the duration of the cycles. Sintering causes changes in the pore shape and in the pore size, as well as an increase in the grain size. In particular, sintering promotes an abatement of the small pores (<220 nm) and the formation of a network of macropores with size >220 nm. In this way, the surface area/volume ratio decreases with the number of cycles. The formation of macropores occurs by means of a mechanism of volume diffusion, determined by the minimization of the surface energy, which promotes a decrease of particle porosity (Fennel et al., 2007b; Manovic et al., 2009). In other words, the CaO sintering generates a variation of surface texture of limestone from rough to smooth (Abanades et al., 2004; Abanades e Alvarez, 2003; Sun et al., 2007b).

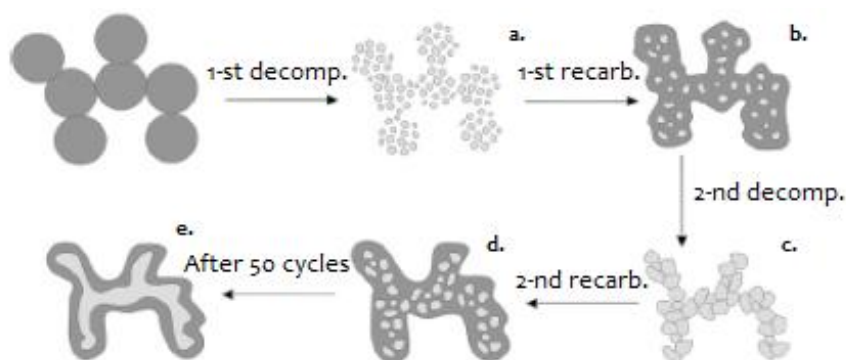


Figure 1.13. Schematic representation of the textural transformation of the CaO sorbent over iterated cycles. The CaO phase is shaded light grey and the CaCO₃ phase is shaded dark grey (Lysikov et al., 2007).

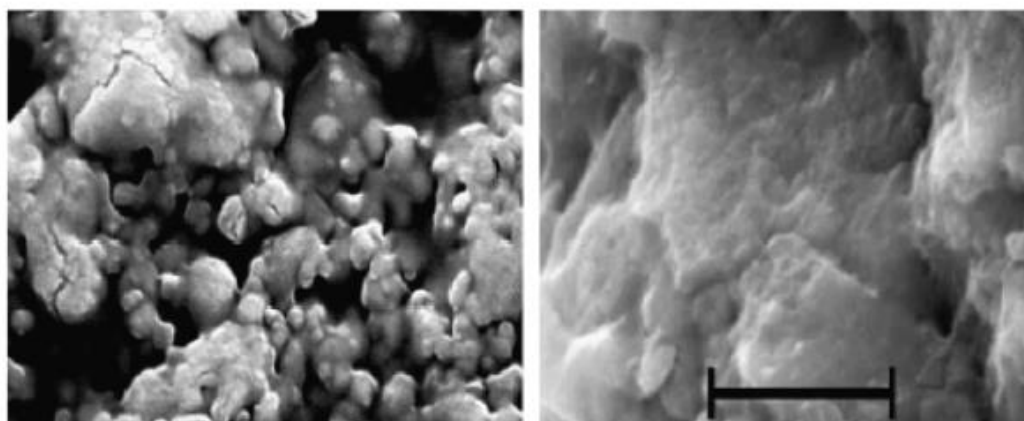


Figure 1.14. SEM images of particles of Purbeck limestone. On the left side: external surface of a particle calcined once. On the right side: interior of a particle calcined 20 times and re-carbonated 19 times. All images were taken with the same magnification, the scale bar corresponding to 5 mm (Fennell et al., 2007b).

Figure 1.13 shows a schematization of the sorbent behaviour during repeated cycles. The initial sorbent, that is after the first calcination, has many pores with small size and very rough surface (Figure 1.13a). The following carbonation is not complete because of pore sealing and sintering process (Figure 1.13b). Some pores remain closed during the consecutive calcinations (Figure 1.13c-d) and this process goes on up to obtaining a sorbent with low reactivity and a rigid structure (Figure 1.13e). It is possible to observe this

structure change in Figure 1.14. The image on the left side shows a particle after the first calcination which appears rough and full of many small pores. On the right side, a particle after 20 calcinations and 19 carbonations is reported, which shows a smoother surface and few pores with large size.

As shown in Figure 1.15, sintering induces significant effects above 975°C, in inert atmosphere, producing a strong reduction of surface area and porosity in a short time (15 min) (Borgwardt, 1989a). Further studies of Borgwardt (1989b) confirm that sintering is promoted by the presence of CO₂ and H₂O. The effect of temperature on sintering is very clear in Figure 1.16, where the CO₂ capture capacity (indicated as a percentage uptake capacity) of the Havelock limestone is reported, as a function of the number of cycles, at atmospheric pressure, with a CO₂ concentration of 15% but at different calcination temperatures. Ultimately, sintering is promoted during calcination, i.e. at high temperature, inducing a fast decay of CO₂ capture capacity, while carbonation has a negligible effect on sintering (Sun et al., 2007c).

German (1976) has proposed a model to describe the sintering process:

$$6. \left(\frac{S_0 - S}{S} \right)^\gamma = K_i \times t$$

where S is the specific surface area at time t , S_0 is the initial specific surface area and K_i is a rate constant which includes diffusion coefficient (a function of temperature), surface tension and other constants. The exponent γ is mechanism dependent and is found in the case of CaO to be 2.7 (Borgwardt, 1989a)

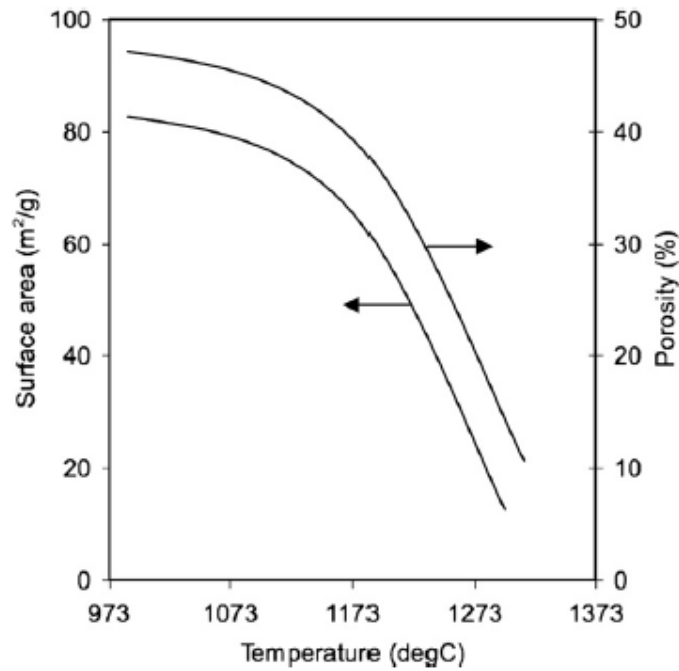


Figure 1.15. Porosity and surface area of 2 mm limestone-derived CaO particles after 15 min heating under a nitrogen atmosphere (adapted from Borgwardt, 1989a).

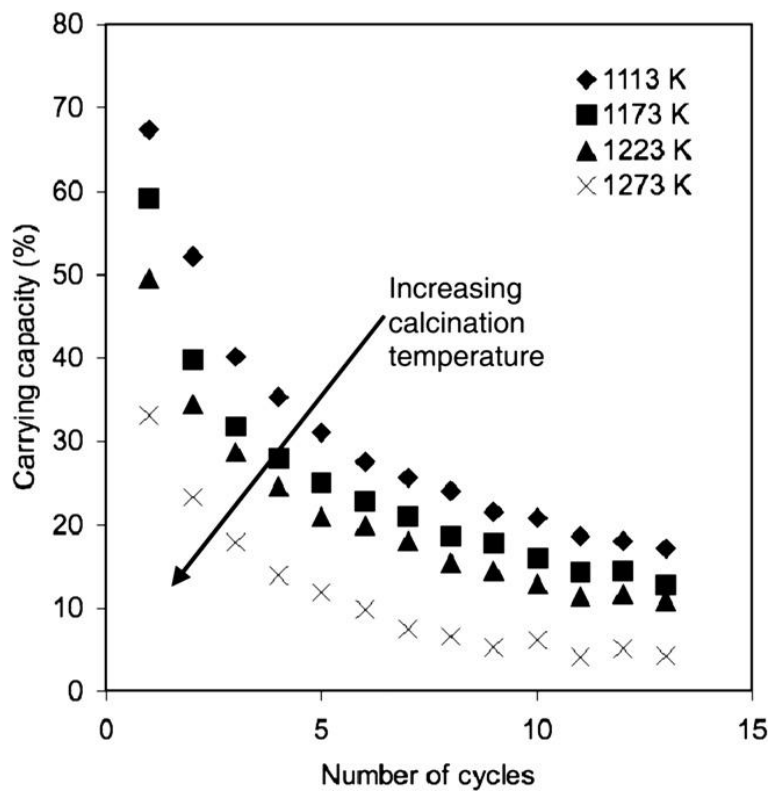
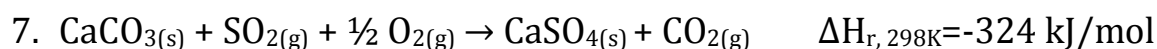


Figure 1.16. Decay of CO₂ capture capacity over iterated cycles at different temperatures (Blamey et al., 2010a).

1.5. Sorbent deactivation induced by sulphation

Another problem related to the decay of the CO₂ capture capacity is represented by the possible presence of SO₂ in the flue gas processed in the carbonator, which reacts with lime to form CaSO₄. Furthermore, SO₂ is generated during combustion of coal which typically has sulphur content up to 8% by weight (Smith, 2007). Hence, SO₂ is also present in the calciner where, as discussed previously, an auxiliary fuel, such as coal, is oxyfired to sustain calcination. The reaction between lime and SO₂ is already used in the *in situ* desulphurization of flue gas in fluidized bed combustors, using natural sorbents such as limestone and dolomite.

Direct sulphation of limestone:



occurs when the CO₂ partial pressure in the reactor does not permit the calcination of CaCO₃ (Smith, 2007). Otherwise, indirect sulphation of CaO takes place:



Unfortunately, sulphation is irreversible in the temperature range of interest so that lime reacted with SO₂ is permanently lost (Anthony and Granatstein, 2001). On the other hand this reaction, even if reduces the CO₂ capture capacity of the sorbent, is not completely undesired as it may be directed to remove SO₂ from the flue gas whose emissions have stringent legal limitations.

Several studies have been carried out on the indirect sulphation of sorbent (Anthony et al., 2007), which confirm that sorbent calcination is faster than sulphation. Furthermore, the higher molar volume of CaSO₄ compared to CaO

and CaCO_3 induces pore plugging with a core-shell structure (Dam-Johansen and Østergaard; 1991). The sulphation effects depend on the particle size: for large particles sulphation produces an unreacted core of CaO (Figure 1.17a); if a network of large pores is present, a number of small unreacted cores are formed (Figure 1.17b), while if the particles are sufficiently small, then the sulphation is uniform (Figure 1.17c).

Moreover, the sulphated external layer hinders intraparticle diffusion of CO_2 (Stanmore and Gilot, 2005; Blamey et al., 2010b; Montagnaro et al., 2010, Anthony and Granatstein, 2001; Scala et al., 2008; Ryu et al., 2006), determining a loss of CaO available for CO_2 capture. The extent of this loss depends on the properties of the sorbent and on CO_2 partial pressure in the system (Grasa et al., 2006). In particular, it was observed that high CO_2 concentrations promote slower deactivation (Sun et al., 2007b). The competition between reaction with CO_2 and SO_2 depends on the morphology of the calcined sorbent (porosity, grain size etc.) and on the properties of the sulphated particles. It is important to underline that sorbent deactivation (promoted by sintering) could result in improved capture of SO_2 (Grasa et al., 2008), due to the presence of large pores in the sorbent which has undergone many carbonation/calcination cycles (Li et al., 2005b).

A useful method to prevent sorbent deactivation by SO_2 is to use spent sorbent reactivated by hydration. Hydration, with either liquid water or steam, represents an efficient method to regenerate the ability of spent sorbent to uptake both CO_2 and SO_2 , because it generates a better sorbent morphology (Manovic and Anthony, 2007b; Manovic et al., 2008b) in terms of pore surface area, which promotes CO_2 capture (Alvarez and Abanades, 2005), and size distribution of pores, which facilitates SO_2 capture (Ives et al., 2008).

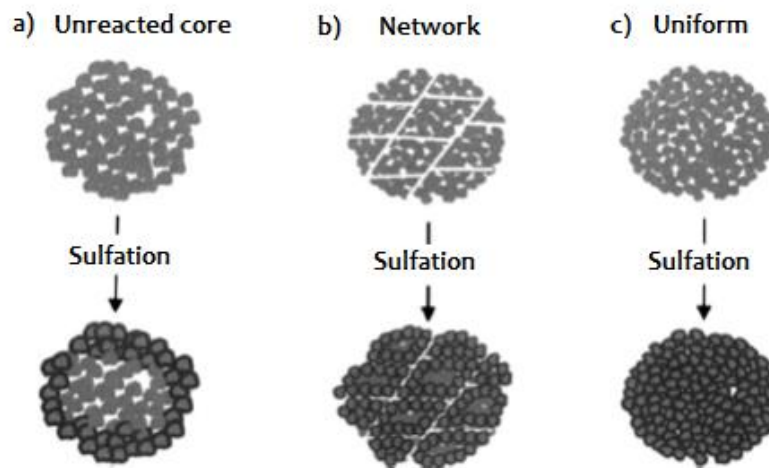


Figure 1.4 Schematic sequence of sulphation of three different types of sulphated limestone particles (Laursen et al., 2000).

1.6. Synthetic and natural alternative sorbents

The use of dolomite, rather than limestone, to accomplish flue gas desulphurization during fluidized bed combustion has been reported in the literature (Stantan, 1983; Anthony and Granatstein, 2001; Scala and Salatino, 2003). Dolomites are generally more reactive (on a Ca molar basis) than limestone with a more elevated resistance toward sintering, but their use implies a larger mass feed rate necessary to obtain a required Ca/S feed ratio. Moreover, dolomites show a higher propensity toward attrition/fragmentation phenomena.

Most of the experimental work on calcium looping reported to date has been directed to characterize the performance of limestones. Only a few studies have considered dolomite, whose potential has been characterized either in thermo-gravimetric (Silaban et al., 1996; Chrissafis et al., 2005; Chen et al.,

2009) or in fluidized bed (Fang et al., 2009) reactors. Early studies showed that dolomite provides larger active surface area than limestone, a feature that results in improved carbonation (Silaban et al., 1996; Chrissafis et al., 2005).

The decomposition of MgCO_3 to MgO and CO_2 occurs, from a thermodynamic viewpoint, at about 305°C at atmospheric pressure with a CO_2 concentration of 100%v/v. The reverse reaction with 10%v/v of CO_2 requires a temperature below about 247°C which is incompatible with the temperature of a carbonator ($650\text{-}700^\circ\text{C}$). Accordingly, MgO does not take part in CO_2 absorption in the carbonator, as carbonation is fully hindered at temperatures typical of the carbonator. However this oxide plays an important role in calcium looping, as it has a structure-stabilizing effect that provides a higher cyclic stability of calcium compounds compared to raw limestone. As a consequence, most dolomites show a higher long-term CO_2 capture capacity than limestone. The structure-stabilizing effect of MgO is made evident by the following features: i) the sorbent porosity is preserved over iterated cycles by the framework of the unreacted MgO ; ii) MgO has a higher melting point than CaO and, therefore, effectively prevents sorbent sintering.

A recent study and patent by Iyer and Fan (2006) reports on the use of waste from food manufacture, like mussel or chicken-egg shells. These waste material are characterized by high calcium content and remarkable particle strength. Ives et al. (2008) repeatedly cycled mussel shells and chicken-egg shells under mild conditions in an atmospheric pressure fluidized bed reactor, and found that both sorbents displayed similar reactivity upon cycling compared to the reference Purbeck limestone, despite showing different initial pore size distributions.

Synthetic sorbents can exhibit a higher reactivity than natural limestone thanks to better tailored microstructural properties. Fan and co-workers

(Agnihotri et al., 1999; Gupta and Fan, 2002) developed a wet precipitation process to produce a precipitated calcium carbonate (PCC) with a high surface area. This sorbent features a large extension of mesopores which are less subjected to pore closure than micropores. Other researchers have synthesized sorbents based on dispersing CaO on various inert supporting materials: Li et al (2005a, 2006) with mayenite ($\text{Ca}_{12}\text{Al}_{14}\text{O}_{33}$), Aihara et al. (2001) with CaTiO_3 . The use of synthetic sorbents in calcium looping is attractive but is generally associated with availability and cost issues. Li et al. (2008a) have reported that modification of dolomite using acetic acid yielded a sorbent with significantly higher activity than that of the original sorbent. An independent study showed that carbonation of CaO, when modified using a solution of ethanol and water, was more complete than for CaO hydrated with distilled water (Li et al., 2008b). Doping of limestones with aqueous solutions (0.002–0.5 M) of different salts such as Na_2CO_3 or NaCl yields only marginal improvements in the long-term reactivity (Fennel et al., 2007b). In some cases doping of natural sorbents induced a decrease of the sorbent reactivity, as was the case for Salvador et al. (2003) who used aqueous solutions of Na_2CO_3 or NaCl. The utilization of high-capacity sorbents entails a reduction of the make-up (Rodriguez et al., 2008), hence an improvement of the process economics. However, chemical or physical treatments of the sorbent involve costs, and their practical feasibility can only be assessed by specific economic analysis (Lisbona et al., 2010).

1.7. Sorbent reactivation and pretreatment

Several studies have investigated measures to reactivate spent sorbents or to reduce the decay of the capture capacity. Among the proposed techniques one might recall thermal preactivation and reactivation of sorbent by hydration.

Studies on thermal pretreatment (Lysikov et al., 2007; Manovic and Anthony, 2008a) have showed that thermally treated sorbents are more reactive than untreated ones for a higher number of cycles. Chen et al. (2009) found that thermally preactivated particles can retain a more elevated asymptotic value of the capture capacity as compared with untreated material. Moreover, thermal pretreatment is generally effective in reducing sorbent attrition phenomenon. Different optimal pretreatment conditions may apply for different sorbents, related also to the presence and nature of impurities and structural differences.

Hydration is currently considered a relatively cheap, and hence a promising way to reactivate spent sorbents for SO₂ capture (Montagnaro et al., 2004, 2006a, 2008; Anthony et al., 2007; Smith, 2007). This process relies on the CaO conversion to Ca(OH)₂, according to the following reaction:



This reaction increases the molar volume (from 16.9 cm³/mol (CaO) to 33.7 cm³/mol (Ca(OH)₂), (Dam-Johansen e Østergaard, 1991)) of the CaO-rich core of spent sorbent particles, producing cracks and fissures in the external sulphate layer. Upon injection of the hydrated sorbent into the hot reactor, dehydration produces a sorbent with elevated surface area and porosity. Montagnaro et al. (2008) discussed strengths and drawbacks of this reactivation method for desulphurization process. In particular, hydration by liquid water requires shorter reaction times (in the order of minutes) than steam hydration (in the order of hours). Moreover, reactivation by liquid water determines sulphur redistribution inside the particles, contributing to an increase of the capture capacity of the reactivated sorbent. This redistribution is related to ion mobility in the aqueous phase associated with a solubilisation-precipitation mechanism driven by concentration gradients (Scala et al., 2001). The ion mobility could be responsible for the observed changes of pore volume along with hydration. This “cramming” phenomenology, consisting of coalescence of fine pores into larger

ones, broadly resembles pore volume changes associated with high-temperature sintering.

However, hydration emphasizes the attrition propensity of the particles, probably because of the lower hardness of Ca(OH)_2 than CaO/CaCO_3 (Montagnaro et al., 2006b; Materić et al., 2010).

Hydration takes place both on calcined and carbonated sorbents, but recent studies have demonstrated that calcined sorbents are more reactive, because they have a higher surface area and a better reactivity toward CO_2 (Manovic and Anthony, 2007b; Fennel et al., 2007a).

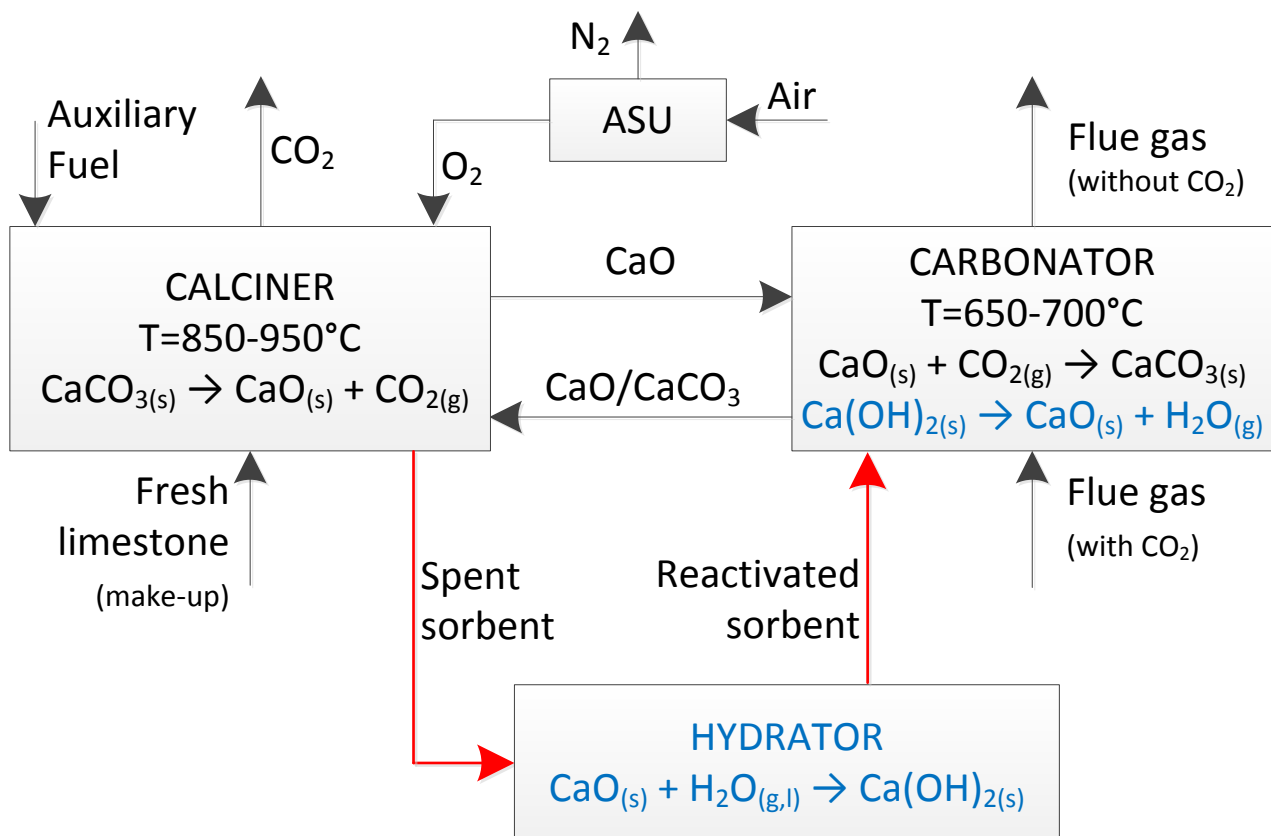


Figure 1.18. Typical scheme of a double-loop calcium looping process based on sorbent reactivation by hydration.

The use of hydration as a reactivation strategy for spent sorbents in the context of CO_2 capture has been recently proposed (Hughes et al., 2004; Fennel

et al., 2007a; Manovic and Anthony, 2007b; Manovic et al., 2008a, 2008b; Sun et al., 2008; Zeman, 2008; Arias et al., 2010; Blamey et al., 2010b; Wu et al., 2010; Martínez et al., 2011). It has been shown that the reactivity of spent sorbent can be nearly doubled after hydration (Fennel et al., 2007a; Manovic and Anthony, 2007a, 2008b). Fennel et al. (2007a) concluded that the sorbent activity is closely related to the total volume of pores.

Zeman (2008) has proposed the addition of a third reactor in the calcium looping process where hydration occurs (Figure 1.18). The spent sorbent is retrieved from the calciner, hydrated in the hydrator and send to the carbonator (Arias et al., 2010). In this way a CaO-rich sorbent is hydrated and the endothermic dehydration occurs in the carbonator simultaneously with the exothermic carbonation. Different operating condition for the hydration process are reported in the literature: steam hydration at high pressure (Manovic e Anthony, 2007b, 2008, 2009); steam hydration at atmospheric pressure (Manovic e Anthony, 2007a; Manovic et al., 2008a, 2008b; Sun et al., 2008; Wu et al., 2010; Martínez et al., 2011); steam hydration at atmospheric pressure and presence of CO₂ (Zeman, 2008); hydration by wet air (Fennel et al., 2007a); hydration by liquid water (Sun et al., 2008). Hydration conditions determine sorbents with different surface area and porosity, and hence with different performances. The steam hydration of CaO can take place at temperatures up to 520°C, but with relevant rates only up to 400°C, at atmospheric pressure (Zsako and Hints, 1998).

The disadvantages of hydration lie in the utilization of a third reactor (hydrator), which involves an increase of plant costs. Moreover, the reactor size depends on the hydration degree, on the residence time of the particles and on the flow rate of the spent sorbent to be reactivated. All these variables must be optimized, in order to make the hydration process economically more attractive than other options, such as the use of a high flow rate of make-up sorbent.

1.8. Calcium-Looping reactor configuration

The typical reactor configuration for the calcium looping process consists of two interconnected fluidized beds. This configuration permits the circulation of the solids between the reactors and ensures an intimate contact between the solid and gas phases. The fluidizing gas in the carbonator is the flue gas coming from the combustion process, while the fluidizing gas in the calciner may be either CO₂ recycled from the outlet gas or a CO₂/H₂O mixture.

One of the issues related to this technology is the optimization of the reactor configuration and of the material loss due to attrition phenomena (Blamey et al., 2010a, Curran et al., 1967; Barker, 1973; Silaban e Harrison, 1995; Abanades, 2002; Abanades e Alvarez, 2003; Grasa e Abanades, 2006).

The applicability of calcium looping has been successfully proved in lab-scale experiments (Abanades et al., 2004). In the next step it is necessary to further develop and optimize the process at the semi-industrial or demonstration scale before the technology will finally be applied to large scale power plants. In order to scale up calcium looping at larger scale, a 1MW_{th} pilot plant has been design and constructed close to a 50 MW_e CFB power plant in La Pereda (Spain), in the framework of the CaOling project (Sánchez-Biezma et al., 2012). In this facility the CO₂ capture efficiencies were larger than 90%, while SO₂ capture in the CFB carbonator was larger 95%. A 1 MW_{th} pilot plant was erected at the Technische Universität Darmstadt. Calcium looping experiments were performed in this test facility (Kremer et al., 2012). CO₂ capture efficiencies larger than 80% were achieved in the carbonator. Taking the oxyfuel-fired calciner into account the pilot plant was operated with total CO₂ capture rates exceeding 90%. It was shown that CO₂ capture can be limited by either chemical equilibrium or chemical kinetics.

1.9. Attrition phenomena

Particles in a fluidized bed are subject to attrition phenomena which produce both coarse and fine fragments. The latter may be dragged out (elutriated) from the reactor by the fluidizing gas, with a consequent material loss from the bed. Therefore, it is necessary to evaluate the fines generation rate to correctly design a fluidized bed calcium looping system.

Attrition is due to both the abrasion and the fragmentation of the sorbent particles (Werther and Reppenhagen, 2003). Abrasion refers to the removal of asperities from the particle surface yielding fine fragments which does not involve a significant size change of the parent particle. On the contrary, fragmentation entails a breakage which affects the entire particle with a significant decrease of the average particle diameter; consequently, a pronounced change of the particle size distribution occurs (Figure 1.19).

The propensity to attrition, which is certainly dependent on the mechanical properties of the material, are also strongly related to process conditions and parallel course of chemical reactions. The only reliable way to assess attrition under realistic process conditions is to carry out tests under conditions simulating real fluidized bed operation.

Based on studies performed on several limestones in a bubbling bed, Salatino and coworkers (Scala et al., 1997 and 2000; Di Benedetto and Salatino, 1998) classified sorbent attrition on the basis of the breakage mechanisms and on the size of the generated fragments, as summarized in Table 1.2: primary fragmentation, which occurs immediately after the injection of the particles in the hot bed, is due to the thermal stress and internal particle overpressure as result of the CO₂ release, and produces both coarse and fine fragments; attrition

by abrasion generates fine fragments and is due to the impacts among the particles and the reactor internals; secondary fragmentation takes place with the same mechanism of the attrition by abrasion, but yields coarse fragments.

Table 1.2. Classification of Attrition Phenomena Occurring to Limestone (adapted from Scala et al., 1997)

Attrition Phenomenon	Cause	Product
Primary fragmentation	Carbon dioxide release Thermal shock	Coarse and fine particles
Secondary fragmentation	Impacts	Coarse particles
Attrition by abrasion	Surface wear	Fine particles

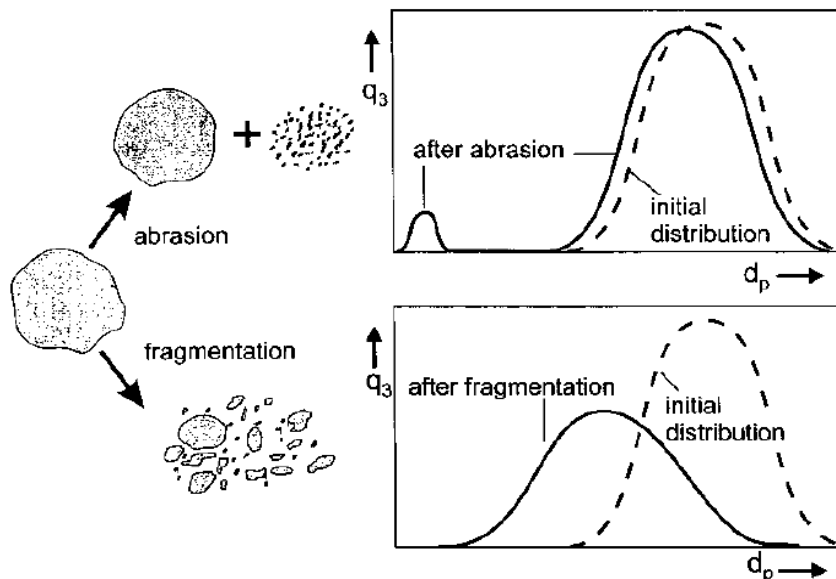


Figure 1.19. Attrition modes and their effects on the particle size distribution (q_3 = mass density distribution of particle sizes d_p) (Werther and Reppenhagen, 2003).

Studies carried out on several sorbents, during calcination-sulphation processes (Scala et al., 2000) display large elutriation rates at the beginning of the calcination stage. Figure 1.20 shows that the elutriation rate E of fine particles (evaluated during calcination and the following sulphation) has a decreasing exponential trend, with an initial peak. This peak is due to both the rounding-off of the rough surface, with a consequent decrease of the surface asperities, and fines generation caused by primary fragmentation. The former

highly depends on the type of sorbent; the latter is common for all limestones. Moreover, primary fragmentation influences the elutriation rate along a twofold pathway: on the one hand it directly generates elutriable fines, on the other it produces coarse fragments with many asperities, which can undergo further rounding-off. Fines generation by primary fragmentation occurs in short times after the sorbent injection into the hot reactor, while attrition by abrasion takes place along the whole particle residence time in the reactor.

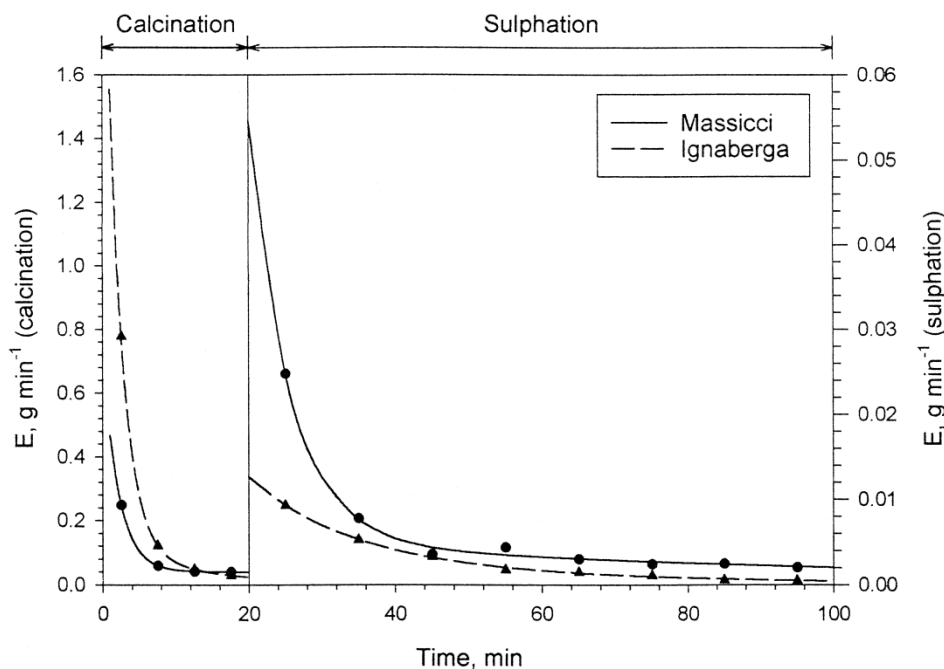


Figure 1.20. Sorbent elutriation rate during subsequent limestone calcination and sulphation for two different sorbents (Scala et al., 2000).

Elutriation is characterized by a smaller rate during sulphation compared with calcination because of the formation of a sulphated external layer which presents a high resistance toward abrasion. Altogether, calcination and sulphation affect the mechanical properties of particles (Scala et al., 2000, 2007; Chen et al., 2007), determining the mechanism and the extent of attrition.

Impact tests have showed that calcination, sulphation and re-carbonation strongly affect the fragmentation degree. In particular, raw limestone displays a better resistance than the calcined material (Scala et al., 2000, 2007; Scala and Salatino, 2003).

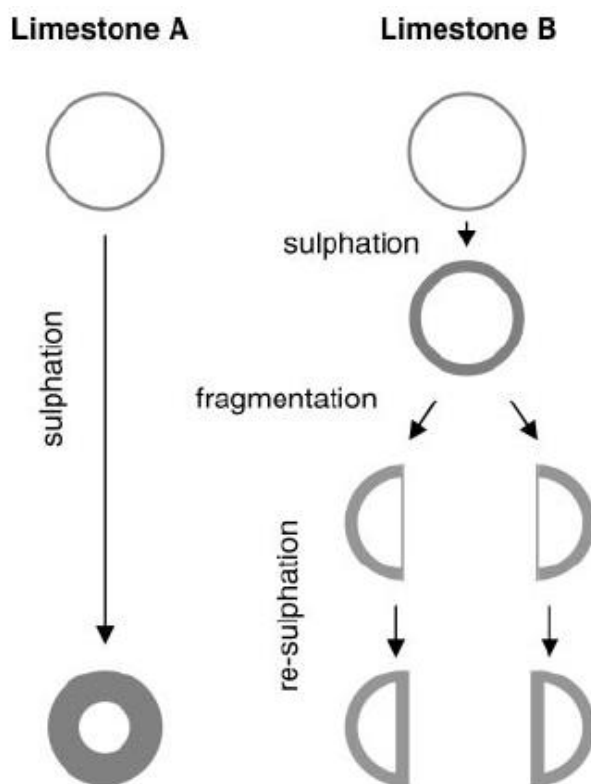


Figure 1.21. Phenomenological model of sorbent particle sulphation/breakage (Scala et al., 2008).

Salatino and co-workers (Scala et al., 2008) have shown that there is a relationship between attrition propensity of particles and their microstructure. Attrition and fragmentation during calcination and sulphation in a fluidized bed are more extensive for limestones with small and non polydispersed pores. This finding is probably due to a different thickness of the sulphated external layer. This layer is thicker for limestones with large and polydispersed pores and hence it has a stronger mechanical resistance, as schematized in Figure 1.21. The higher propensity toward attrition phenomena promotes a further exposition of the unreacted core of CaO increasing the sorbent capture capacity. This

underlines the important role of attrition phenomena to increase the capture capacity.

The sorbent attrition, widely studied for desulphurization processes in fluidized bed, is very important for the calcium-looping process (Fennell et al., 2007b; Jia et al., 2007; Koppatz et al., 2009; Charitos et al., 2010; González et al., 2010). Unfortunately, there is a lack of data on attrition of limestones during repeated cycles of calcination and carbonation (Blamey et al., 2010a).

2. Objectives and contribution to knowledge of the present work

The objective of the present study is to investigate specific features of the calcium looping concept which have been proven to have a key impact on the feasibility and competitiveness of this technology.

The research activity was focused on the characterization of attrition phenomena and of the CO₂ capture capacity of a set of natural sorbents. The calcium looping process has been simulated in a lab-scale bubbling fluidized bed with repeated calcination/carbonation cycles under realistic conditions. The following key aspects have been specifically scrutinized:

- the influence of multiple cycles of alternated calcination and carbonation on limestone performance, as related to process temperatures and reaction environments;
- the comparison of the performance of different natural limestones.
- the effect of the presence of SO₂, assessed by quantifying the influence of the parallel course of sulphation on the CO₂ sorption capacity and mechanical resistance to attrition of the sorbent.
- the potential of using alternative natural sorbents, like dolomite.

Moreover, the issue of the possible re-use of spent sorbent has been addressed. Feeding of make-up sorbent and disposal of the spent one represent critical aspects relevant to the economics and environmental compatibility of the calcium looping process. The potential of regenerating the sorption capacity of spent sorbents by water hydration has been assessed. The effectiveness of sorbent reactivation and the physico-chemical and microstructural changes

induced by hydration have been examined by means of a combination of different experimental techniques. Moreover, the reactivated sorbent performances, in terms of CO₂ capture capacity and attrition propensity, have been evaluated.

The research program has been developed in the Dipartimento di Ingegneria Chimica, dei Materiali e della Produzione Industriale of Università degli Studi di Napoli Federico II and of Istituto di Ricerche sulla Combustione of Consiglio Nazionale delle Ricerche in Naples. Most of the research activities have been carried out in the framework of the European Commission – Research Fund for Coal and Steel Contract no. RFCR-CT-2010-00013 (CAL-MOD) (<http://cal-mod.eu-projects.de>).

3. Experimental

3.1. Materials and experimental set-up

Six high-calcium limestones (calcite > 94% by weight) and one dolomite coming from different European countries (Italy, Germany, Greece and Poland) have been used in calcium looping tests. The chemical composition of the sorbents is given in Table 3.1.

Table 3.1. Chemical composition of sorbents (% by weight)

Sample	Origin	SiO ₂	Al ₂ O ₃	Fe ₂ O ₃	CaO	MgO	K ₂ O	Na ₂ O	SO ₃	TiO ₂	LOI	Sum
Massicci	Italy	1.11	0.37	0.14	54.53	0.44	0.06	0.02	0.00	0.02	43.13	99.82
Schwabian Alb	Germany	3.51	0.50	0.18	53.64	0.51	0.08	0.02	0.00	0.02	41.94	100.40
EnBW	Germany	0.30	0.13	0.08	56.01	0.26	0.00	0.02	0.00	0.01	43.50	100.31
Xirorema Sand	Greece	0.83	0.26	0.36	55.13	0.56	0.00	0.01	0.00	0.02	42.87	100.04
Tarnow Opolski	Poland	1.73	0.34	0.39	54.04	0.94	0.00	0.02	0.00	0.02	42.64	100.12
Czatkowice	Poland	3.91	0.39	0.31	52.88	0.99	0.00	0.02	0.00	0.03	41.43	99.96
Redziny (dolomite)	Poland	0.91	0.22	0.25	31.80	20.90	0.00	0.00	0.00	0.02	45.12	99.21

Experiments were carried out in a stainless steel (AISI 240) bubbling fluidized bed reactor, 40 mm ID operated at atmospheric pressure (Figure 3.1). The reactor consists of three sections: a) the preheater/premixer section of the fluidizing gas, 0.66 m high; b) the fluidization column, 0.95 m high; c) the brass two-exit head placed on top of the reactor with a hopper to feed the solids in the reactor and connected with the exhaust line.

The gas distributor is a perforated plate with 55 holes of 0.5 mm diameter in a triangular pitch. The reactor is electrically heated with two semi-cylindrical furnaces placed around the upper part of the preheater/premixer and the lower part of the fluidization column. A type-K thermocouple, located 40 mm above the gas distributor, allows measuring the reactor temperature. The thermocouple is connected with a PID temperature controller (Ascom SN) which regulates the electrical power supply for the furnaces. The two-exit head is used to convey flue gases through either of two cylindrical sintered brass filters, whose filtration efficiency is 1 for $> 10 \mu\text{m}$ -particles. Alternated use of the filters enables time-resolved capture of elutriated fines at the exhaust. Gases are supplied to the reactor by means of three mass flow meters/controllers (Bronkhorst EL-Flow). Downstream of the two-exit head, a fraction of the exhaust gas is continuously sampled to measure CO_2 and SO_2 concentrations with a NDIR analyser (ABB AO2020-uras 14) in order to monitor the progress of reactions. Concentration signals are logged on a PC at a sampling rate of 1 Hz.

3.2. Procedures

3.2.1. Procedure for the calcium looping tests

Five calcination/carbonation cycles were carried out in all the experiments (except for reactivation tests whose procedure is discussed in detail below, see § 3.7), using an initial amount of 20 g of fresh limestone, sieved in the range size 400-600 μm . Limestone was diluted in a bed of sand to avoid excessive temperature variations during calcination and carbonation reactions. The bed consisted of 150 g of silica sand in the size range 850-1000 μm and the fluidizing velocities were 0.7 and 0.6 m/s in the calcination and in the carbonation stages, respectively; these velocities ensure bubbling fluidization in

the bed. In particular, the difference in the size between sorbent material and sand permits an easy separation among them at the end of each stage. It should be underlined that the presence of sand may somewhat enhance sorbent attrition as discussed by Scala et al. (1997).

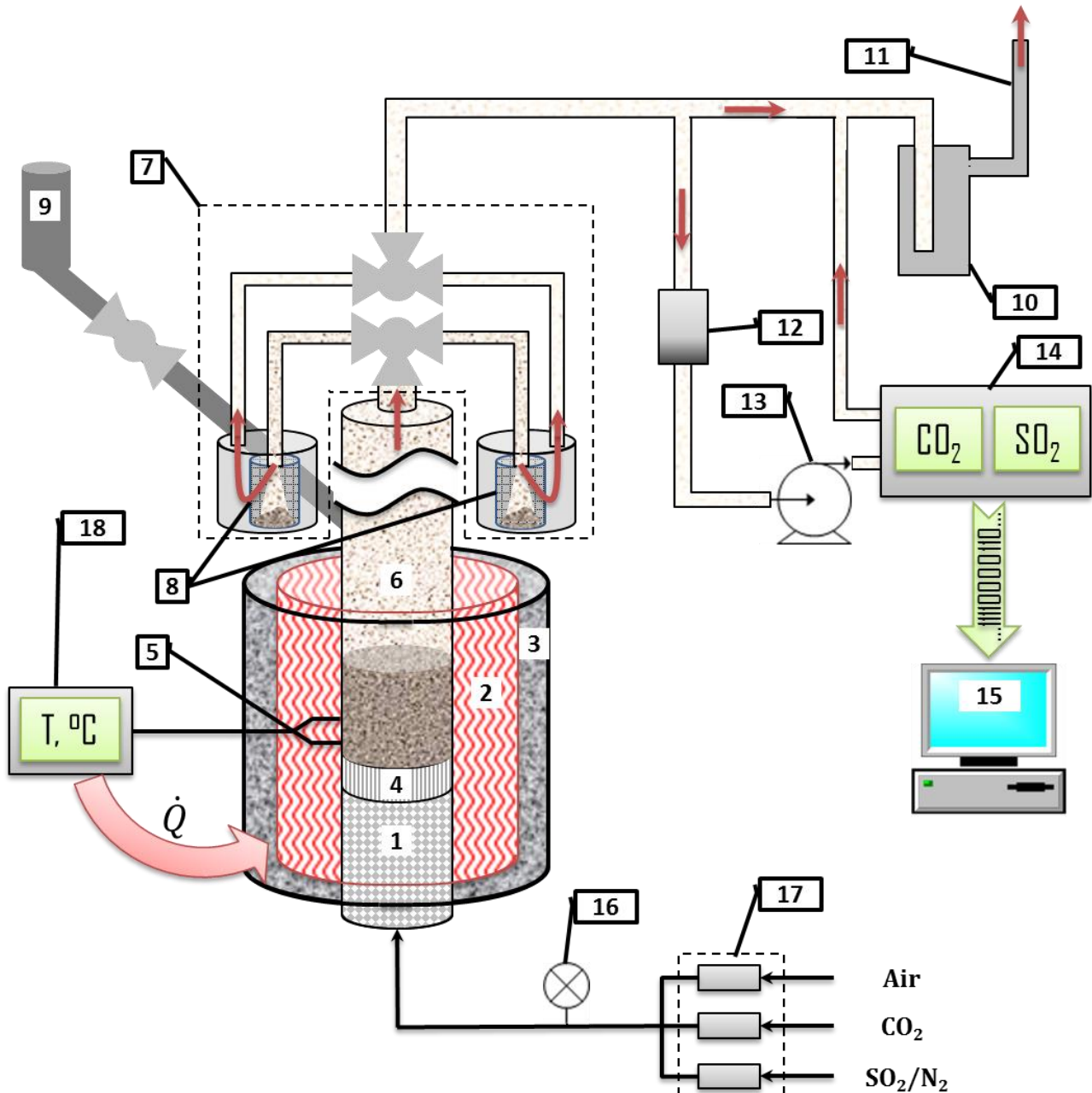


Figure 3.5. Experimental apparatus. (1) gas preheating/premixing section; (2) electrical furnaces; (3) ceramic insulator; (4) gas distributor; (5) thermocouple; (6) fluidization column; (7) two-exit head; (8) sintered brass filters; (9) hopper; (10) SO₂ scrubber; (11) stack; (12) cellulose filter; (13) membrane pump; (14) gas analyzer; (15) personal computer; (16) manometer; (17) mass flow meter/controller; (18) PID controller.

Before each test the reactor was charged with silica sand and heated up to the desired temperature using air as fluidizing gas. When the set temperature was reached, the bed was fluidized with the gas mixture chosen for the calcination and the limestone particles were injected in the reactor by means of the hopper placed on the two-exit head. After injection, the sorbent underwent rapid heating from ambient temperature to the reactor temperature, resulting in a thermal shock. The progress of calcination was followed during the run by measuring the CO₂ concentration at the exhaust by means of the analysers. The run ended when calcination was almost complete (specifically when the fast calcination stage was over):

$$10. C_{CO_2}^{in} \approx C_{CO_2}^{out}$$

At this point the bed was rapidly discharged and cooled down. The sand was separated from the limestone by sieving and re-injected in the fluidized bed reactor. The temperature of the bed was then set to the carbonation temperature. When the new temperature was reached the carbonation reaction was started by fluidizing the bed with the gas mixture containing CO₂, and injecting the calcined sorbent particles through the hopper. The progress of carbonation was followed during the run by measuring the CO₂ concentration at the exhaust by means of the analysers. Again, the run ended when carbonation was almost complete (when the fast carbonation stage was over), except for some tests (see § 3.4) where the effect of a prolonged sulphation during carbonation was investigated and in this case the run ended when sulphation was almost completed:

$$11. C_{SO_2}^{in} \approx C_{SO_2}^{out}$$

The bed was rapidly discharged and cooled down (in 100% CO₂ to avoid possible calcination). The procedure described before was then repeated in all the cycles. The same duration of the first calcination stage was used for the successive calcination stages, and the same criterion was applied for the duration of the carbonation stages.

It must be noted that, because of the above procedure, the limestone particles underwent a more severe thermal shock than that occurring in a real calcium looping process, where the particles are not cooled down to ambient temperature. This implies that sorbent attrition rates measured in this investigation are likely to somewhat overestimate particle attrition.

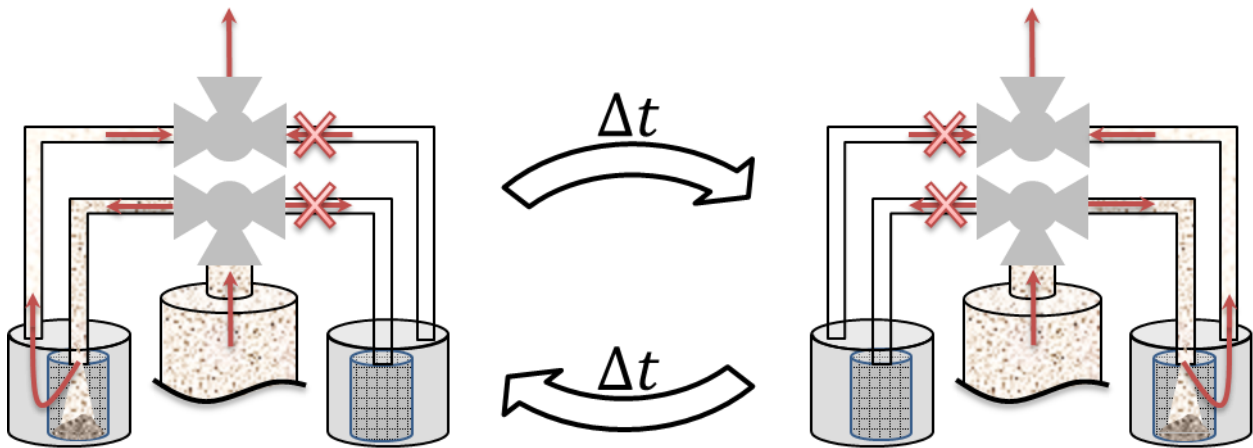


Figure 3.6. The alternated use of filters for the measurement of fines elutriation rate.

3.2.2. Evaluation of attrition/fragmentation phenomena

During the experiments the rates of fines generation were determined by measuring the amount of fines carried over by the fluidizing gas and elutriated from the reactor. The assumption underlying this procedure was that the residence time of elutriable fines in the reactor could be neglected and that the elutriation rate could be assumed to be equal to the rate of fines generation by

attrition at any time during limestone conversion. Elutriated fines were collected by means of the two-exit head previously described by letting the flue gas flow alternately through sequences of filters for definite time periods, as shown in the Figure 3.2. The difference between the weight of filters after and before operation, divided by the time interval during which the filter was in operation, gave the average fines elutriation rate $E(t)$ relative to that interval:

$$12. \quad E(t) = \frac{\Delta m}{\Delta t}$$

where Δm is the difference between the mass of the filter after and before its utilization and Δt is time interval of utilization.

The Particle Size Distribution (PSD) of the sorbent was determined by sieving the sorbent material after each calcination and carbonation stage. Before evaluating the PSD, the sorbent material was separated from sand by means of a 710 μm -sieve. Sieving was carried out gently to avoid further attrition of the particles, but rapidly, because of the propensity of the calcined sorbent to absorb moisture when in contact with ambient air. The sieve size ranges used for the PSD evaluation are the following:

Size range [μm]
0 - 53
53 - 112
112 - 180
180 - 212
212 - 250
250 - 300
300 - 350
350 - 400
400 - 600

Moreover, from the PSD analysis it was possible to determine the mean Sauter diameter d_s of the distribution:

$$13. \quad d_S = \frac{1}{\sum_i \frac{x_i}{d_i}}$$

where x_i is the mass fraction of particles having mean diameter d_i .

3.2.3. Evaluation of the CO₂ capture capacity

The CO₂ capture capacity of the sorbent during the carbonation stage was evaluated from the CO₂ concentration profile at the exhaust by means of the gas analyzer. The total amount of CO₂ uptaken during the experiment, divided by the initial amount of sorbent, gave the sorbent capture capacity. In particular, it is possible to calculate the CO₂ capture capacity (or calcium conversion to carbonate) expressed as moles of CO₂ captured per moles of Ca as:

$$14. \quad X_{Ca(CaCO_3)} = \frac{\int_0^t [F_{CO_2}^{in} - F_{CO_2}^{out}(t)] dt}{m_0} \times \frac{M_{CaCO_3}}{M_{CO_2} \times w_{CaCO_3}}$$

where $F_{CO_2}^{in}$ and $F_{CO_2}^{out}$ the inlet and outlet CO₂ mass flow rates respectively and m_0 the initial mass of sorbent, M_{CaCO_3} and M_{CO_2} are the molecular weights of CaCO₃ and CO₂ respectively and w_{CaCO_3} is the CaCO₃ mass fraction of the sorbent. In particular, the mass flow rates are calculated from the inlet and outlet CO₂ concentrations ($C_{CO_2}^{in}$ and $C_{CO_2}^{out}$) and the volumetric flow rates (Q^{in} and Q^{out}), so that the integral in the equation 14 becomes:

$$15. \quad \int_0^t [F_{CO_2}^{in} - F_{CO_2}^{out}(t)] dt = M_{CO_2} \int_0^t [Q^{in} C_{CO_2}^{in} - Q^{out} C_{CO_2}^{out}(t)] dt$$

Moreover, knowing $X_{Ca(CaCO_3)}$, it is possible to calculate the CO₂ capture capacity expressed as mass of CO₂ captured per mass of initial sorbent from $X_{Ca(CaCO_3)}$ and vice versa:

$$16. \quad CO_2 \text{ Capture Capacity} = X_{Ca(CaCO_3)} \times \frac{M_{CO_2} \times w_{CaCO_3}}{M_{CaCO_3}} = \frac{\int_0^t [F_{CO_2}^{in} - F_{CO_2}^{out}(t)] dt}{m_o}$$

From a practical point of view, the integral is discretized and substituted by the summation:

$$17. \quad \int_0^t [F_{CO_2}^{in} - F_{CO_2}^{out}(t)] dt \approx \sum_{i=0}^{t_f} [F_{CO_2}^{in} - F_{CO_2}^{out}(t_i)] \Delta t_i$$

where t_f is the total time of a single stage of calcination or carbonation, while Δt_i is the time interval which, as discussed previously, is equal to 1 s for all tests.

For all tests the inlet CO₂ concentration during the carbonation stage was set at 15-16%v/v, in order to simulate realistic values of CO₂ concentrations in flue gases.

3.2.4. Evaluation of the calcium conversion degree to sulphate

When SO₂ is present during the tests, the calcium conversion degree to sulphate was calculated from the SO₂ concentration profile at the exhaust

measured by the gas analyzer. Because the sulphation reaction is irreversible in the temperature range of interest for the calcium looping process, in each stage the conversion degree $X_{Ca(CaSO_4)}^N$ is evaluated by two terms: an integral, which takes into account the conversion degree for the current stage of calcination or carbonation plus a term which refers to the cumulative conversion degree reached in the previous stage:

$$18. X_{Ca(CaSO_4)}^N = X_{Ca(CaSO_4)}^{N-1} + \frac{\int_0^t [F_{SO_2}^{in} - F_{SO_2}^{out}(t)] dt}{m_o} \times \frac{M_{CaCO_3}}{M_{SO_2} \times w_{CaCO_3}}$$

where $F_{SO_2}^{in}$ and $F_{SO_2}^{out}$ are the inlet and outlet SO_2 mass flow rates, respectively, m_o is the initial mass of sorbent, M_{CaCO_3} and M_{SO_2} are the molecular weights of $CaCO_3$ and SO_2 respectively and w_{CaCO_3} is the $CaCO_3$ mass fraction of the sorbent, while $X_{Ca(CaSO_4)}^{N-1}$ is the conversion degree reached in the previous stage. As discussed about the evaluation of CO_2 capture capacity, also in this case the mass flow rates are calculated from the inlet and outlet SO_2 concentrations ($C_{SO_2}^{in}$ and $C_{SO_2}^{out}$) and the volumetric flow rates (Q^{in} and Q^{out}) and it is also possible to express the SO_2 capture capacity in terms of mass of SO_2 captured per mass of initial sorbent using $X_{Ca(CaSO_4)}^N$:

$$19. SO_2 \text{ Capture Capacity} = X_{Ca(CaSO_4)}^N \times \frac{w_{CaCO_3} \times M_{SO_2}}{M_{CaCO_3}}$$

Again the integral is approximated by summation:

$$20. \int_0^t [F_{SO_2}^{in} - F_{SO_2}^{out}(t)] dt \approx \sum_{i=0}^{t_f} [F_{SO_2}^{in} - F_{SO_2}^{out}(t_i)] \Delta t_i$$

Table 3.2. Operating conditions of the calcination/carbonation experiments on Massicci limestone for conditions 1, 2 and 3.

Calcination/ Carbonation	Condition 1	Condition 2	Condition 3
Duration [min]	15/15	35/15	20/15
Temperature [°C]	850/700	850/700	900/700
Inlet CO ₂ [%v/v]	0/16	20/16	44/16

3.3. Effect of temperature and CO₂ partial pressure during calcination

In order to evaluate the influence of the calcination temperature and of the reaction environment (in particular the effect of CO₂ concentration during the calcination stage) on sorbent attrition/fragmentation and CO₂ capture capacity, a preliminary experimental campaign on Massicci limestone was carried out, whose operative conditions are given in Table 3.2, Conditions 1, 2 and 3. The carbonation conditions are the same for the three investigated conditions, while during the calcination conditions there are significant differences. In particular, comparing condition 1 and 2 there is a different inlet CO₂ concentration during the calcination stage that involves a more extended calcination time, which passes from 15 min (Condition 1) up to 35 min (Condition 2), due to a slower reaction rate. This parameter, as it will be shown in the next section, has relevant consequences on the capture capacity and on the attrition phenomena.

The higher calcination temperature (900°C) for Condition 3 was used to study its effect on the sintering process of particles; in this regard the inlet CO₂ concentration during the calcination stage (44 %v/v) was chosen such as to

limit the effects due to a too rapid calcination reaction. In particular, the ratio between CO₂ partial pressure and the CO₂ equilibrium pressure (this latter calculated by equation 5) is the same (0.4 atm/atm) for Condition 2 and 3, which ensures the same driving force for the calcination reaction.

Table 3.3. Operating conditions of the calcination/carbonation experiments with SO₂ during carbonation using Massicci limestone.

Calcination/ Carbonation	0 ppm	110 ppm	1800 ppm	1800 ppm CS
Duration [min]	35/15	35/15	35/15	35/45
Temperature [°C]		850/700		
Inlet CO ₂ [%v/v]		20/16		
Inlet SO ₂ [ppmv]	0/0	0/110	0/1800	0/1800

3.4. Effect of SO₂ during carbonation

The presence of SO₂ in the flue gas (during the carbonation stage), at different concentrations, was investigated on the Massicci limestone, whose chemical composition is reported in Table 3.1. The conditions are indicated by the inlet SO₂ concentration used during the carbonation stage (0, 110, 1800 ppm and 1800 ppm CS) as reported in Table 3.3.

In particular, two SO₂ concentrations were tested (110 and 1800 ppmv), representing typical values of pre-desulphurized and uncontrolled flue gas, respectively. Results of these tests were compared with those obtained in a test without SO₂ (0 ppm) in the same conditions. In particular, the temperatures and the inlet CO₂ concentrations during calcination and carbonation stages were the

same for all conditions investigated (see Table 3.3). Some tests at 1800 ppmv SO₂ were also repeated using a longer duration of the carbonation stage (45 min instead of 15 min) in order to investigate the effect of a more extensive particle sulphation (as discussed in § 3.2.1). These tests (1800 ppm CS) were indicated with the acronym CS (complete sulphation).

Table 3.4. Operating conditions of the calcination/carbonation experiments on the six different limestones under oxy-firing conditions during calcination.

Calcination/ Carbonation	<i>Without SO₂</i> NO SO ₂	<i>With SO₂</i> intermediate conditions	<i>With SO₂</i> severe conditions
Duration [min]	20/15	20/15	20/15
Temperature [°C]	940/650	940/650	940/650
Inlet CO ₂ [%v/v]	70/15	70/15	70/15
Inlet SO ₂ [ppmv]	0/0	750/75	1500/1500

3.5. Oxy-firing conditions and the effect of SO₂ using limestone as sorbent

Attrition and capture capacity of the six different limestones (Table 3.1) were studied during calcium looping cycles under realistic conditions representative of a process with calcination in an oxy-firing environment. The operating conditions are given in the Table 3.4. In particular, it was found in preliminary tests that a bed temperature as high as 940°C was necessary to calcine the limestone at reasonable rates in an environment containing 70% v/v CO₂. (Figure 3.3).

The bed temperature and CO₂ inlet concentration during the carbonation stage were 650°C and 15%v/v respectively. The effect of SO₂ on calcium looping was studied under two conditions (Table 3.4): intermediate conditions (75ppm SO₂ during carbonation and 750ppm SO₂ during calcination) simulating CO₂ capture from already desulphurized flue gas and calcination in an oxy-fired calciner burning medium-sulphur coal; severe conditions (1500ppm SO₂ during both carbonation and calcination) simulating CO₂ capture from uncontrolled flue gas and calcination in an oxy-fired calciner burning high-sulphur coal. Calcium conversion to sulphate during calcination/carbonation was evaluated from SO₂ concentration profiles at the exhaust.

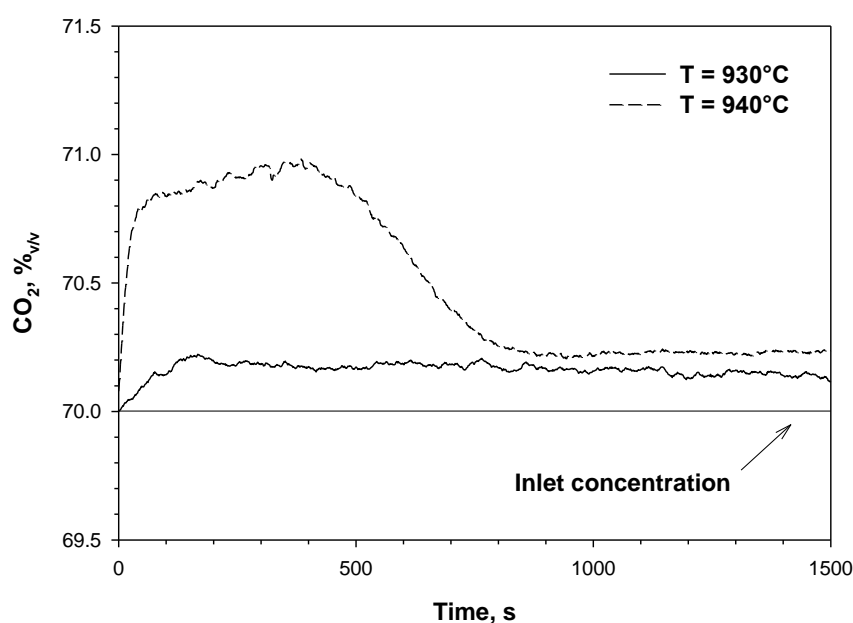


Figure 3.3. Measured CO₂ outlet concentration during preliminary calcination experiments at different bed temperatures and 70% CO₂ inlet concentration with Massicci limestone.

3.6. Oxy-firing conditions and the effect of SO₂ using dolomite as sorbent

The Polish dolomite Redziny was used in these tests, whose chemical composition is reported in Table 3.1. In particular, the dolomite was studied during calcium looping cycles under the same realistic conditions, representative of a process with calcination in an oxy-firing environment, used to study the six limestones (see Table 3.4) and under the same inlet SO₂ concentrations: intermediate conditions and severe conditions. Moreover, to make clear the results proposed in the next section, they were compared with those of the limestones (in terms of capture capacity and attrition propensity) studied in the same conditions. Also for the dolomite, the initial amount of tested sorbent was 20 g sieved in the size range 400-600 μm and capture capacity, PSD and fines generation were evaluated after each stage of calcination and carbonation.

3.7. Reactivation by hydration

The raw sorbent used in these tests was Massicci limestone. The test rig was a bubbling FB lab-scale reactor described above (see § 3.1). Details on the sorbent properties are reported in Table 3.1. The procedure for preparation of the spent sorbent is essentially the same used for the other tests, with the only exception related to the cycle number: indeed, in this case a cyclic sequence of five calcination/four carbonation stages was performed (instead of five complete cycles) retrieving, in this way, a high CaO-based sorbent after the 5th

calcination. The operating conditions are those reported in the Table 3.4 for the tests without SO₂ (NO SO₂), starting with 20 g of raw sorbent in the size range 400-600 μm.

Deactivated sorbent particles (spent sample, retrieved after the 5th calcination) were reactivated by liquid-phase hydration in a thermostatic bath kept at 25°C. Batches of spent sorbent (10 g) blended with a large excess of distilled water (water/solid weight ratio=25) were charged to sealed polyethylene bags and put in the thermostatic bath for curing times of 10, 30 and 60 min (samples water hydrated *WHY_10*, *WHY_30* and *WHY_60*, respectively). At the end of each hydration experiment, samples were retrieved from the bags, vacuum filtered, left overnight at 110°C and then stored in a desiccator. Sorbent particles were characterized by means of the following experimental techniques: *i*) non-isothermal thermogravimetric (TG) analysis, from room temperature to 1000°C at a heating rate of 10°C/min under inert atmosphere (Ar) in a Netzsch STA409CD apparatus; *ii*) scanning electron microscopy (SEM) analysis, performed at magnifications up to 3000× in a FEI Inspect apparatus; *iii*) porosimetric analysis, carried out in a Micromeritics AutoPore IV apparatus for pore sizes ranging from 3 nm to 100 μm. In particular, TG analysis allowed calculating the hydration degree X_H :

$$21. X_H = \frac{n_{CaO}^H}{n_{CaO}^S}$$

where n_{CaO}^H is the number of CaO moles reacted by hydration starting from the number of CaO moles present in the spent sorbent (n_{CaO}^S). Reactivated (*WHY*) material, sieved again in the particle size range 400-600 μm, was re-injected in the FB reactor for a new series of looping tests (now starting from the 5th

carbonation step and ending to the 8th carbonation step), under the same operating conditions held before reactivation. Care was taken to make sure that the mass of CaO (not carbonated) available for the 5th carbonation, i.e. the first stage after reactivation, was the same as that remaining in the sample after the 5th calcination, i.e. the last stage before reactivation. Again, the capture capacity, the PSD and the fines generation were evaluated after each stage of calcination and carbonation.

4. Results and discussion

4.1. Effect of temperature and CO₂ partial pressure during calcination

4.1.1. CO₂ Capture Capacity

Figure 4.1 reports the sorbent capture capacity (as $g_{CO_2}/\text{initial } g_{\text{Sorbent}}$) and the calcium conversion degree to carbonate as a function of the number of cycles, for the conditions 1, 2 and 3 (see Table 3.2 reported here for convenience).

Table 3.2. Operating conditions of the calcination/carbonation experiments using Massicci limestone for conditions 1, 2 and 3.

Calcination/ Carbonation	Condition 1	Condition 2	Condition 3
Duration [min]	15/15	35/15	20/15
Temperature [°C]	850/700	850/700	900/700
Inlet CO₂ [%v/v]	0/16	20/16	44/16

As expected, the capture capacity decreases with the number of cycles towards an asymptotic value. It is noted that the highest capture capacity was obtained in condition 1, i.e., when calcination was carried out in air. In condition 2 (calcination in 20% CO₂), a slightly lower capacity was found during all the cycles. A possible explanation for this result lies in the experimental evidence that the presence of CO₂ during calcination enhances sintering (Borgwardt, 1989). A higher calcination temperature (condition 3) determines a significant fall in the capture capacity at each cycle. This result underlines the important role of the thermal history of the sorbent particles. Again, this behaviour can be

explained by an enhancement of sintering at higher temperature. It is also interesting to note that in this case, the capture capacity reaches a plateau already after the fourth cycle.

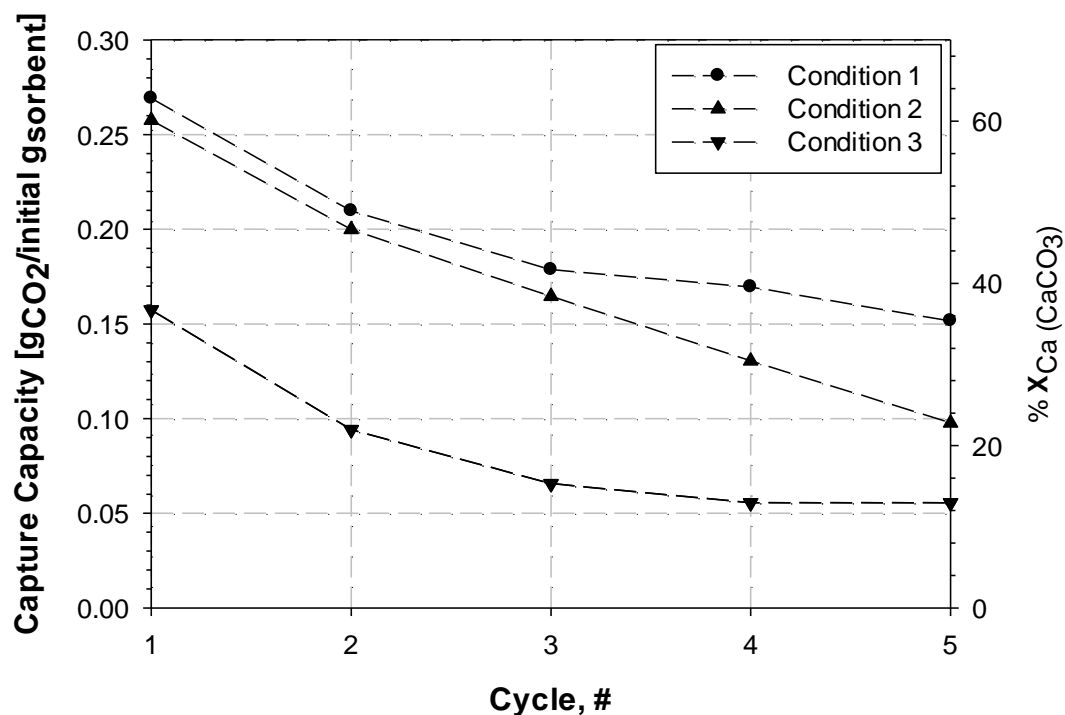


Figure 4.1. CO₂ capture capacity and calcium conversion degree to carbonate of the sorbent as a function of the number of cycles for the three experimental conditions investigated (Table 3.2).

4.1.2. Particle Size Distribution

Figure 4.2 reports the cumulative particle size distributions (PSDs) of the limestone during a test in condition 1. The PSD was evaluated after every calcination and carbonation stage, but in the figure, only the PSDs after the first calcination, the third carbonation, and the fifth carbonation were plotted, for clarity, since all the other PSDs were very similar to each other. It can be observed that the PSD does not change appreciably during the cycles, indicating a limited occurrence of particle fragmentation. Indeed, the qualitative features of

the PSD after the first calcination remain approximately constant after the following cycles.

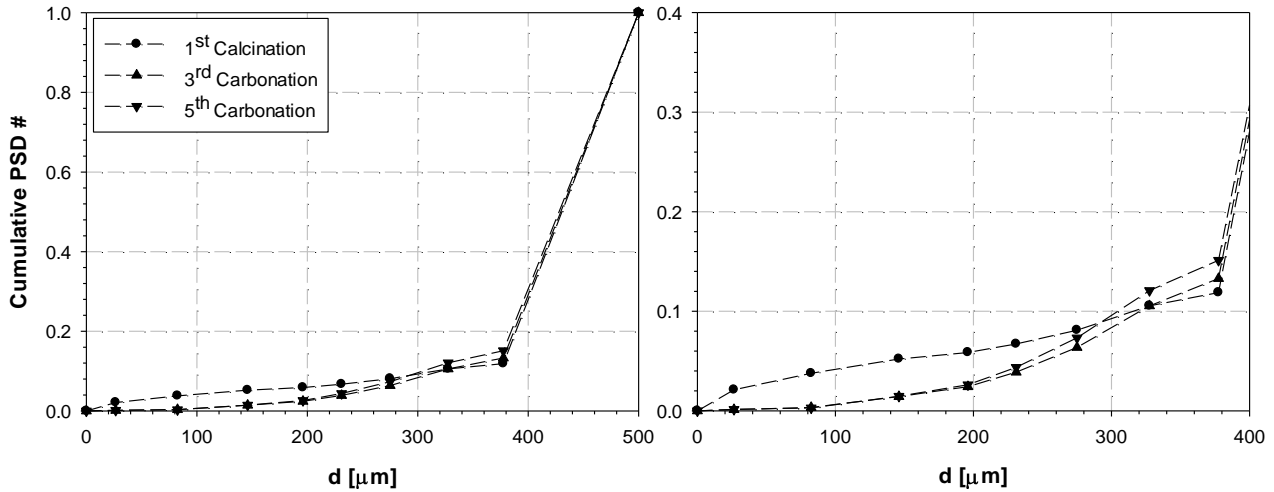


Figure 4.2. Cumulative particle size distribution (PSD) of the sorbent during a test in condition 1 (Table 3.2), after 1st calcination, 3rd carbonation, and 5th carbonation. Left: complete PSD. Right: PSD for particles with a size below 400 μm (fragments).

The only significant difference is the amount of fines ($<100 \mu\text{m}$) appearing after the first calcination that was not found in the following cycles, as shown by the changing of mean Sauter diameter d_S , which passes from 323 μm , after first calcination, to 438 μm , after the third carbonation. This result is more evident in the right-hand panel of Figure 4.2, where the PSD refers only to particles (fragments) with a size below 400 μm . By “fragments” are indicated all the collected particles whose size falls below the lower limit of the feed size interval: accordingly all the collected particles finer than 400 μm were classified as “fragments” in the context of the present study. Generation of fines is mostly due to particle rounding off of the fresh particles during the first calcination (Scala et al., 1997). When rounding off is complete, less fines are generated by attrition, as will be shown in the next paragraph. It should be noted that the fines generated during the first calcination stage were re-injected (after the PSD analysis) in the reactor together with the coarser particles in the next carbonation stage, where

they were eventually elutriated together with the newly attrited fines. In the whole discharge–injection procedure, the loss of fines was always very limited. Tests carried out under the other two experimental conditions showed the same qualitative trend.

Figure 4.3 compares the measured PSDs of the sorbent particles after the fifth carbonation in tests under the three operating conditions investigated. It can be observed that all the PSD curves have a similar shape, with only slight differences in the amount of produced fragments. Altogether, analysis of the PSD curves indicates that, irrespective of the operating conditions, only limited particle fragmentation occurs, in particular about 70% of the particles preserve their initial sizes (400–600 μm) and the PSD remains approximately constant over the cycles.

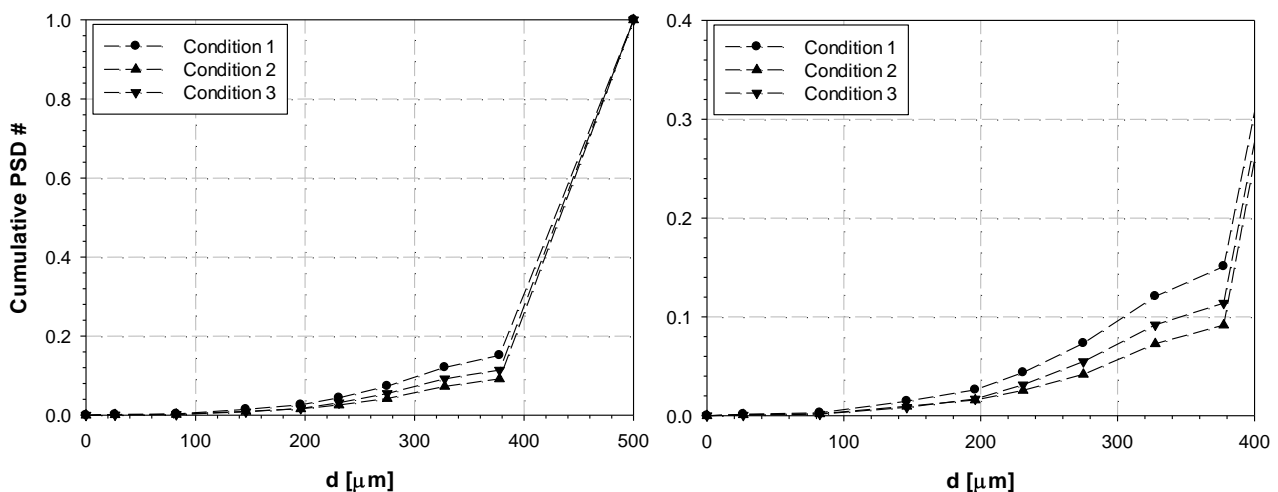


Figure 7.3. Cumulative particle size distribution (PSD) of the sorbent during tests in all experimental conditions investigated (Table 3.2), after 5th carbonation. Left: complete PSD. Right: PSD for particles with a size below 400 μm (fragments).

Comparing the PSDs among them (Figure 4.3), it is possible to note that condition 1 shows a higher fragmentation than the others ($d_5=432 \mu\text{m}$), while condition 2 exhibits a lower quantity of generated fragments ($d_5=456 \mu\text{m}$). A possible explanation of such differences can be imputed by a combination of CO_2 concentration and temperature during the calcination. In particular, under

condition 1 inside the particles elevated overpressures are generated, due to a fast release of CO_2 during calcination, which entail a higher primary fragmentation than the other conditions; this fast release is induced by the absence of CO_2 in the calcination environment and further consequences of this are shown in the section on the elutriation rate (see § 4.1.3). The lower fragmentation under condition 2 is likely due to the presence of CO_2 (20% v/v), which determines a slower CO_2 release and a more pronounced sintering process (as disclosed by data on CO_2 capture capacity in § 4.1.1), which in turn increases the particle hardness. On the contrary, a faster CO_2 release and a more elevated thermal shock after the particle injection into the bed, due to the increase of calcination temperature (condition 3), promote a more elevated primary fragmentation than in condition 2.

4.1.3. Elutriation Rate

Figure 4.4 reports the fines elutriation rate E (as mass of elutriated material per minute) as a function of time, measured in a test carried out in condition 1. Similar results were obtained in the other two conditions. As a general trend, it is noted that the fines elutriation rate decreases with the number of cycles. This suggests that hardening of the particle surface takes place over the cycles, which is consistent with the progressive sintering of the sorbent. In each cycle, the elutriation rate shows a typical trend with a peak of fines generation at the beginning. This peak is caused by a combination of the following effects: rounding off of the rough particles (Scala et al., 1997), thermal shock after injection in the hot bed, and elutriation of re-injected fines (if any). During calcination, a further process is the rapid release of CO_2 that causes overpressures inside the particles (see § 4.1.2) and may change the mechanical properties of the solid. Figure 4.4 shows a remarkable feature: during the first

calcination, the elutriation rate shows a slightly different trend with a peak shifted to about 2 min after the beginning of the test. This behaviour was not observed in tests carried out under conditions 2 and 3, where CO₂ was present in the inlet gas stream and calcination was slower (Table 3.2). This finding suggests that the peak might be related to the large rate of CO₂ release during calcination in condition 1.

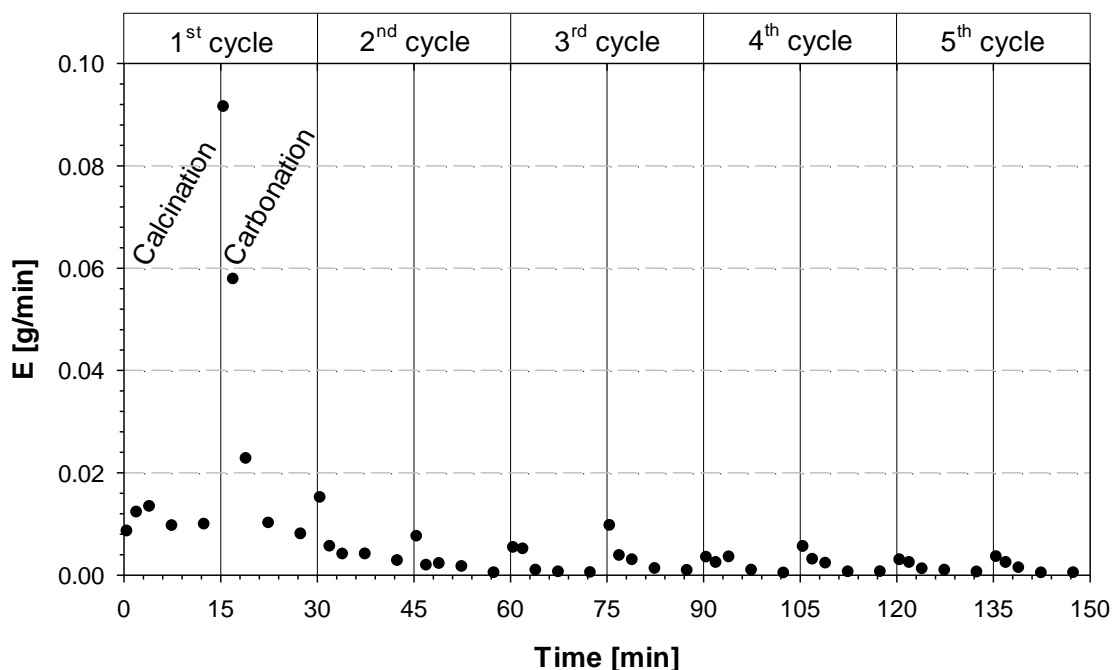


Figure 4.8. Sorbent elutriation rate as a function of time during alternated calcinations and carbonations for a test in condition 1 (Table 3.2).

Figure 4.5 reports the measured fines elutriation rate and CO₂ concentration at the exhaust during the first calcination stage in condition 1 (where the gas sampling line delay time of 13 s was taken into account). The figure clearly shows that the peak of the elutriation rate occurs approximately at the same time as the CO₂ concentration peak. Figure 4.6 reports the total amount of fines, as % mass of elutriated fines per mass of initial sorbent, collected during each calcination and carbonation stage as a function of the number of cycles. In all conditions, the amount of fines decreases with the cycle number. When considering that the calcination stages have a different duration under the

different experimental conditions (Table 3.2), the average fines elutriation rate is approximately the same during the calcination and the carbonation stages.

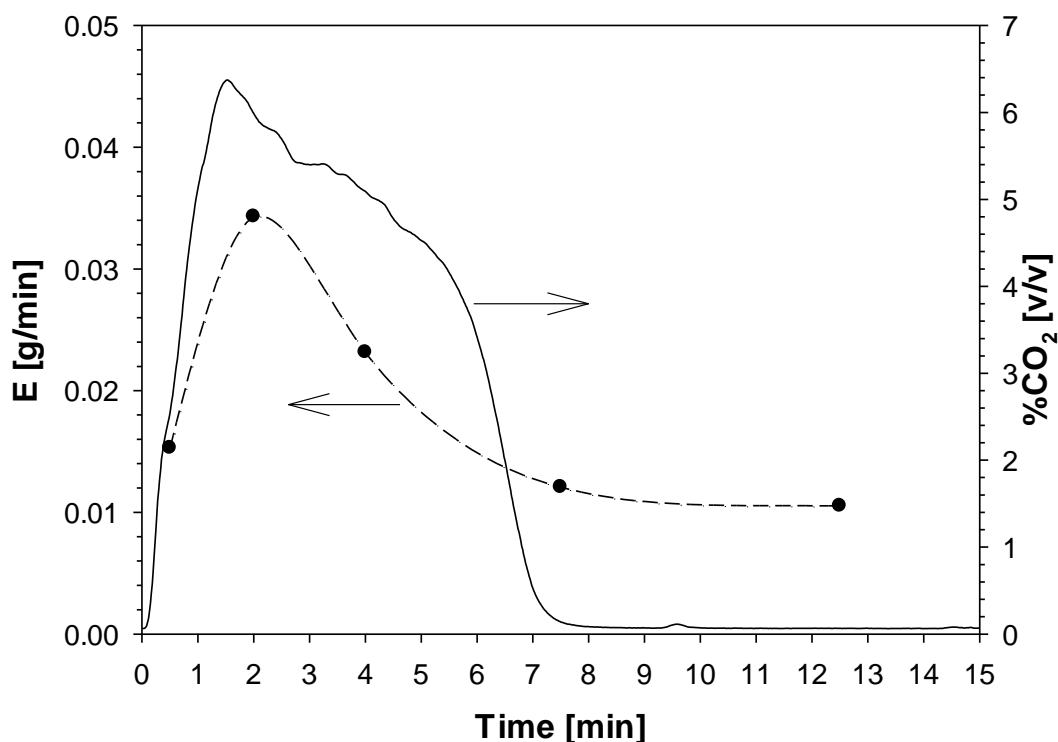


Figure 4.9. Sorbent elutriation rate and measured CO₂ outlet concentration as a function of time during the 1st calcination stage for a test in condition 1 (Table 3.2).

The largest amount of fines was obtained in the tests carried out in condition 1 (Figure 4.6-top). Fines generation was much smaller under condition 2 (Figure 4.6-center), where the only difference was the presence of 20% CO₂ in the fluidizing gas during calcination. This behaviour is most likely due to the absence of CO₂ during calcination in condition 1, which determines on the one hand a fast release of CO₂ and a consequent higher overpressure in the particles, and on the other hand a less pronounced sintering. When the calcination temperature is increased to 900 °C (condition 3, Figure 4.6-bottom), a larger amount of fines was collected when compared with results obtained under condition 2. Again, this behaviour should be related to the faster release of CO₂ due to the higher temperature, and possibly to a more pronounced

thermal shock. On the basis of the above results, an average limestone loss rate by elutriation from a dual fluidized bed system can be estimated in the range 0.05–0.2%/h for Massicci limestone. The calculation was made from results reported in Figure 4.6, excluding data relative to the first two cycles for each condition.

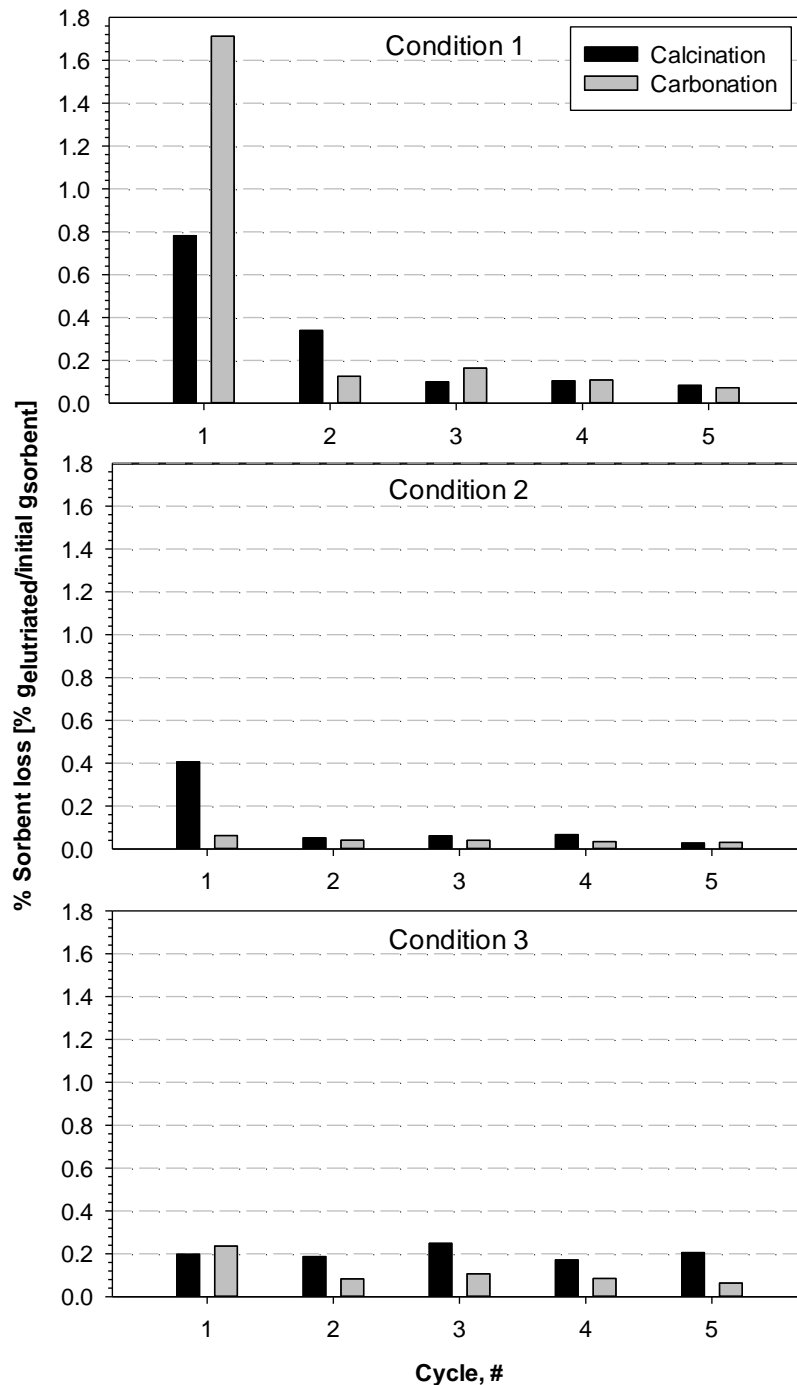


Figure 4.10. Total amount of elutriated fines as a function of number of cycles in each calcination and carbonation stage for the condition 1 (top), condition 2 (center) and condition 3 (bottom) (Table 3.2).

4.2. Effect of SO₂ during carbonation

4.2.1. Calcium conversion to sulphate

Figure 4.7 reports the SO₂ capture capacity of the sorbent and the calcium conversion degree to sulphate as a function of the cycle number, for tests carried out in conditions given in the Table 3.3 (reported here for convenience).

Table 3.3. Operating conditions of the calcination/carbonation experiments with SO₂ during carbonation on Massicci limestone.

Calcination/ Carbonation	0 ppm	110 ppm	1800 ppm	1800 ppm CS
Duration [min]	35/15	35/15	35/15	35/45
Temperature [°C]		850/700		
Inlet CO ₂ [%v/v]		20/16		
Inlet SO ₂ [ppmv]	0/0	0/110	0/1800	0/1800

At the end of the 5th carbonation stage the cumulative calcium conversion to sulphate (CaSO₄) was about 1.5%, 27% and 14% for conditions investigated, respectively. The significant difference between the measured conversion at 110 ppm SO₂ and those found at 1800 ppm SO₂ is clearly a consequence of the SO₂ concentration level, differing by more than one order of magnitude. Finding a mechanistic explanation for the measured difference between conversion of calcium to sulphate in conditions 1800ppm and 1800ppm CS is less straightforward. Tests in conditions 1800ppm were performed using a duration of the carbonation stage of 15 min. This time was long enough to obtain almost full carbonation of the sorbent, while complete sulphation was only approached. On the other hand, at the end of the carbonation stage during tests in condition

1800ppm CS the duration (45 min instead of 15 min) was long enough to bring both carbonation and sulphation to near-completion. This was clearly visible in the SO₂ concentration profiles measured at the exhaust (not reported here), and was reflected by the difference between the sorbent sulphation degrees after the first cycle, as shown in Figure 4.7 (5.8% and 6.2% in conditions 1800ppm and 1800ppm CS, respectively).

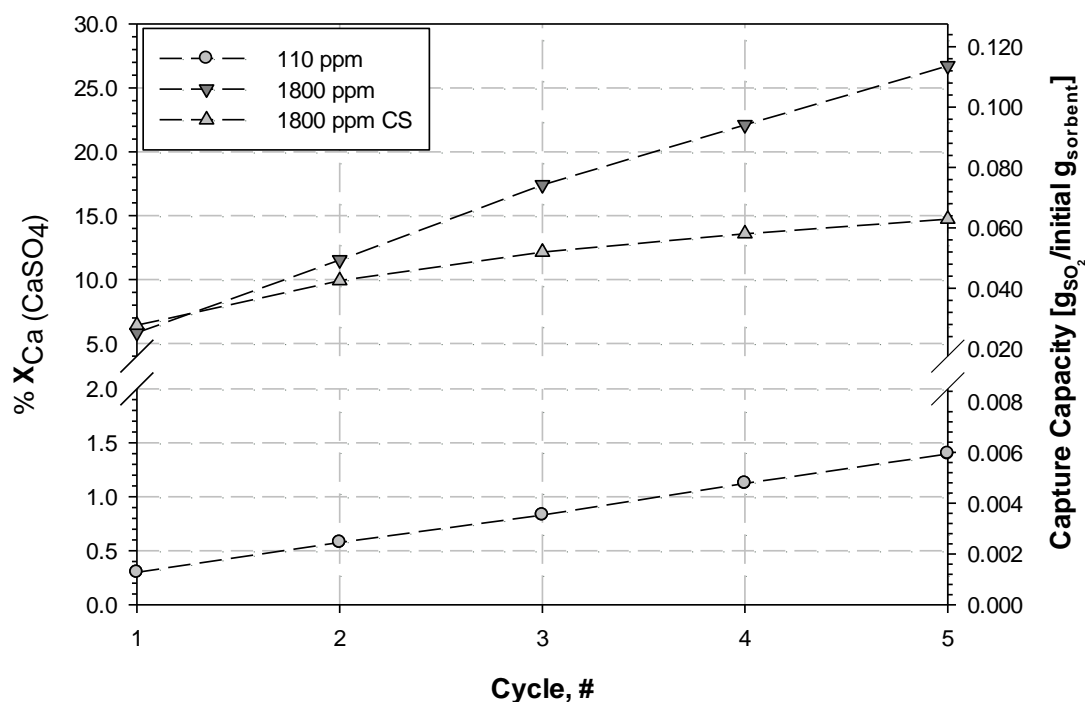


Figure 4.11. SO₂ capture capacity and calcium conversion degree to sulphate of the sorbent as a function of the number of cycles, at different inlet SO₂ concentrations during the carbonation stage (Table 3.3).

From the second cycle on, calcium conversion to sulphate in condition 1800ppm was always larger than that measured in condition 1800ppm CS. It may be speculated that the more prolonged sorbent sulphation in condition 1800ppm CS is responsible for a stronger sorbent deactivation due to pore plugging and “chemical sintering” (to an extent that is only partly reflected by the marginal increase of the Ca sulphation degree) which is retained in the

subsequent cycles. The formation of a more compact CaSO_4 layer would hinder effective SO_2 diffusion inside the sorbent particle, even after the subsequent calcination stages. This mechanistic explanation is consistent with experimental findings of Sun et al. (2007b). A further explanation could be related to fragmentation phenomena, in fact, as reported in the § 4.2.3, condition 1800 ppm shows a more pronounced fragmentation than condition 1800 ppm CS, yielding in this way additional available surface for sulphation.

4.2.2. CO_2 capture capacity

Figure 4.8 reports the sorbent CO_2 capture capacity (as $\text{g}_{\text{CO}_2}/\text{initial g}_{\text{Sorbent}}$) and the calcium conversion degree to carbonate as a function of the number of cycles, for the four conditions investigated reported in the Table 3.3. The capture capacity decreased with the number of cycles (from 0.18–0.26 to 0.036– 0.098 $\text{g}_{\text{CO}_2}/\text{initial g}_{\text{Sorbent}}$). It is noted that the largest capture capacity was obtained in condition 0ppm, i.e. when carbonation was carried out without SO_2 . The presence of SO_2 in the gas (conditions 110ppm, 1800ppm and 1800ppm CS) determined a significant fall in the capture capacity at each cycle. The higher the SO_2 concentration, the lower was the carbonation capacity (0.098, 0.044 and 0.036 $\text{g}_{\text{CO}_2}/\text{initial g}_{\text{Sorbent}}$ after the 5th cycle for SO_2 concentration equal to 0, 110 and 1800 ppm, respectively). This behaviour can be explained by the formation of a calcium sulphate shell around the particles that hinders the diffusion of CO_2 in the pores of the sorbent. However, the effect of the SO_2 concentration level was not as large as expected. This seems to indicate that, in these conditions, even a small quantity of SO_2 is sufficient to significantly hinder the CO_2 capture capacity of the sorbent, since no remarkable changes occurred when increasing the SO_2 concentration from 110 to 1800 ppm. Also the duration of sulphation did not influence the CO_2 capture capacity to any significant extent: after the first

cycle results of tests in conditions 1800ppm and 1800ppm CS are nearly the same.

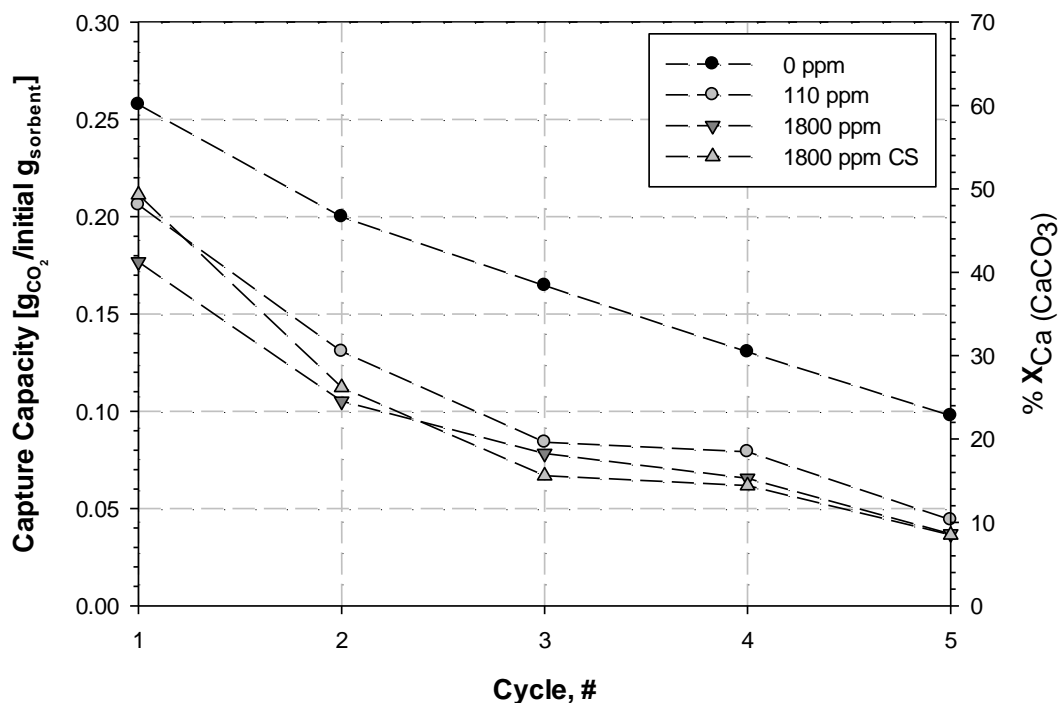


Figure 4.12. CO₂ capture capacity and calcium conversion degree to carbonate of the sorbent as a function of the number of cycles. In the legend: SO₂ concentration during carbonation stage (Table 3.3).

4.2.3. Particle size distribution

Figure 4.9 reports the cumulative particle size distributions (PSDs) of the limestone after the tests in the four conditions given in the Table 3.3. The PSD was evaluated after every calcination and carbonation stage, but in the figure only the PSDs after the 5th carbonation were plotted, for clarity, since all the other PSDs were very similar to each other. It can be noted that the PSD does not change appreciably as a result of the cycles, indicating a limited occurrence of particle fragmentation. Tests carried out under the four experimental conditions investigated showed the same trend, with only slight differences in the amount

of produced fragments. This indicates that the presence of SO_2 has only a minor influence on particle fragmentation. Notably, tests carried out in condition 1800ppm showed a slightly larger amount of fragments, as shown by the value of $d_5=394 \mu\text{m}$, which is lower than the others, whose values are included in the range 456-463 μm . This seems to indicate a lower resistance of particles that have undergone sulphation at high SO_2 concentrations. However, when sulphation was carried out for a longer time (condition 1800ppm CS), particle fragmentation was less pronounced. Probably, for the same sulphation time (conditions 110 ppm and 1800 ppm), low SO_2 concentrations produce a thin external sulphate layer which is not able to change significantly the fragmentation propensity. On the other hand, for the same SO_2 concentration (conditions 1800 ppm and 1800 ppm CS), prolonged sulphations generates a more compact and harder sulphate layer.

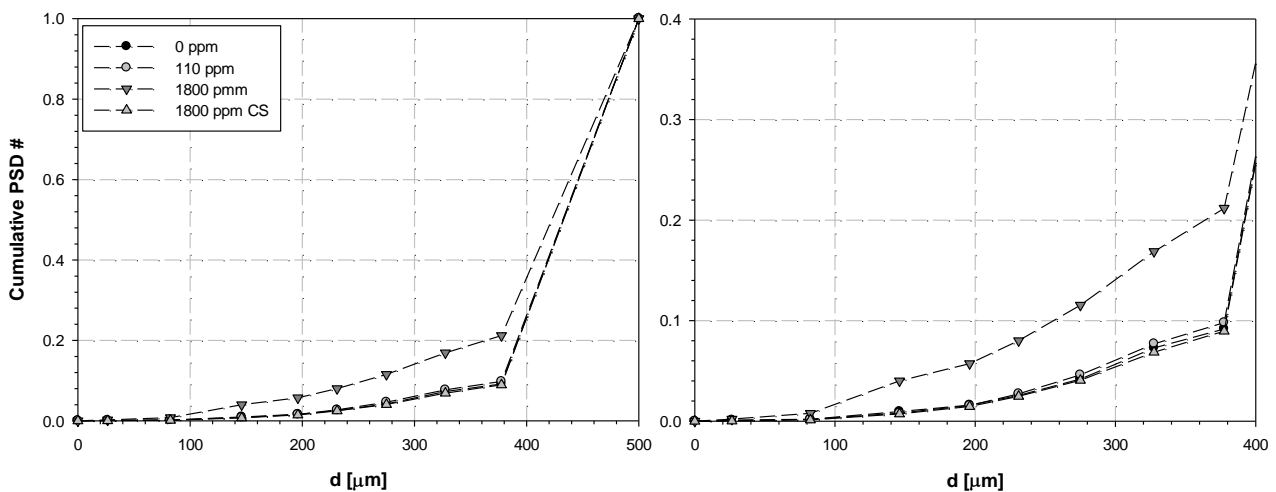


Figure 4.13. Cumulative particle size distribution of the sorbent during tests in all experimental conditions investigated, after 5th carbonation. In the legend: SO_2 concentration during carbonation stage (Table 3.3).

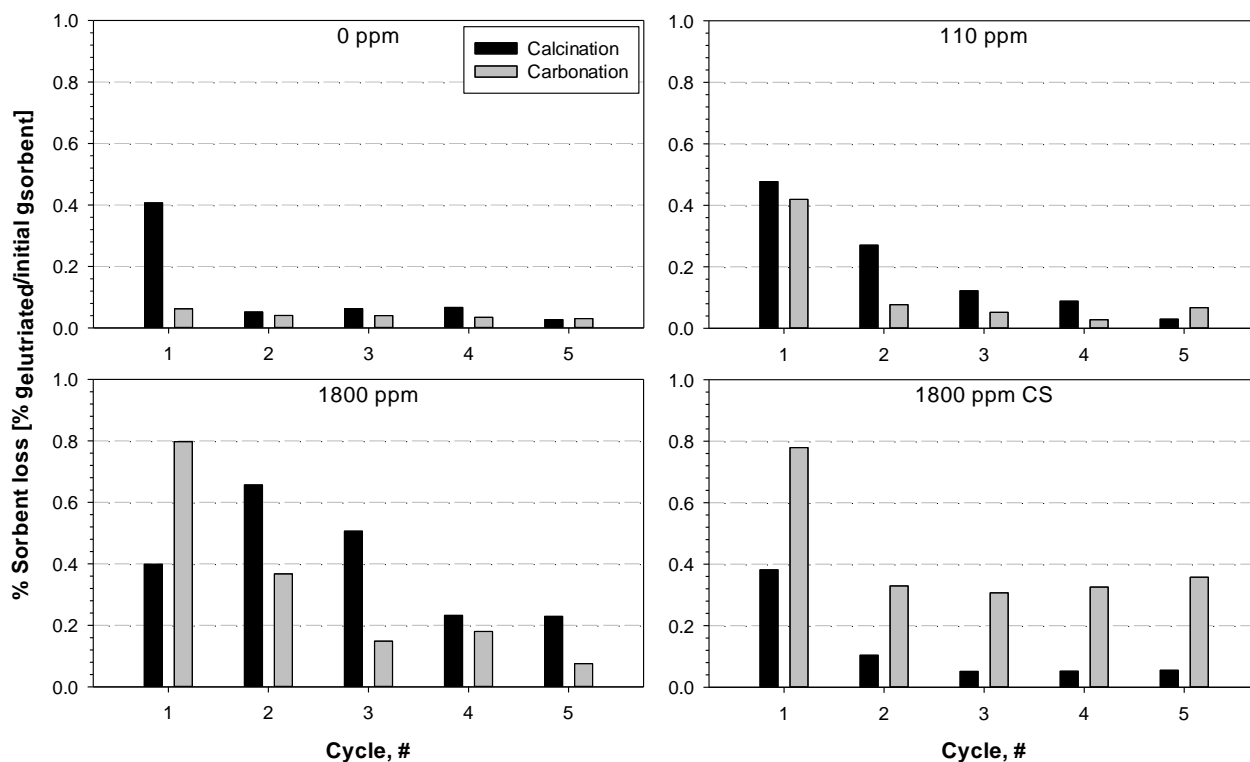


Figure 4.14. Fractional (percent) sorbent loss in elutriated fines as a function of the number of cycles in each calcination and carbonation stage for the four conditions investigated (Table 3.3).

4.2.4. Elutriation rate

Figure 4.10 reports the fractional sorbent loss in fines (expressed as per cent mass of elutriated fines referred to the mass of sorbent initially loaded in the reactor) collected during each calcination and carbonation stage as a function of the number of cycles for the four conditions investigated (Table 3.3). The amount of fines decreased with the cycle number under all the conditions tested. This suggests that hardening of the particle surface takes place over the cycles, which is consistent with the progressive sintering of the sorbent. Once the extent of elutriation is related to the different duration of the calcination and carbonation stages in the tests (Table 3.3), the average fines elutriation rate turns out to be nearly the same during calcination and carbonation. Comparison of the results under the four operating conditions indicates that the elutriation

rates are similar, slightly larger when SO_2 is present in the gas during carbonation. Similarly to the CO_2 capture capacity, experimental results indicate that even a small quantity of SO_2 induces an appreciable change of the attrition behaviour of the sorbent. This result is probably caused by the lower hardness of calcium sulphate at the particle surface as compared with calcium carbonate or by negative synergistic effects between the two calcium compounds with respect to resistance to wear. Again, a moderately larger attrition rate was recorded in condition 1800ppm. It is likely that in this condition a surface layer containing a large amount of sulphate but in a poorly structured and less compact form is generated.

4.3. Oxy-firing conditions and the effect of SO_2

4.3.1. CO_2 capture capacity

Figure 4.11 reports the sorbent CO_2 capture capacity as a function of the number of cycles for the six limestones tested under the operating conditions given in Table 3.4 (reported here for convenience).

Table 3.4. Operating conditions of the calcination/carbonation experiments with the six different limestones under oxy-firing conditions during calcination.

Calcination/ Carbonation	<i>Without SO_2</i> NO SO_2	<i>With SO_2</i> intermediate conditions	<i>With SO_2</i> severe conditions
Duration [min]	20/15	20/15	20/15
Temperature [°C]	940/650	940/650	940/650
Inlet CO_2 [%v/v]	70/15	70/15	70/15
Inlet SO_2 [ppmv]	0/0	750/75	1500/1500

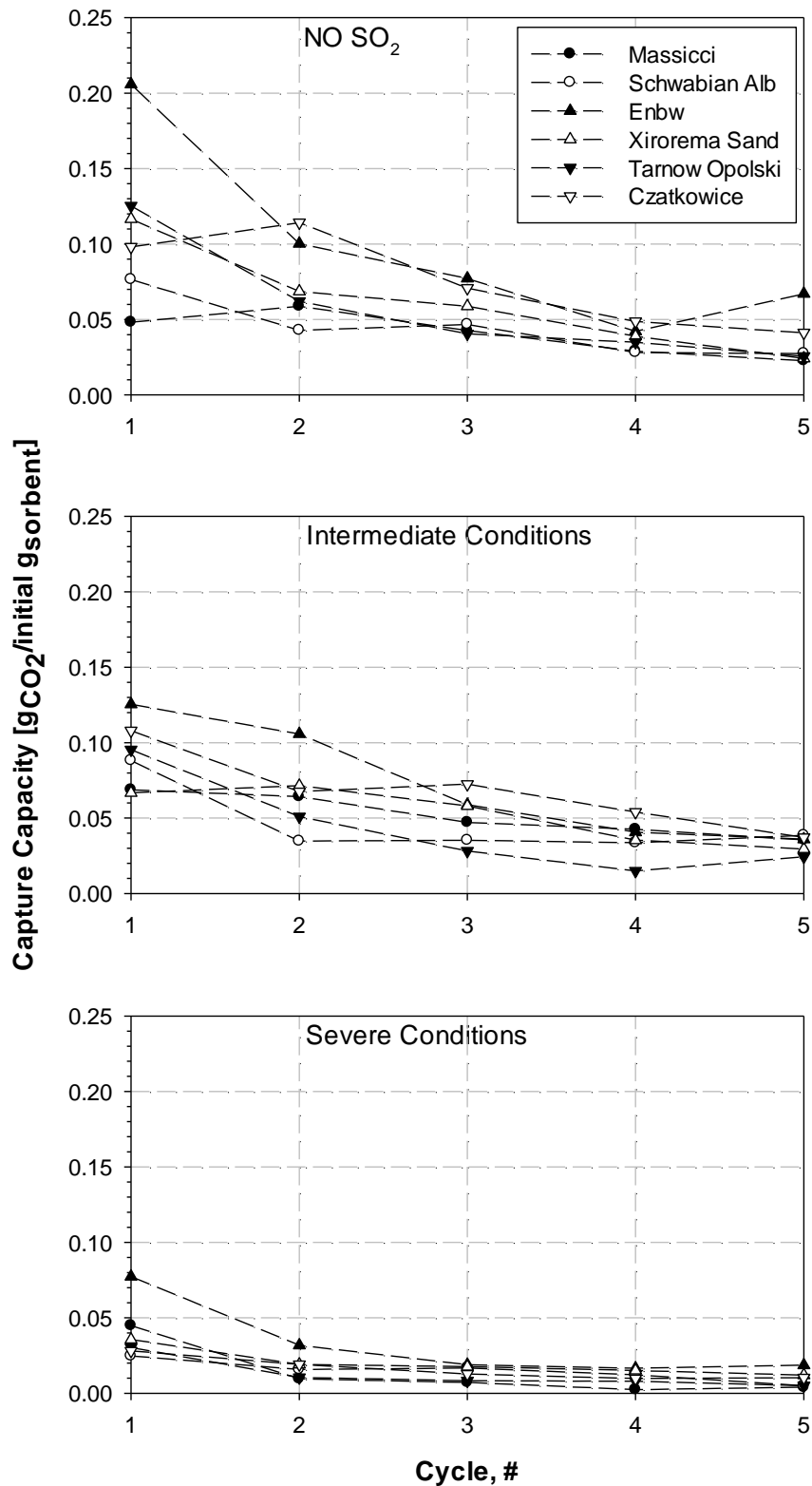


Figure 4.15. CO₂ capture capacity of the six limestones as a function of the number of cycles for experiments carried out without SO₂ (left) and with SO₂ under intermediate conditions (center) and severe conditions (right) (Table 3.4).

Results of tests with or without SO_2 are compared. As expected, the capture capacity decreases with the number of cycles for all the limestones reaching an asymptotic value already after the fourth cycle. This residual capture capacity ($0.02\text{-}0.07 \text{ g}_{\text{CO}_2}/\text{initial g}_{\text{Sorbent}}$ in the tests without SO_2 , Figure 4.11–top) is much lower than that typically found under milder conditions (of the order of $0.1\text{-}0.2 \text{ g}_{\text{CO}_2}/\text{initial g}_{\text{Sorbent}}$ as reported by Blamey et al., 2010a). The explanation for this result lies in the combination of high temperature and high concentration of CO_2 during calcination that significantly enhances sintering (Borgwardt, 1989). The relative ranking of the six limestones, from the best to the worst capture capacity, is: EnBW, Czatkowice, Xirorema Sand, Tarnow Opolski, Schwabian Alb and Massicci.

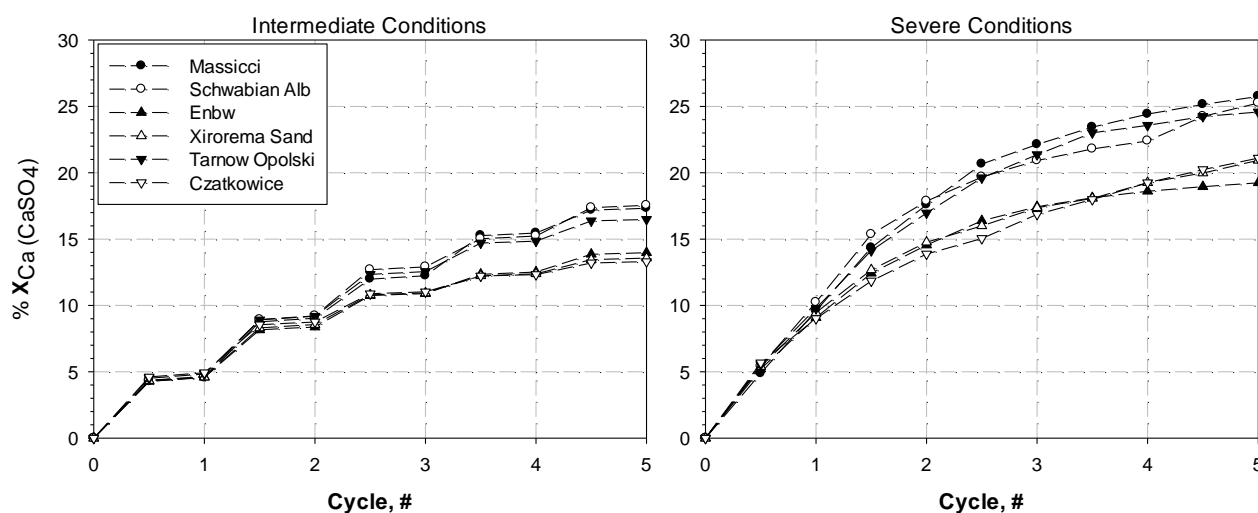


Figure 4.16. Cumulative calcium conversion degree to sulphate of the six limestones as a function of the number of cycles under intermediate conditions (left) and severe conditions (right). Each data point represents conversion after half cycle (Table 3.4).

When a high SO_2 concentration is present in the gas flow a further decrease of the CO_2 capture capacity (of the order of 3-6 times) is found for all the limestones (Figure 4.11–bottom). The residual capture capacity was $0.004\text{-}0.02 \text{ g}_{\text{CO}_2}/\text{initial g}_{\text{Sorbent}}$ in this case. This behaviour can be explained by the progressive formation of a calcium sulphate shell around the particles that hinders intraparticle diffusion of CO_2 in the pores of the sorbent (Sun et al., 2007). On the other hand, when a low SO_2 concentration was used in the tests

(Figure 4.11–center) results were closer to those obtained in tests without SO₂. This is somewhat different from results reported before (see § 4.2.2) under milder temperature conditions for Massicci limestone. It could be speculated that at very high temperatures (during calcination) sintering dominates the deactivation behaviour of the limestone, unless very high SO₂ concentrations are used. Morphological analysis of the used limestone particles seems to confirm this hypothesis (Itskos et al., 2012). It is interesting to note, however, that the relative ranking of the six limestones towards CO₂ capture is not significantly altered by the presence of sulphur dioxide.

Figure 4.12 reports the calcium conversion degree to sulphate during the tests, as calculated from the SO₂ concentration profiles at the exhaust (note that since SO₂ is present both during calcination and carbonation, each data point represents conversion to sulphate after half cycle). The extent of calcium conversion to sulphate in each stage clearly depends on the relevant SO₂ concentration in the gas phase. It appears that at both SO₂ levels investigated the three best performing limestones with regard to CO₂ capture capacity (EnBW, Xirorema Sand and Czatkowice) are those sulphating to a lower extent.

4.3.2. Particle size distribution

Figure 4.13 compares the measured cumulative particle size distributions (PSDs) of the six limestones after the fifth carbonation stage in tests carried out under the operating conditions reported in Table 3.4, with or without SO₂ in the fluidizing gas. The PSD was evaluated after every calcination and carbonation stage for each limestone. However, only the PSDs recorded after the fifth carbonation were plotted in the figures, for clarity, since all the other PSDs were very similar to one another.

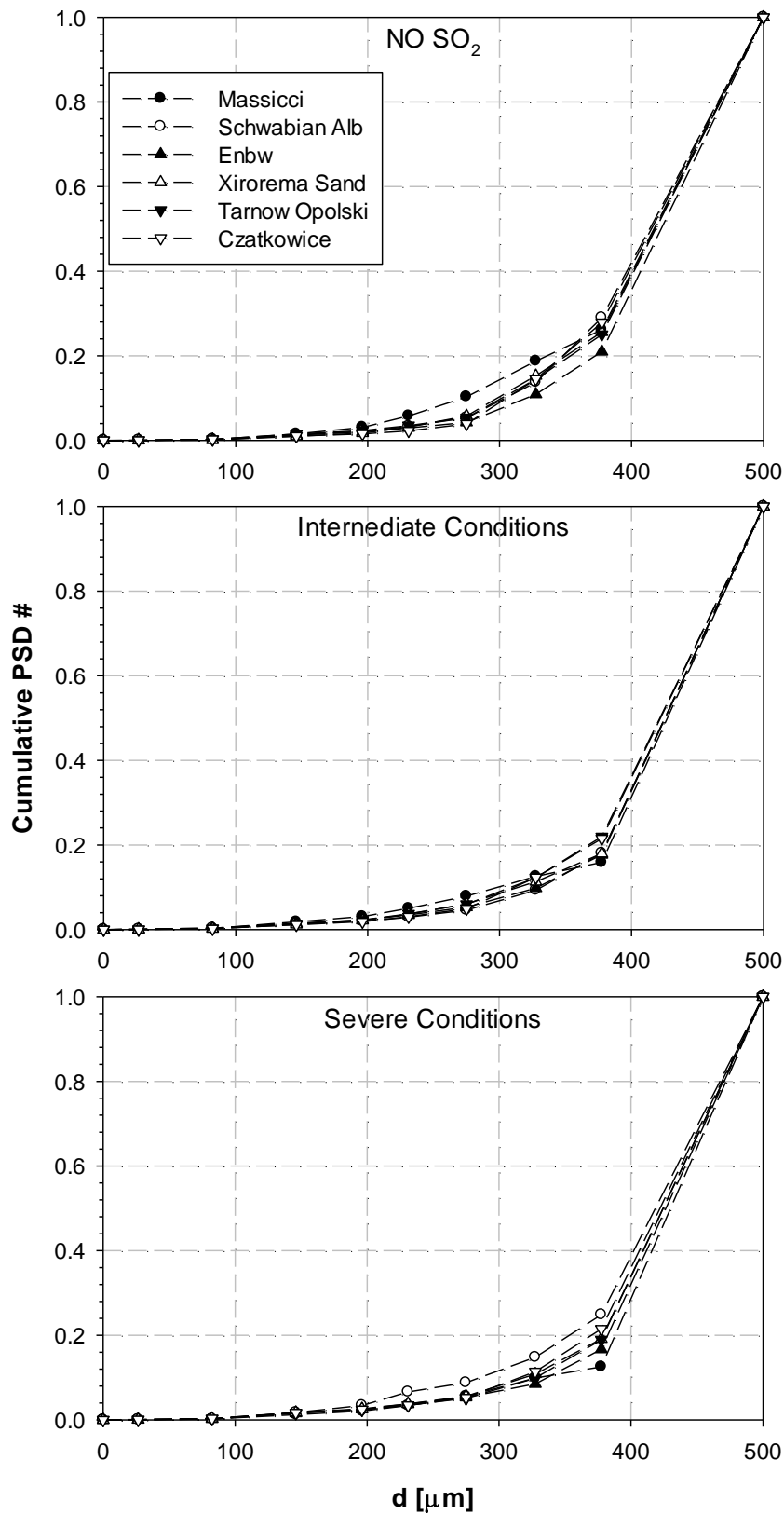


Figure 4.17. Cumulative particle undersize distribution of the six limestones after the 5th carbonation stage for experiments carried out without SO_2 (top) and with SO_2 under intermediate conditions (center) and severe conditions (bottom) (Table 3.4).

It can be observed that all the PSD curves have a similar shape, with only slight differences in the amount of produced fragments among the six limestones. The presence of SO₂ appears to slightly reduce the extent of fragmentation for all the limestones. Altogether, analysis of the PSD curves indicates that particle fragmentation is limited, as witnessed by the small amount of retrieved particles with size < 400 μm. Figure 4.13 shows that the fractional amount of fragments is within the range 20-30% of the initial sample mass for tests without SO₂, decreasing to ~15-20% for tests with SO₂. As regards the fragmentation propensity, the relative ranking of the six limestones (in terms of increasing fragmentation) is: EnBW, Massicci, Tarnow Opolski, Xirorema Sand, Czatkowice and Schwabian Alb.

4.3.3. Elutriation rate

Figures 4.14-4.16 reports the cumulative mass of elutriated fines (as % of the initial mass) collected during each calcination and carbonation stage as a function of the number of cycles, in tests carried out under the operating conditions reported in Table 3.4, with or without the presence of SO₂. As a general trend, it can be noted that for all the limestones the fines elutriation rate is relatively large only during the first cycle and decreases with the number of cycles. This suggests that hardening of the particle surface takes place over the cycles, which is consistent with the progressive sintering of the sorbent.

Comparison of the results with and without SO₂ shows two different trends. When low SO₂ concentrations were used, the fines elutriation rate slightly increased. This is most likely due to a sintering-retarding effect of calcium sulphate on the particle surface (Itskos et al., 2012). On the other hand, when high SO₂ concentrations were used, the fines elutriation rate slightly

decreased. In this case it appears that a more compact calcium sulphate shell is formed increasing the hardness of the particles.

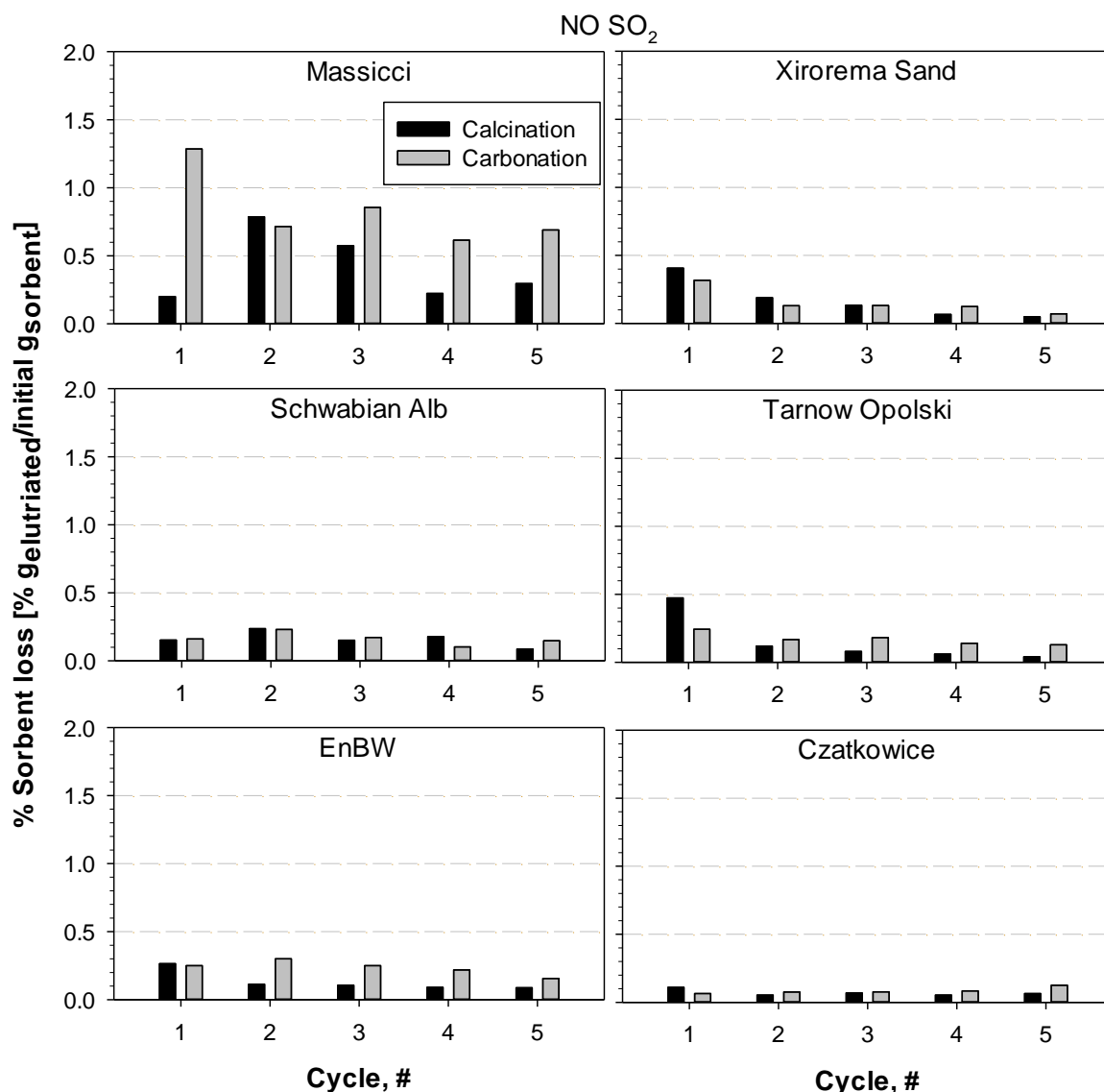


Figure 4.18. Percent mass of elutriated fines for the six limestones as a function of the number of cycles during experiments carried out without SO₂ (Table 3.4).

The average fines elutriation rate is similar during the calcination and the carbonation stages for all the limestones. This indicates that sintering is able to harden the particles irrespective of the chemical composition (CaO or CaCO₃). However, it was noted that in the tests without SO₂ the elutriation rate was slightly larger during the carbonation stage, while the opposite was true in the tests with SO₂ (at both concentration levels). This is clearly visible in Figure 4.17,

reporting a comparison of the measured fines elutriation rate (E) as a function of time during tests without SO₂ and in severe conditions (see Table 3.4) for Tarnow Opolski limestone.

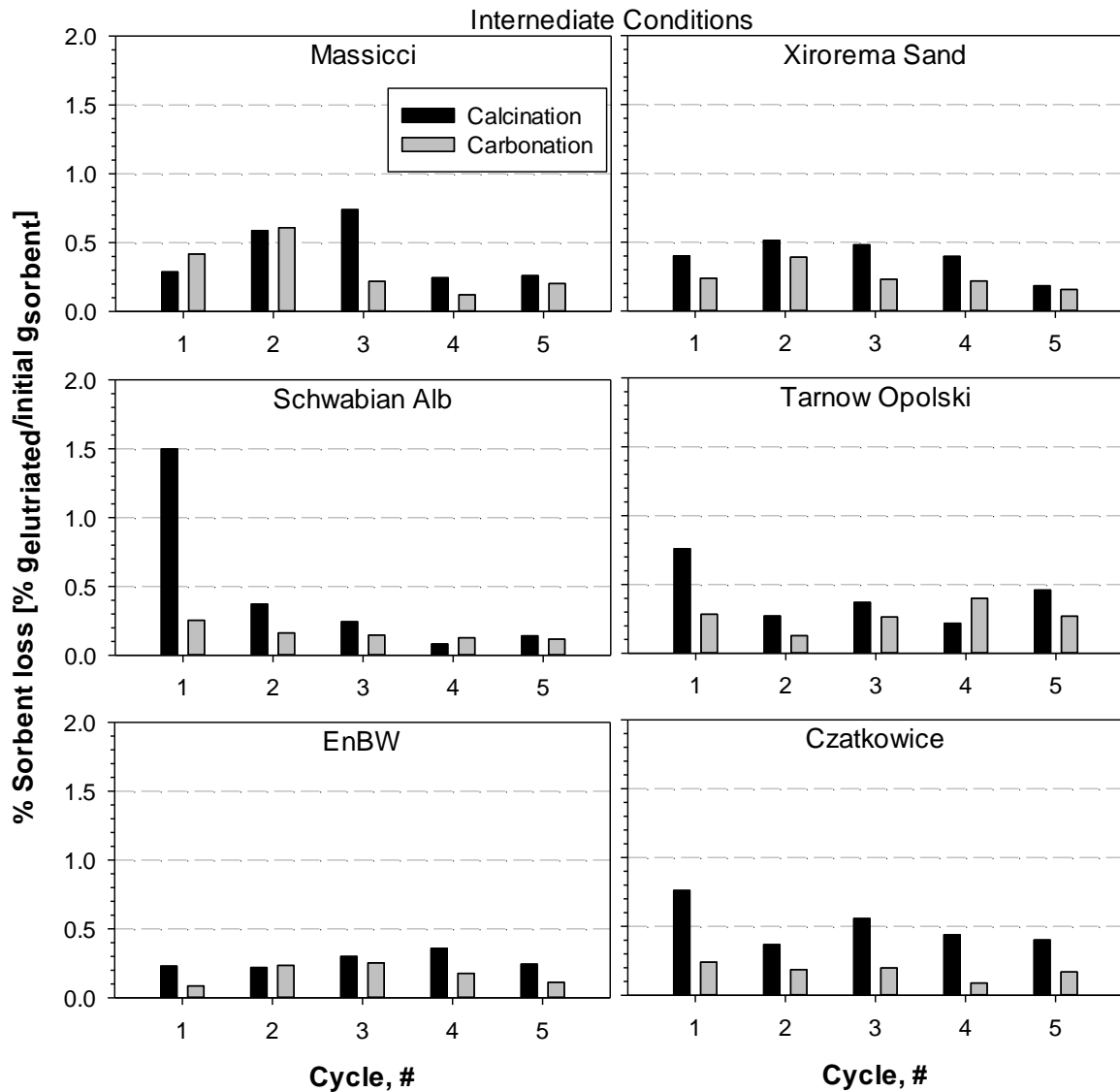


Figure 4.19. Percent mass of elutriated fines for the six limestones as a function of the number of cycles during experiments carried out with SO₂ under intermediate conditions (Table 3.4).

Similar results were obtained for all the other limestones tested. In each cycle the elutriation rate shows a typical trend with a peak of fines generation at the beginning. This peak is caused by a combination of the following effects: rounding off of the rough particles (Scala et al., 1997), thermal shock after

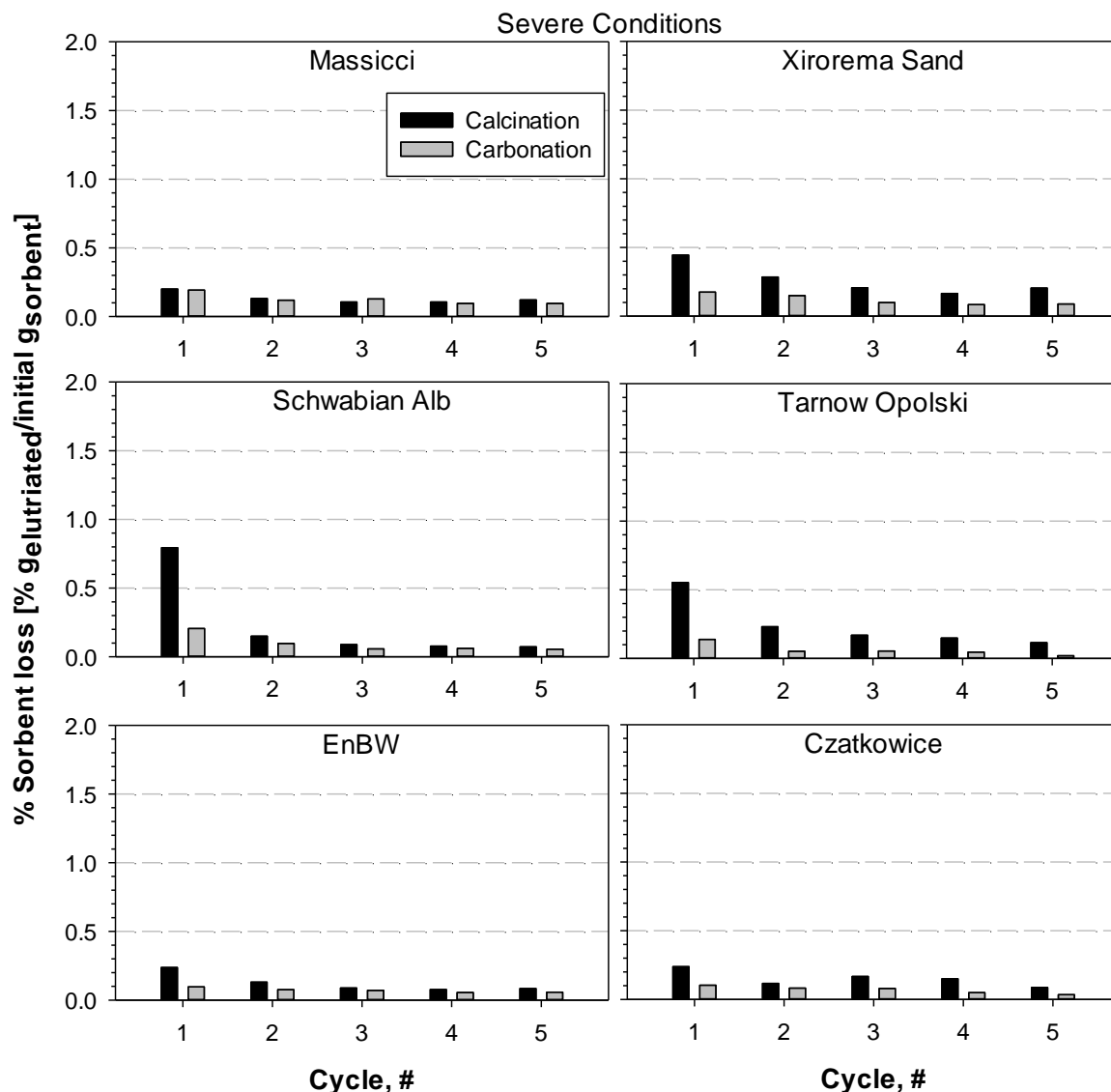


Figure 4.20. Percent mass of elutriated fines for the six limestones as a function of the number of cycles during experiments carried out with SO_2 under severe conditions (Table 3.4).

injection in the hot bed, and elutriation of re-injected fines (if any). During calcination, a further process is the rapid release of CO_2 that causes overpressures inside the particles and may change the mechanical properties of the solid. Inspection of Figure 4.17 indicates that in the tests without SO_2 the fines elutriation rate is always larger during the carbonation stages. This can be easily explained by considering that at the beginning of carbonation a more porous and softer CaO particle produced in the previous calcination stage is injected in the bed. On the other hand, in the tests with SO_2 the fines elutriation

rate is larger during the calcination stages. It is likely that in this case the calcium sulphate shell forming around the particles provides a similar surface hardness to the sorbent in both stages. The measured increase of the elutriation rate during the calcination stage is to be ascribed by the rapid CO_2 evolution from the particle that is able to crack the sulphate shell.

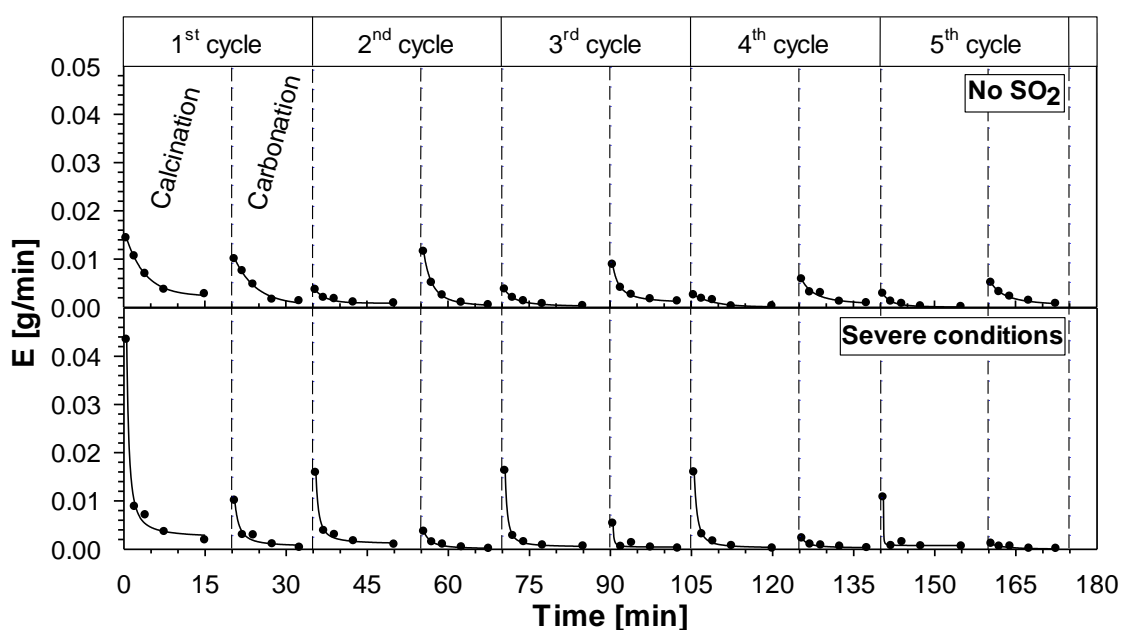


Figure 4.21. Sorbent elutriation rate as a function of time measured during experiments carried out without SO_2 (top) and with SO_2 under severe conditions (bottom) for Tarnow Opolski limestone (Table 3.4).

Figure 4.18 reports a comparison of the measured fines elutriation rate as a function of time during tests in intermediate and severe conditions (see Table 3.4) for Massicci limestone. Again, similar results were obtained for all the other limestones tested. This Figure shows another interesting trend: under low- SO_2 conditions the fines elutriation rate presents a first increasing trend with the cycle number, thereby decreasing towards a low asymptotic value. On the contrary, under high- SO_2 conditions this maximum is not found, and a continuously decreasing trend is always observed. A possible explanation of this

trend relies on the different sorbent sulphation rate in the two cases. Under low-SO₂ conditions, in the first cycles slow sulphate formation induces an enhancement of the sorbent attrition rate due to the lower hardness of calcium sulphate at the particle surface as compared with calcium carbonate, or by negative synergistic effects between the two calcium compounds with respect to resistance to wear (see § 4.2.4). At later stages, when a sufficiently compact sulphate layer at the particle surface establishes, the attrition rate decreases. Under high-SO₂ conditions, instead, a hard and compact sulphate layer is already established in the first cycles leading to a continuous decrease of the elutriation rate.

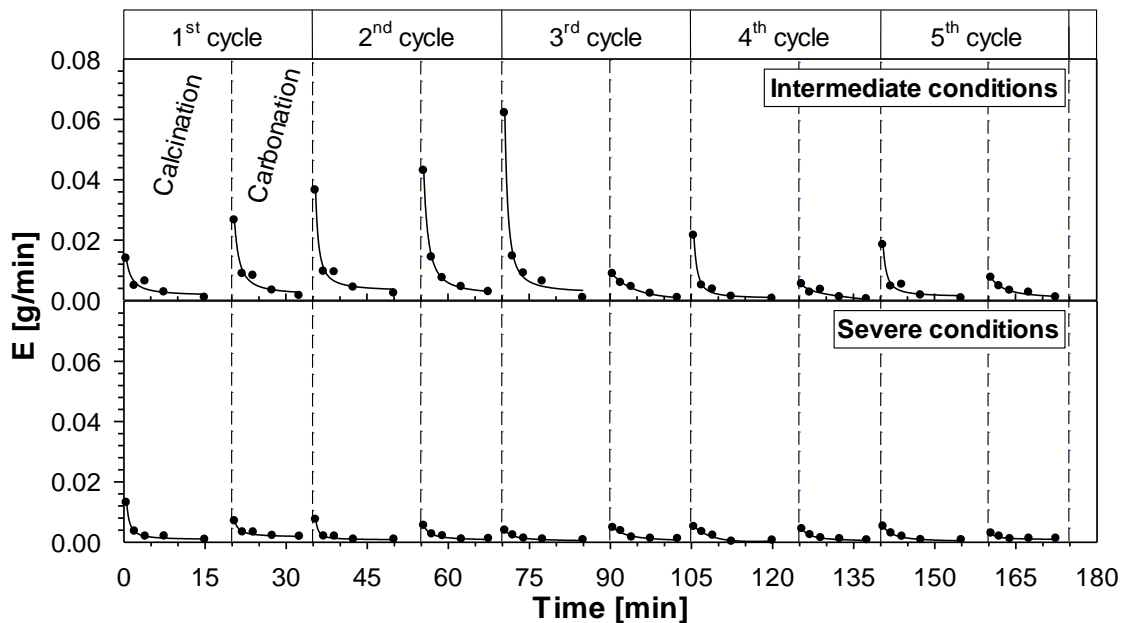


Figure 4.22. Sorbent elutriation rate as a function of time measured during experiments carried out with SO₂ under intermediate conditions (top) and severe conditions (bottom) for Massicci limestone (Table 3.4).

On the whole, as regards the surface abrasion propensity, the relative ranking of the six limestones (in terms of increasing abrasion) is: Czatkowice, EnBW, Tarnow Opolski, Schwabian Alb, Xirorema Sand and Massicci. On the basis of the above results, an average limestone loss rate by elutriation from a dual fluidized bed system can be estimated in the range 0.3-0.5%/h under

realistic conditions (a larger value of 1.3%/h was evaluated for Massicci). These values are lower than the 2%/h found by Charitos et al. (2010) during continuous operation of a 10kWth dual fluidized bed facility. It must be underlined, however, that in this plant the calciner was operated as a high velocity riser (4-6 m/s), and that a limestone with a smaller particle size (200-400 μm) was used in the experiments. On the whole, as discussed by Charitos et al. (2010), these figures would not represent a process limitation, since they are well below the expected sorbent make-up rate required to maintain sufficient sorbent activity.

4.4. Oxy-firing conditions and the effect of SO_2 using dolomite as sorbent

4.4.1. CO_2 capture capacity

Figure 4.19 reports the CO_2 capture capacity of the dolomite as a function of the number of cycles, tested under the operating conditions given in Table 3.4 (reported here for convenience).

Table 3.4. Operating conditions of the calcination/carbonation experiments with the six different limestones under oxy-firing conditions during calcination.

Calcination/ Carbonation	<i>Without SO_2</i> NO SO_2	<i>With SO_2</i> intermediate conditions	<i>With SO_2</i> severe conditions
Duration [min]	20/15	20/15	20/15
Temperature [$^{\circ}\text{C}$]	940/650	940/650	940/650
Inlet CO_2 [%v/v]	70/15	70/15	70/15
Inlet SO_2 [ppmv]	0/0	750/75	1500/1500

Results of tests with or without SO_2 are compared. The figure also reports for the same tests the calcium conversion to carbonate for each cycle (right axis). As expected, the capture capacity and the Ca conversion decreased with the number of cycles, approaching an asymptotic value after the fifth cycle. The residual capture capacity ($\sim 0.12 \text{ g}_{\text{CO}_2}/\text{initial g}_{\text{sorbent}}$ in the tests without SO_2) was larger than that typically found for limestone under the same operating conditions ($0.02\text{-}0.07 \text{ g}_{\text{CO}_2}/\text{g}_{\text{sorbent}}$, § 4.3.1), in spite of the lower Ca content of the sorbent and of the high temperature and CO_2 concentration during calcination. This result highlights the positive effect of the large magnesium content of the dolomite in preserving Ca reactivity and reducing particle sintering. The residual Ca conversion was as high as $\sim 50\%$, as compared with values below 15% for limestone under the same operating conditions).

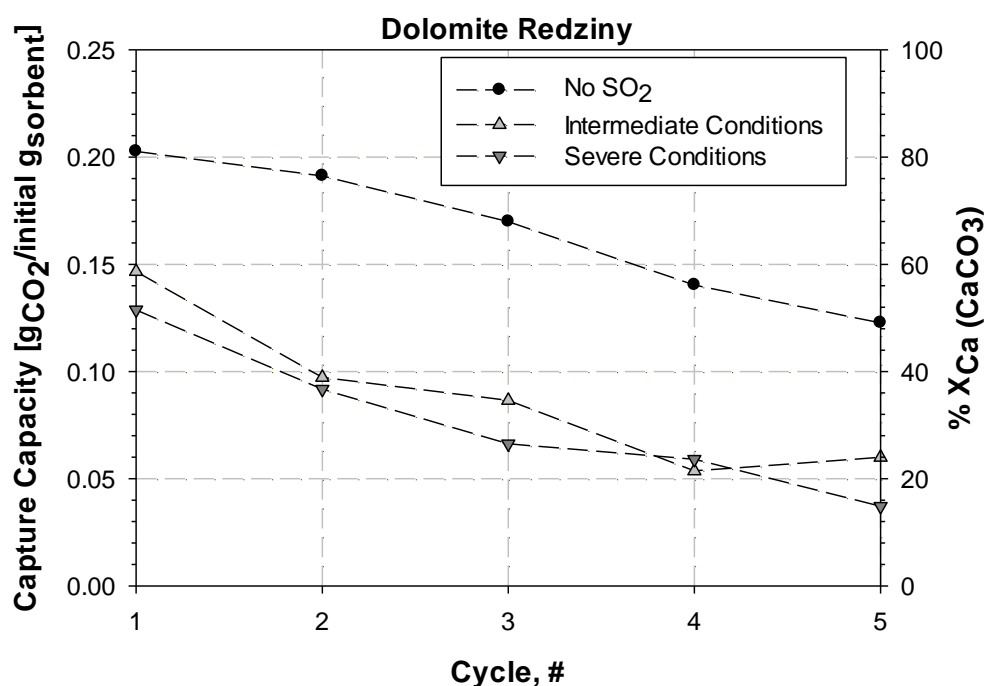


Figure 4.19. CO_2 capture capacity and calcium conversion to carbonate of the dolomite as a function of the number of cycles for experiments carried out without and with SO_2 (Table 3.4).

When SO_2 was present a further decrease of the CO_2 capture capacity and of the Ca conversion of the dolomite (of the order of 2-3 times) was found. This behaviour can be explained by the progressive formation of a calcium sulphate shell around the particles (both during calcination and carbonation) that hinders intraparticle diffusion of CO_2 in the pores of the sorbent. The residual capture capacity of the dolomite was 0.04-0.06 $\text{g}_{\text{CO}_2}/\text{initial g}_{\text{sorbent}}$ in this case, corresponding to a residual Ca conversion of about 20%. Noteworthy, this CO_2 capture capacity was still larger than that of limestone under the same operating conditions (0.004-0.04 $\text{g}_{\text{CO}_2}/\text{initial g}_{\text{sorbent}}$, § 4.3.1).

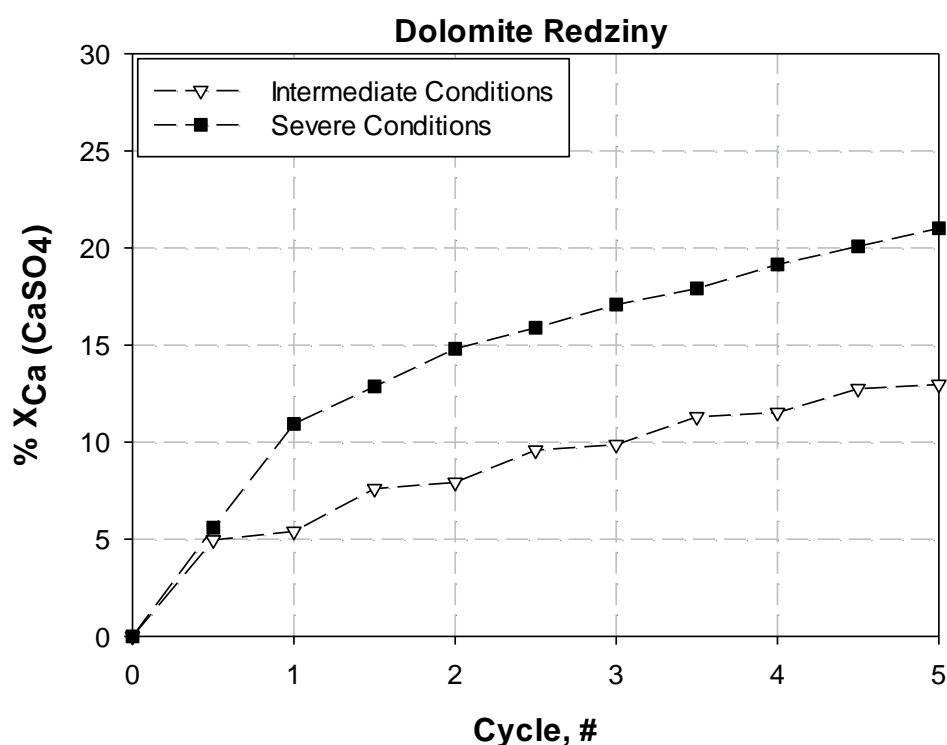


Figure 4.20. Calcium conversion degree to sulphate of the dolomite as a function of the number of cycles (each data point represents conversion after half cycle) (Table 3.4).

It is interesting to note that results under low- SO_2 and high- SO_2 conditions were very similar to each other for the dolomite, indicating that even a small quantity of SO_2 is sufficient to significantly hinder the CO_2 capture capacity of the sorbent. This result was similar to that obtained with a limestone under mild conditions (see § 4.2.1), but was different from that found for a number of

limestones under the same operating conditions (high temperature and high CO₂) reported in the § 4.3.1. In fact, in that case it was observed that when a low SO₂ concentration was used in the tests, limestone capture capacity results were closer to those obtained in tests without SO₂ rather than to those obtained in high-SO₂ tests. Altogether these results suggest that when SO₂ is present the CO₂ capture capacity of the sorbent is determined by the competition between sulphation and sintering. All factors reducing the effect of sintering (high Mg content, low temperature and CO₂) enhance the relative effect of particle sulphation with respect to sintering.

Figure 4.20 reports the cumulative calcium conversion degree to sulphate during the tests, as calculated from the SO₂ concentration profiles at the exhaust (note that since SO₂ is present both during calcination and carbonation, each data point represents conversion to sulphate after half cycle). The extent of calcium conversion to sulphate in each stage clearly depends on the relevant SO₂ concentration in the gas phase, and it is approximately the same as that found for limestone under the same two operating conditions (§ 4.3.1).

4.4.2. Particle size distribution

Figure 4.21 compares the measured cumulative particle size distributions (PSDs) of the dolomite after the fifth carbonation stage in tests carried out under the operating conditions reported in Table 3.4, with or without SO₂ in the fluidizing gas. In the same figure, the shaded area contains all the experimental results obtained with a number of limestones under the same operating conditions (§ 4.3.1), for reference. Contrary to limestone, particle fragmentation was extensive for the dolomite. The presence of SO₂ appears to slightly reduce

the extent of fragmentation. The fractional amount of fragments after the 5th cycle was ~65% of the initial sample mass for tests without SO₂, decreasing to ~55% for tests with SO₂. This mass fraction of fragments was about three times more than that found for limestone. It is recalled here that by “fragments” we mean all the collected particles whose size falls below the lower limit of the feed size interval: accordingly all the collected particles finer than 400 μm were classified as “fragments” in the context of the present study.

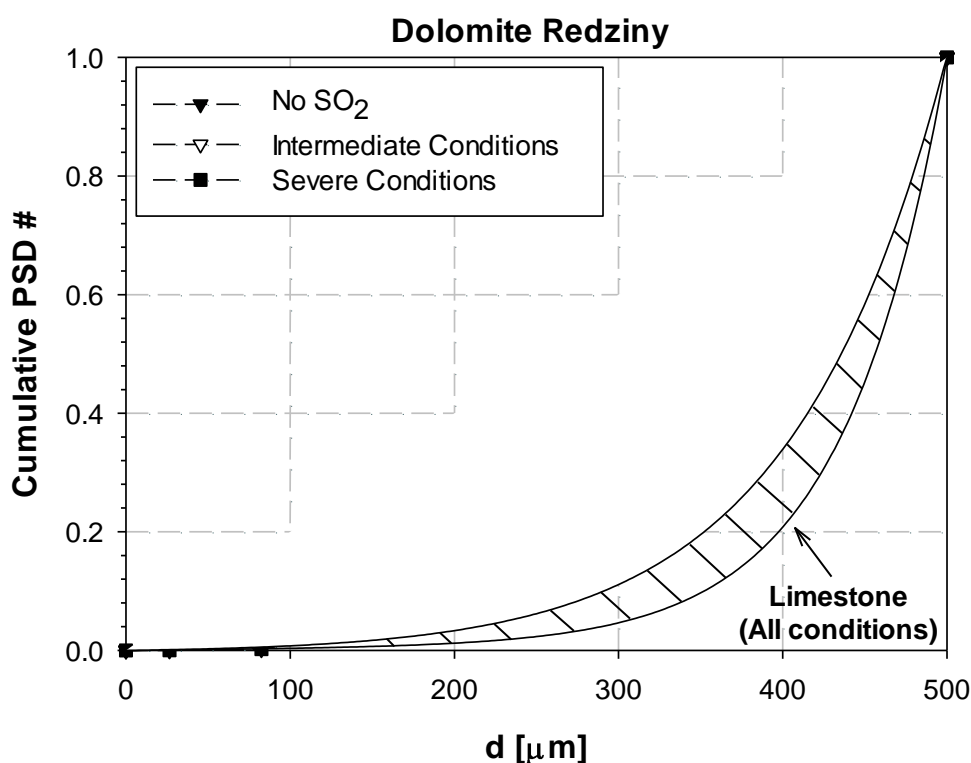


Figure 4.21. Cumulative particle undersize distribution of the dolomite after the 5th carbonation stage for experiments carried out without and with SO₂ (Table 3.4). The shaded area represents results for limestone under the same conditions.

Figure 4.22 compares the PSDs of the dolomite after the 1st calcination, the 3rd carbonation and the 5th carbonation stages for experiments carried out under severe conditions. Similar results were obtained under the other two conditions tested. The PSD curves are very close to one another indicating that particle fragmentation was mostly active upon the 1st calcination. The most likely reason

for this result is that decomposition of magnesium carbonate only occurs during this stage, since magnesium does not contribute to the CO₂ capture process during the carbonation stages.

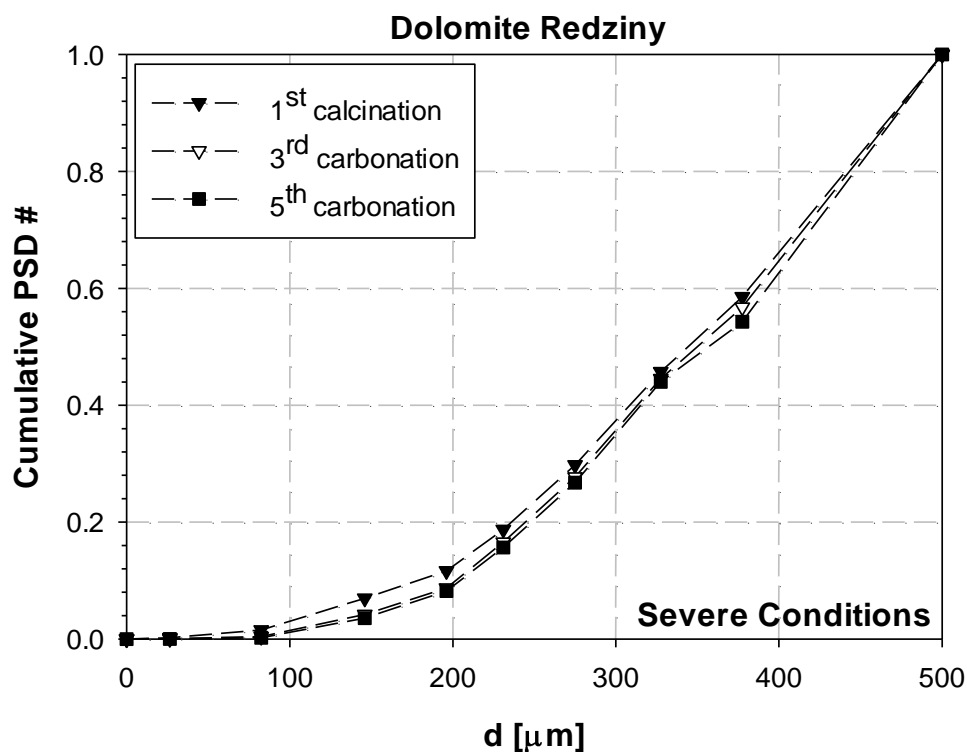


Figure 4.22. Cumulative particle undersize distribution of the dolomite after the 1st calcination, the 3rd carbonation and the 5th carbonation stage for experiments carried out under severe conditions (Table 3.4).

4.4.3. Elutriation rate

Figure 5 reports a comparison of the measured dolomite fines elutriation rate as a function of time in tests carried out under the operating conditions reported in Table 3.4, with or without SO₂ in the fluidizing gas. In each cycle the elutriation rate shows a typical trend with a peak of fines generation at the beginning. This peak is caused by a combination of the following effects: rounding off of the rough particles (Scala et al., 1997), thermal shock after injection in the hot bed, and elutriation of re-injected fines (if any). During

calcination, a further process is the rapid release of CO_2 that causes overpressures inside the particles and may change the mechanical properties of the solid. In all conditions the fines elutriation was relatively large during the first cycle and significantly decreased from the second cycle on. In fact, hardening of the particle surface takes place over the cycles, as a consequence the progressive sintering of the sorbent. This result is also consistent with the PSD data showing that significant fragmentation occurred during the 1st calcination stage. Particle fragmentation enhances attrition in two ways (Scala et al., 2000): on the one hand it may directly lead to the generation of elutriable fragments; on the other it gives rise to relatively coarse fragments with a highly angular shape, which are therefore more prone to surface wear.

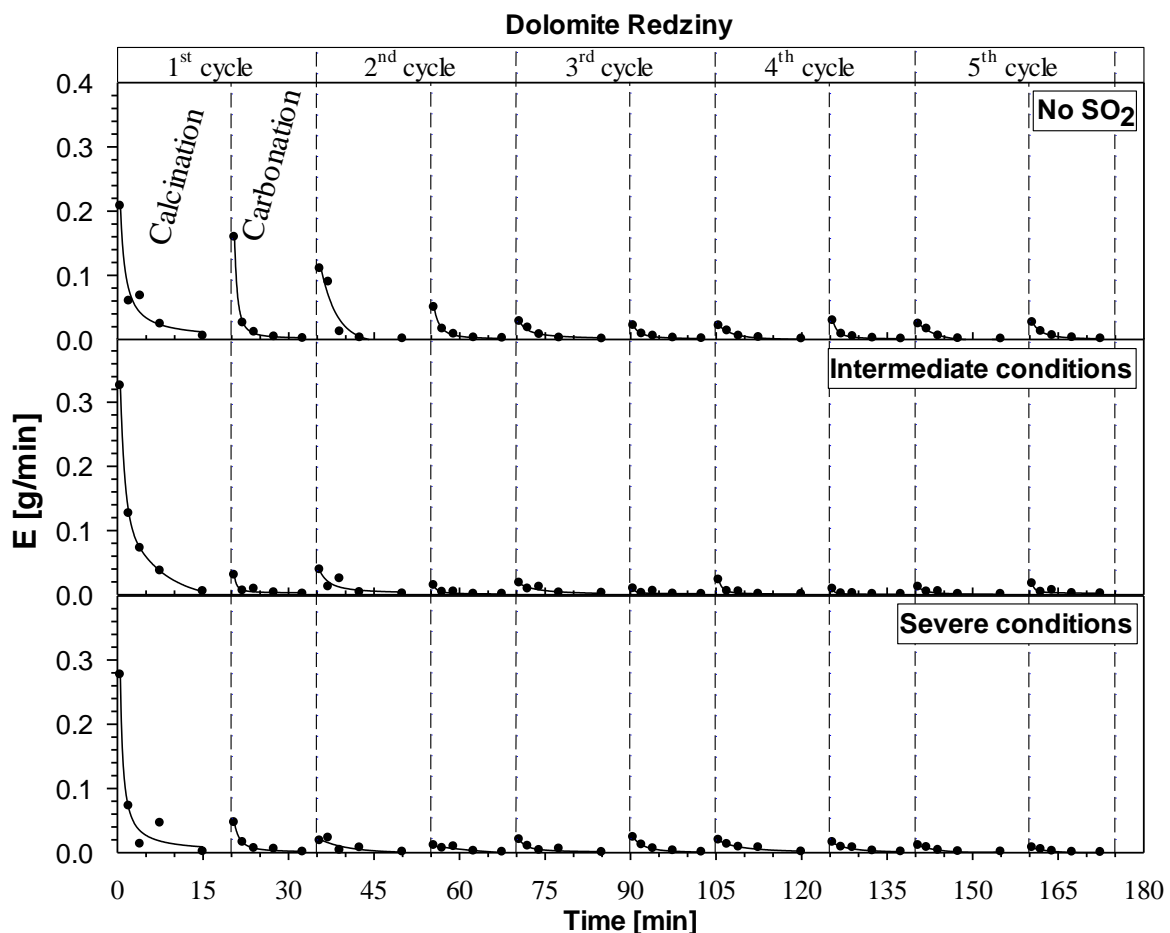


Figure 4.23. Dolomite elutriation rate as a function of time measured during experiments carried out without SO_2 (top) and with SO_2 under intermediate conditions (center) and severe conditions (bottom) (Table 3.4).

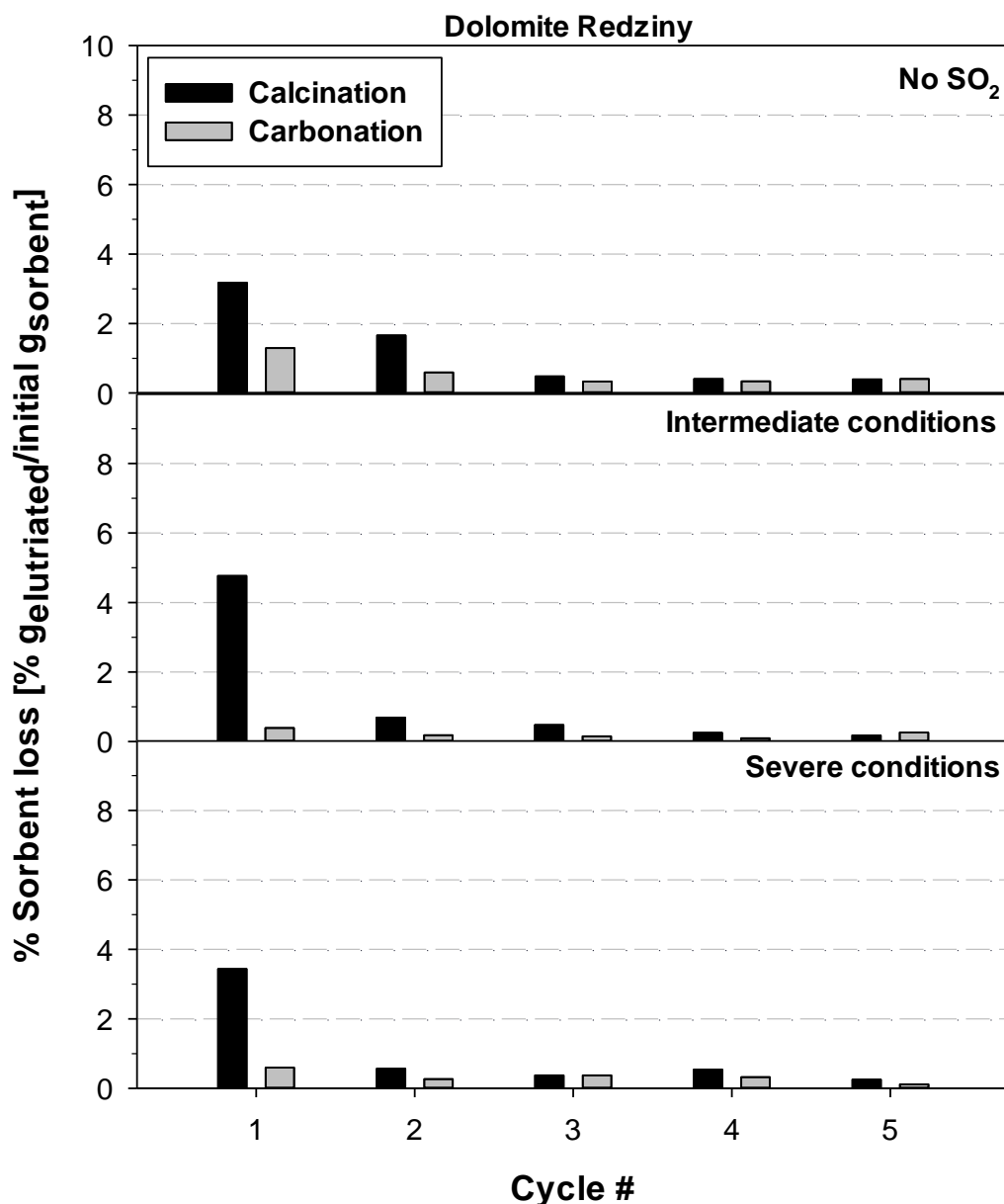


Figure 4.24. Average fines elutriation loss for dolomite as a function of the number of cycles for experiments carried out without SO₂ (top) and with SO₂ under intermediate conditions (center) and severe conditions (bottom) (Table 3.4).

It can be noted that for the dolomite the average fines elutriation rate was approximately the same during the calcination and the carbonation stages. This indicates that the combination of the large MgO content and of the hardening effect of sintering/sulphation were able to make the particle surface properties independent of the calcium chemical form (CaO or CaCO₃). Comparison of the

results with or without SO₂ indicates that the elutriation rates were similar, slightly lower when SO₂ was present in the gas (except during the 1st calcination stage).

Figure 4.24 reports the cumulative mass of elutriated fines (as % of the initial mass) collected during each calcination and carbonation stage as a function of the number of cycles, in tests carried out under the operating conditions reported in Table 3.4, with or without the presence of SO₂. On the basis of these results, an average sorbent loss rate by elutriation from a fluidized bed system can be estimated of the order of 2.0%/h for dolomite, as compared to a typical value of 0.3-0.5%/h for limestone (§ 4.3.1). This result can be attributed to two concurring factors. On the one side, sintering appears to be reduced for this sorbent, making the particles softer than limestone. On the other side, as discussed before, the extensive particle fragmentation (Figure 4.21) increases the sorbent surface area subject to attrition in the bed.

4.5. Reactivation by hydration

4.5.1. Microstructural characterization of reactivated sorbent

Table 4.1. Hydration degree for reactivated Massicci limestone and total cumulative specific porosity and for sizes < 200 nm for spent and reactivated Massicci limestone.

Material	Hydration Degree	Total cumulative specific porosity	Cumulative specific porosity for sizes < 200 nm
Spent	-	253 mm ³ g ⁻¹	65 mm ³ g ⁻¹
WHY_10	52.4%	571 mm ³ g ⁻¹	215 mm ³ g ⁻¹
WHY_30	54.6%	601 mm ³ g ⁻¹	198 mm ³ g ⁻¹
WHY_60	55.2%	590 mm ³ g ⁻¹	181 mm ³ g ⁻¹

Table 4.1 reports the hydration degree and specific porosity data for the spent Massicci limestone and for the three different hydrated sorbent (WHY_10,

WHY_30 and WHY_60). Procedure and conditions for preparation of spent material are reported in the specific section (see § 3.7); a summary is given in Table 4.2.

Table 4.2. Operating conditions for preparation and for subsequent hydration of the spent material

<i>Conditions for preparation of spent material (five calcination/four carbonation)</i>		<i>Conditions for hydration of spent material</i>	
Duration [min]	20/15	Duration [min]	10, 30, 60 (WHY_10, WHY_30, WHY_60)
Temperature [°C]	940/650	Temperature [°C]	25
Inlet CO₂ [%v/v]	70/15	Water/solid ratio [g/g]	25

TG analysis of the samples indicated that the spent sorbent was mostly composed of CaO with some residual CaCO₃ (9.8%wt) that was left unconverted after the last (5th) calcination. The hydration degree of the water-reactivated samples increased from 52.4% for WHY_10 to 55.2% for WHY_60, suggesting that chemical hydration is fairly fast and practically complete after the first 10 min. Further increase of hydration degree was likely hindered by the spent sorbent chemical (e.g., presence of residual CaCO₃) and physical (e.g., reduced porosity of the sintered spent sample) properties. Figure 4.25 reports selected SEM micrographs of the samples. Visual comparison of the morphology of Spent and WHY samples indicates that hydration brought about an increased degree of “softness” of the external surface of the samples. Quantitative considerations were obtained by analyzing porosimetric results (Table 4.1), which were referred to the pore size range finer than 200 nm, since it has been reported in the literature (Fennel et al., 2007a, Sun et al., 2008) that this is the range mostly affected by sintering/deactivation phenomena upon cycling. Therefore, in order for hydration to be effective, it must restore this “fine” porosity. The cumulative specific “fine” porosity was 65 mm³/g for spent sorbent, and the hydration

treatment was effective in increasing this porosity: 215 mm³/g (WHY_10), 198 mm³/g (WHY_30) and 181 mm³/g (WHY_60). The hydration treatment was therefore able to induce an intra-particle pore regeneration process which underlies reactivation. Moreover, the most pronounced increase in the <200 nm-porosity was observed just after 10 min-hydration, while longer hydration times resulted into a slight decrease in porosity with respect to that measured for WHY_10. This should be related to the competing effects of particle swelling (related to the chemical hydration process and, therefore, significant only during the initial hydration period and low-temperature cramming/chemical sintering phenomena (relevant for longer hydration times and already observed in (Montagnaro et al., 2004) when hydrating spent sorbents from flue gas FB desulphurization). Hydration results indicated that the most interesting reactivated sample is WHY_10, which was subjected to further Calcium-Looping tests. To assess the effect of the hydration time, the performance of WHY_10 was compared with that of the potentially less interesting WHY_60 sample.

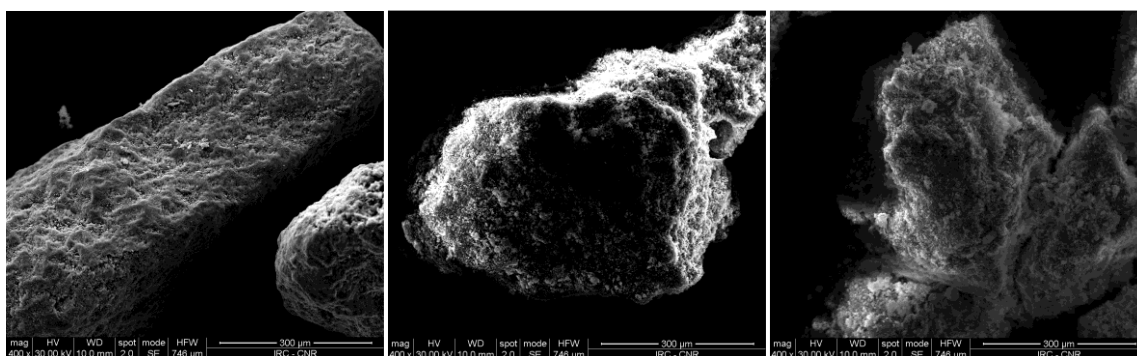


Figure 4.25. SEM micrographs of spent sorbent (left), and WHY materials at two different times (center, 10 min; right, 60 min).

4.5.2. CO₂ capture capacity

Figure 4.26 shows the CO₂ capture capacity values, as mass of CO₂ captured per mass of sorbent initially injected into the bed, obtained for WHY_10 and WHY_60, as a function of the number of carbonation stages and with reference to a 0.03 g_{CO2}/initial g_{Sorbent} baseline, the value obtained after the 4th carbonation, i.e. the last carbonation before hydration for Massicci limestone in the same conditions reported in the Table 4.2.

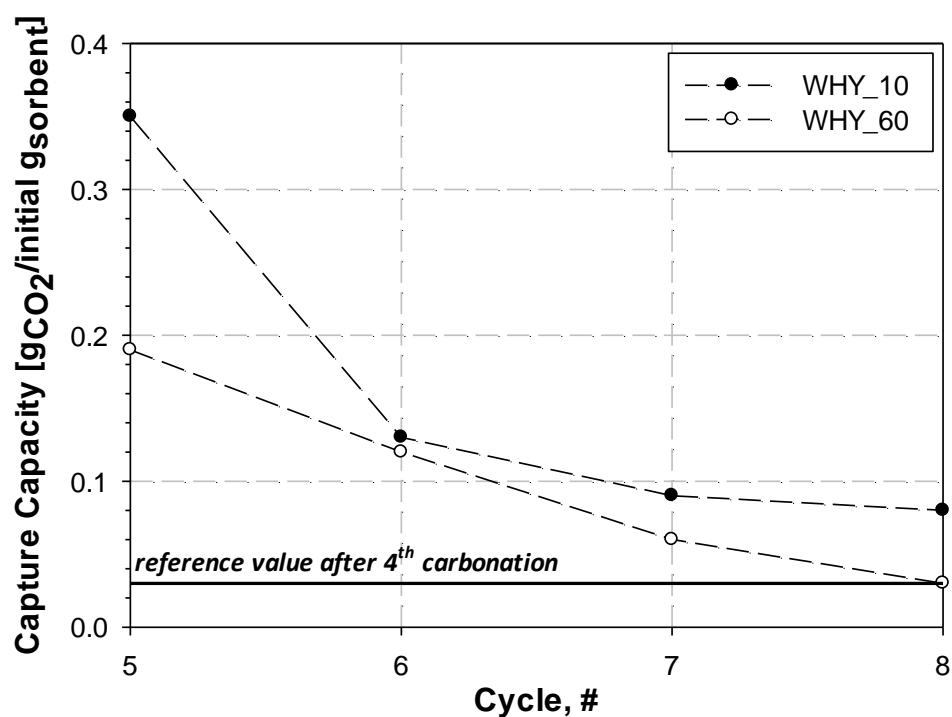


Figure 4.26. CO₂ capture capacity for the reactivated WHY_10 and WHY_60 samples as a function of the number of carbonation stages (the 5th carbonation is the first carbonation step after hydration).

Results confirmed the effectiveness of the hydration treatment in regenerating the sorbent activity toward CO₂ capture. The capture capacity decreased from 0.35 to 0.08 g_{CO2}/initial g_{Sorbent} (WHY_10) and from 0.19 to 0.03 g_{CO2}/initial g_{Sorbent} (WHY_60) along with the carbonation stages, highlighting that

deactivation phenomena occurred also for the reactivated materials. In particular, at the 8th carbonation WHY_60 reaches the same value of raw Massicci after the 4th carbonation canceling the reactivation effect, while it seems that WHY_10 shows a more durable reactivation than WHY_60. Moreover, WHY_10 sample resulted more effective in CO₂ capture capacity than WHY_60, and this should be mostly ascribed to the larger porosity achieved when hydrating for short hydration times, so to exploit the “chemical” hydration effect without suffering the long-term “physical” crumpling effect.

4.5.3. Particle size distribution

Figure 4.27 reports the cumulative particle size distributions (PSD) for WHY_10 and WHY_60 after 5th carbonation (the first after reactivation), 6th calcination and 8th carbonation. As described in the procedure section (see § 3.7), the initial size range for the hydrated sorbent is 400-600 μm .

For WHY_10, PSD results showed that particle fragmentation was limited during the 5th carbonation, when compared with the following cycles, in particular the percentage of fragments (<400 μm) represents the 14% of the total sorbent.

Fragmentation phenomena undergo an appreciated increase during the 6th calcination (i.e., the first calcination after reactivation), with a fractional mass of fragments of about 30%. This was ascribed to the more severe conditions to which the reactivated sorbent underwent upon its first calcination, in terms of thermal shock. For all the other cycles, the PSD did not show significant changes, even if a somewhat larger fragmentation tendency was observed along the cycles: altogether, an amount of fragments in the range 14-38% was recorded. Similar considerations hold for WHY_60 (Figure 4.27-bottom): about 15% of

fragments after the 5th carbonation, about 26% of fragments after the 6th calcination and, in general, an amount of fragments in the range 15-34%. It is important to underline that WHY_10 and WHY_60 show a very similar fragmentation propensity. In particular, slight differences are appreciable after the 6th calcination, where WHY_10 is a little more fragile. Comparing the fragmentation propensity of reactivated sorbent with spent one (Figure 4.28) it is clear that hydration involves a particle embrittlement. Probably, this behaviour is related to the higher porosity of reactivated materials which increases particle fragility.

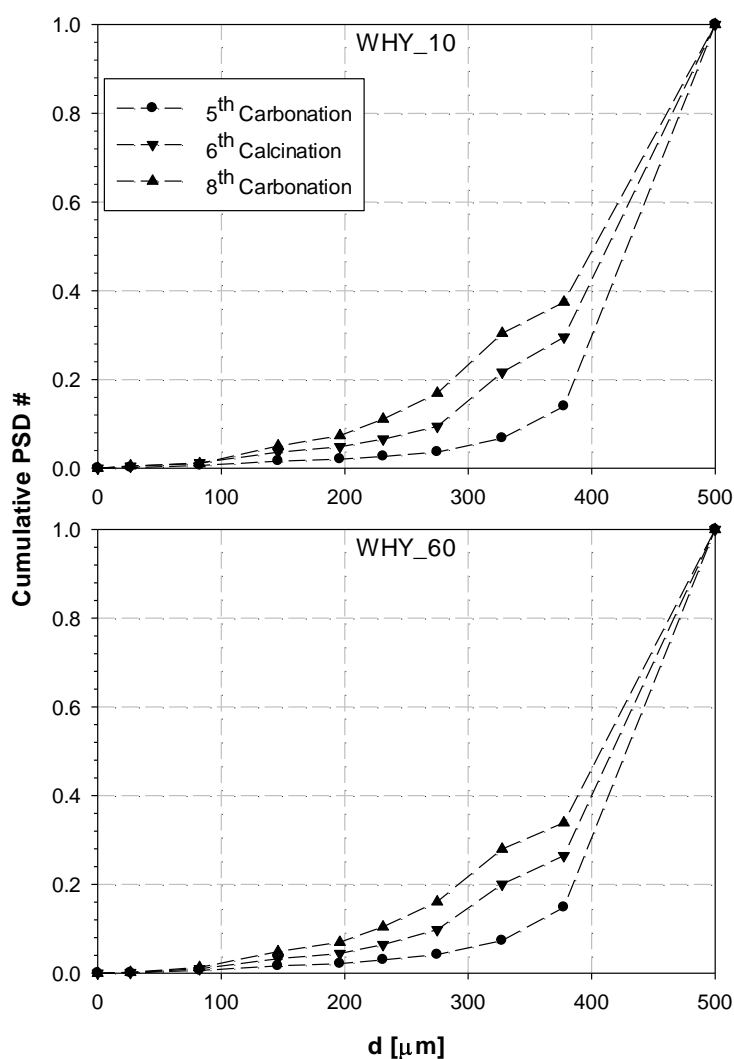


Figure 4.27. Cumulative particle size distribution (PSD) for the reactivated WHY_10 (top) and WHY_60 (bottom) samples after the 5th carbonation, the 6th calcination and 8th carbonation stage.

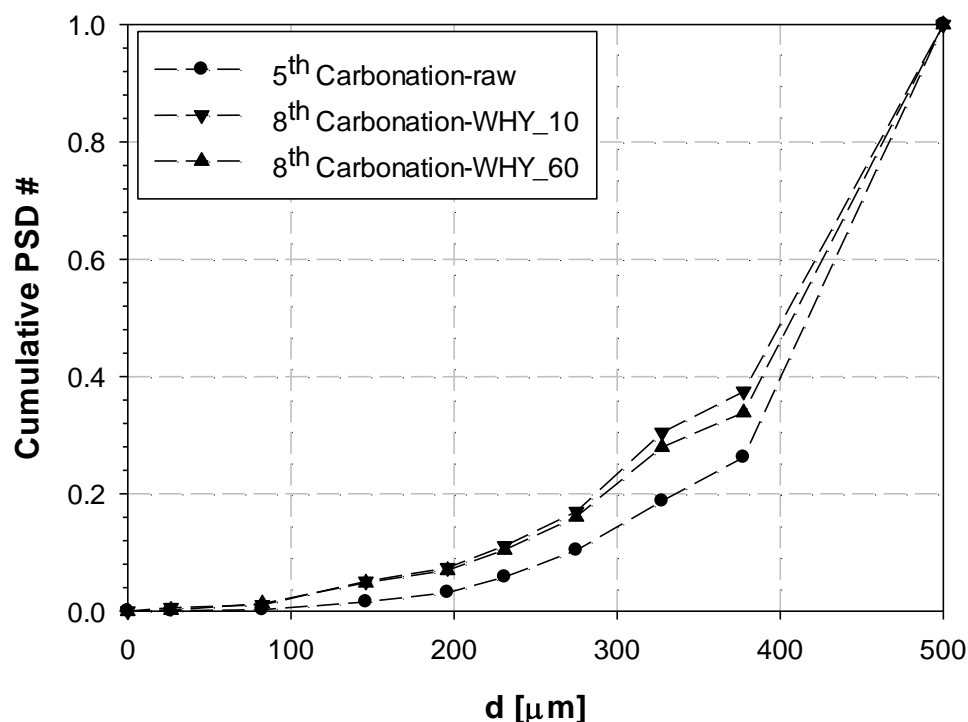


Figure 4.28. Cumulative particle size distribution (PSD) for the raw Massicci limestone after the 5th carbonation and for the reactivated materials WHY_10 and WHY_60 after the 8th carbonation.

4.5.4. Elutriation rate

Figure 4.29 reports elutriation fine data for the reactivated materials (as % of the initial mass), collected during each calcination and carbonation stage as a function of the number of cycles. In particular, these values are compared with elutriation amount of raw material in the same conditions in the previous cycles. The loss of elutriated material during each calcination and carbonation stage was $0.88 \pm 0.14\%$ and $0.70 \pm 0.43\%$, respectively, for WHY_10, and $0.90 \pm 0.60\%$ and $1.00 \pm 0.55\%$, respectively, for WHY_60. The cumulative loss of elutriated fines after 3 complete calcination/carbonation stages (therefore, discarding the datum relative to the 5th calcination) was 5.36% and 6.17% for WHY_10 and

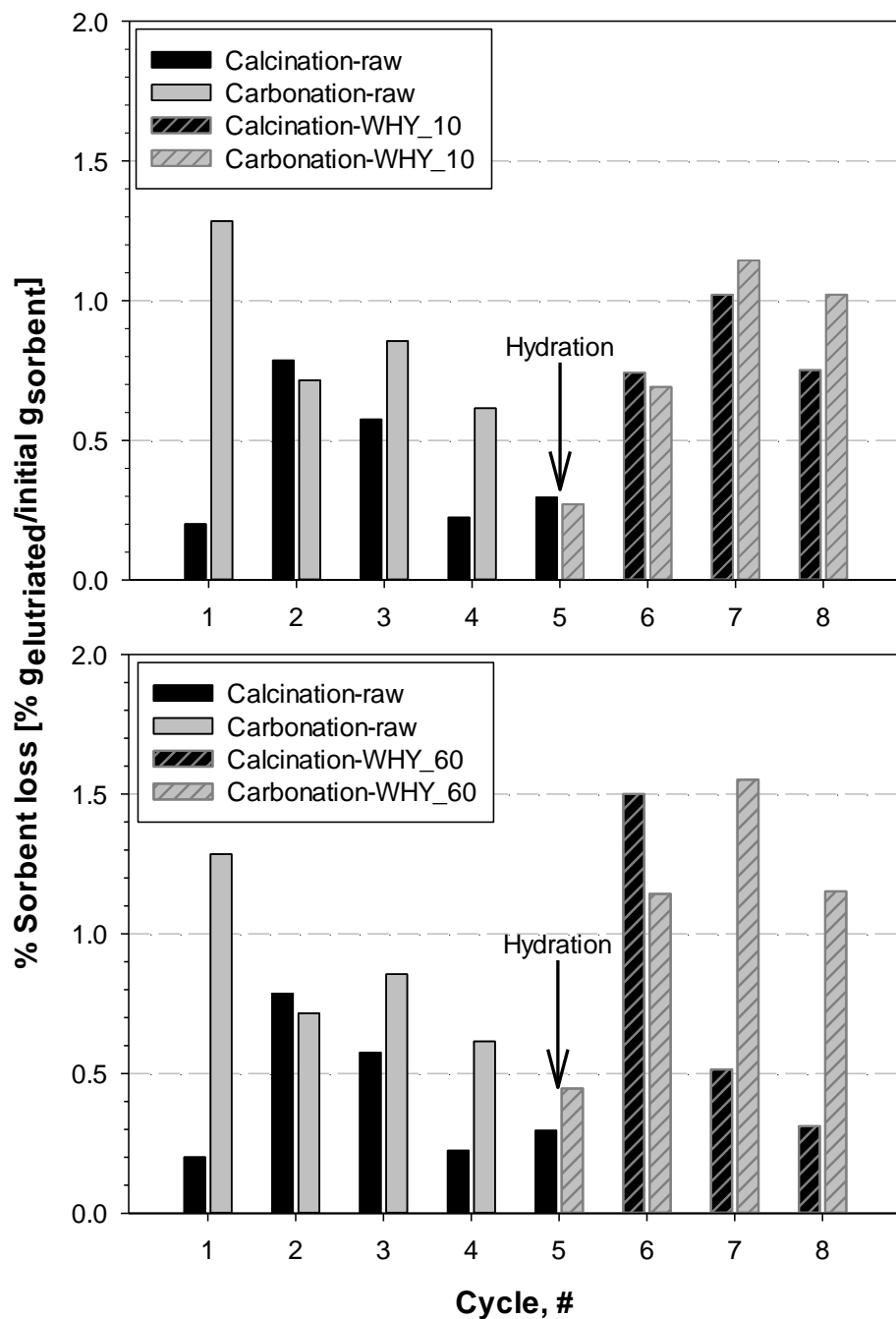


Figure 4.29. Percent mass of elutriated fines for the raw Massicci limestone and for the reactivated materials WHY_10 (top) and WHY_60 (bottom) as a function of the number of cycles during experiments.

WHY_60, respectively. It is possible to see that, except for the first cycles, for the reactivated materials the amount of elutriated fines is higher during the carbonation stage. Moreover, this behaviour is the same as for the raw material

and the possible explanation was already discussed in § 4.3.3. In general, WHY_10 and WHY_60 show a moderate increase toward attrition tendency, in percentage terms, than raw Massicci. This is probably due to a soaking effect which produces a softer particle surface, as shown by the SEM micrographs (see Figure 4.25), and since this effect is time-dependent it exhibits more pronounced consequences for WHY_60. These results suggest that CO₂ capture capacity and attrition propensity are linked one to the other showing that the sorbent should be hydrated for times long enough to get a substantially complete chemical hydration, but short enough to avoid soaking and cramming phenomena.

5. Conclusions

Results obtained in the frame of the present Doctoral Thesis are hereby summarized. They provide a valuable basis for the design of Ca-looping processes, with specific reference to sorbent propensity to attrition and fragmentation, to the mutual interaction between CO₂ and SO₂ uptake, to the performance of dolomitic sorbents as alternative to the more usual limestones, to the potential of spent sorbent reactivation by water hydration to reduce the consumption of make-up sorbent. The main conclusions are detailed in the following sections.

5.1. Effect of temperature and CO₂ partial pressure during calcination

The effects of the calcination temperature and of the CO₂ partial pressure during the calcination stage on CO₂ capture capacity and attrition propensity of a Ca-based sorbent have been investigated. Experiments have been carried out with the Italian Massicci limestone during calcium looping cycles under relatively mild conditions. Results showed that the limestone exhibited the typical decrease of the uptake capacity with increasing number of cycles. The presence of CO₂ during calcination and especially a higher calcination temperature determine a decrease of sorbent capacity for all the cycles, most likely due to the enhancement of particle sintering. Analysis of the particle size distribution (PSD) of the bed material over repeated calcination/carbonation cycles indicated that particle fragmentation was very limited in all the conditions investigated. The fines elutriation rate was relatively large during the

first cycle and decreased with the number of cycles. The presence of CO₂ during calcination led to a significant decrease of fines generation, while a higher calcination temperature produced an increase of the particle attrition rate. These results may be explained by the competition of two opposed effects: on the one hand sintering brings about hardening of the particle surface; on the other side a faster release of CO₂ leads to higher internal overpressures and, in turn, to increased propensity to particle breakage.

5.2. Effect of SO₂ during carbonation

The CO₂ capture capacity and the attrition propensity of an Italian limestone (Massicci) have been assessed in the presence of SO₂ (during the carbonation stage) during calcium looping cycles under relatively mild conditions. Results showed that the presence of SO₂ in the flue gas significantly decreased the sorbent CO₂ capacity, most likely because of the formation of an impervious CaSO₄ layer at the periphery of the particles. The effect of the SO₂ concentration level (110 versus 1800 ppm), however, was less pronounced than expected. In particular, results showed that even a small quantity of SO₂ is sufficient to significantly hinder the CO₂ capture capacity of the sorbent. Analysis of the particle size distribution of bed material over repeated calcination/carbonation cycles indicated that particle fragmentation was very limited in all the conditions investigated. The fines elutriation rate was relatively large during the first cycle and decreased with the number of cycles. The presence of SO₂ during carbonation determined a limited increase of particle attrition. The interplay between the extent of calcium sintering and the properties of the sulphate layer formed on the surface of the sorbent particles

control the attrition propensity of the limestone. Results obtained with 1800 ppm SO₂ showed departures from the other conditions as regards: cumulative particle size distribution of fragments, cumulative elutriated material over five repeated cycles, degree of SO₂ uptake over repeated cycles. The departure was particularly noticeable as results were compared with those obtained under 1800 ppm CS conditions (i.e. when the duration of the carbonation stage was 45 min instead of 15 min, and sulphation approached completion). An explanation is based on the speculation that a poorly structured and less compact sulphate layer is formed during the 1800 ppm tests as compared with that formed than during the 1800 ppm CS tests. This feature would affect the propensity to generate fragments and attritable material and the capacity to further uptake SO₂ at the same time.

5.3. Oxy-firing conditions and the effect of SO₂

The CO₂ capture capacity and the attrition propensity of six high-calcium European limestones were assessed under cyclic calcination/carbonation conditions in a lab-scale fluidized bed reactor under realistic conditions representative of a process with calcination in an oxy-firing environment. Results showed that the CO₂ capture capacity decreased with the cycles, as expected. The presence of a high CO₂ concentration during calcination (70%) and a high calcination temperature (940°C) determined a significant decrease of the sorbent capacity, due to the enhancement of particle sintering. The analysis of the PSD of bed material over repeated calcination/carbonation cycles indicated that particle fragmentation was limited for all the limestones. The fines elutriation rate was relatively large only during the first cycle and decreased with the number of cycles, since the combined chemical-thermal

treatment affected the particle structure making it increasingly hard. The presence of a high SO_2 concentration had a detrimental effect on the CO_2 capture capacity of all limestones, while a low SO_2 concentration had a more limited effect. Attrition was only slightly affected by the presence of SO_2 . On the basis of the experimental data reported in this work, the residual CO_2 capture capacity after the first few cycles is of the order of 0.01-0.05 $\text{g}_{\text{CO}_2}/\text{initial g}_{\text{CaCO}_3}$ depending on the SO_2 concentration. The average limestone loss rate by elutriation can be estimated to be of the order of 0.5%/h under realistic conditions, and should not represent a process limitation.

5.4. Oxy-firing conditions and the effect of SO_2 using dolomite as sorbent

The CO_2 capture capacity and the attrition propensity of a dolomite were assessed during multiple calcination/carbonation cycles in a lab-scale fluidized bed reactor under conditions representative of a process with calcination in an oxy-firing environment. In addition, the effect of the presence of SO_2 in the flue gas was investigated. The performance of the dolomite was compared with that of limestone tested under the same operating conditions.

Results showed that the CO_2 capture capacity decreased with the cycles, as expected. The present experimental conditions, consisting of a high CO_2 concentration during calcination (70%) and a high calcination temperature (940°C), are known to determine a significant decrease of the CO_2 capacity of limestone due to the enhancement of particle sintering. This effect, however, was less important for the dolomite tested in this work. The CO_2 capture capacity of the dolomite was always larger than that of limestone, and remained relatively large along the cycles in spite of the lower calcium content of the

sorbent. This result highlights the positive effect of the large magnesium content of the dolomite in reducing the particle sintering effect. The presence of SO_2 significantly depressed the CO_2 capture capacity, most likely because of the formation of an impervious CaSO_4 layer on the surface of the particles.

The analysis of the particle size distribution (PSD) of the bed material over repeated calcination/carbonation cycles indicated that, contrary to limestone, particle fragmentation was extensive for the dolomite, especially upon the first calcination stage. The fines elutriation rate was also large during the first cycle and decreased with the number of cycles, because of the combined effect of early particle fragmentation and of the chemical-thermal treatment that affected the particle structure making it increasingly hard. Conversely, attrition was only slightly affected by the presence of SO_2 .

5.5. Sorbent reactivation

The CO_2 capture capacity and the propensity to attrition of an Italian limestone (Massicci) reactivated by water hydration were investigated. Tests consisted of calcination/carbonation cycles carried out in a lab-scale fluidized bed reactor under realistic conditions representative of a process with calcination in an oxy-firing environment.

The hydrated spent sorbent displayed enhanced CO_2 capture capacity which, as expected, underwent deactivation over iterated calcination/carbonation cycles. The extent of reactivation depends on the hydration time: short hydration times give rise to more efficient regeneration of the sorption capacity avoiding sorbent “cramming” which is instead observed upon longer hydration. Porosimetric analysis showed the relevance of sorbent porosity, highlighting the important role of small pores (<200 nm). Sorbent

reactivation brings about a moderate increase of attrition. Again, the hydration time affects attrition: longer hydration times apparently emphasize the propensity to sorbent abrasion.

Results provide a valuable basis for the design of a “double loop” process, where, in conjunction with looping between the calciner and the carbonator, spent sorbent is continuously regenerated by water hydration.

References

A

- Aaron D., Tsouris C.: *Separation of CO₂ from flue gas: a review*. Separation Science and Technology 2005; 40; 321-348.
- Abanades J.C.: *The maximum capture efficiency of CO₂ using a carbonation/calcination cycle of CaO/CaCO₃*. Chemical Engineering Journal 2002; 90; 303–306.
- Abanades J.C., Alvarez D.: *Conversion limits in the reaction of CO₂ with lime*. Energy & Fuels 2003; 17; 308-315.
- Abanades J.C., Anthony E.J., Lu D.Y., Salvador C., Alvarez D.: *Capture of CO₂ from combustion gases in a fluidized bed of CaO*. AIChE Journal 2004; 50; 1614-1622.
- Abanades J.C., Anthony E.J., Wang J., Oakey J.E.: *Fluidized bed combustion systems integrating CO₂ capture with CaO*. Environmental Science & Technology 2005; 39; 2861–2866.
- Adánez J., de Diego L.F., García-Labiano F., Gayán P., Abad A.: *Selection of oxygen carriers for Chemical-Looping Combustion*. Energy & Fuel 2004; 18; 371-377.
- Adánez J, Abad A., García-Labiano F., Gayán P., de Diego L.F.: *Progress in Chemical-Looping Combustion and Reforming technologies*. Progress in Energy and Combustion Science 2012; 38; 215-282
- Agnihotri R., Mahuli S.K., Chauk S.S., Fan L.S.: *Influence of surface modifiers on the structure of precipitated calcium carbonate*. Industrial & Engineering Chemistry Research 1999; 38; 2283–2291.

- Aihara M., Nagai T., Matsushita J., Negishi Y., Ohya H.: *Development of porous solid reactant for thermal-energy storage and temperature upgrade using carbonation/decarbonation reaction*. Applied Energy 2001; 69; 225–238.
- Albrecht, B.: *Aerosols, cloud microphysics and fractional cloudiness*. Science 1989; 245; 1227–1230.
- Alonso M., Rodríguez N., González B., Grasa G., Murillo R., Abanades J.C.: *Carbon dioxide capture from combustion flue gases with a calcium oxide chemical loop. Experimental results and process development*. International Journal of Greenhouse Gas Control 2010; 4; 167–173.
- Alvarez D., Abanades J.C.: *Determination of the critical product layer thickness in the reaction of CaO with CO₂*. Industrial & Engineering Chemistry Research 2005; 44; 5608-5615.
- Amann J.-M., Kanniche M., Bouallou C.: *Reforming natural gas for CO₂ precombustion capture in combined cycle power plant*. Clean Techn Environ Policy 2009; 11; 67–76
- Anthony E.J., Granatstein D.L.: *Sulfation phenomena in fluidized bed combustion systems*. Progress in Energy and Combustion Science 2001; 27; 215-236.
- Anthony E.J., Bulewicz E.M., Jia L.: *Reactivation of limestone sorbents in FBC for SO₂ capture*. Progress in Energy and Combustion Science 2007; 33; 171-210
- Anthony E.J. *Solid Looping Cycles: A new technology for coal conversion*. Ind. Eng. Chem. Res. 2008; 47; 1747-1754.
- Arias B., Grasa G.S., Abanades J.C.: *Effect of sorbent hydration on the average activity of CaO in a Ca-looping system*. Chemical Engineering Journal 2010; 163; 324-330.
- Arjmand M., Azad A.M., Leion H., Lyngfelt A., Mattisson T.: *Prospects of Al₂O₃ and MgAl₂O₄-supported CuO oxygen carriers in Chemical-Looping Combustion (CLC) and Chemical-Looping with Oxygen Uncoupling (CLOU)*. Energy & Fuels 2011; 25; 5493-5502.

B

- Baker E.H.: *The CaO-CO₂ system in the pressure range 1-300 atm.* Journal of the Chemical Society 1962; 464-470.
- Barker R.: *Reversibility of the reaction CaCO₃ = CaO + CO₂.* Journal of Applied Chemistry & Biotechnology 1973; 23; 733-742.
- Benson, S.M.: *Overview of geologic storage of CO₂.* in Thomas, D.C. and Benson, S. (eds). Capture and Separation of Carbon Dioxide from Combustion Sources 2005, Volume 2 (Elsevier Science, Oxford, UK).
- Bhatia S.K., Perlmutter D.D.: *Effect of the product layer on the kinetics of the CO₂-lime reaction.* AIChE Journal 1983; 29; 79-86.
- Blamey J., Anthony E.J., Wang J., Fennel P.S.: *The calcium looping cycle for large-scale CO₂ capture.* Progress in Energy and Combustion Science 2010a; 36; 260-279.
- Blamey J., Paterson N.P.M., Dugwell D.R., Fennel P.S.: *Mechanism of particle breakage during reactivation of CaO-based sorbents for CO₂ capture.* Energy & Fuels 2010b; 24; 4605-4616.
- Borgwardt R.H.: *Sintering of nascent calcium oxide.* Chemical Engineering Science 1989a; 44; 53-60.
- Borgwardt R.H.: *Calcium oxide sintering in atmospheres containing water and carbon dioxide.* Industrial & Engineering Chemistry Research 1989b; 28; 493-500.
- Bosoaga A., Masek O., Oakey J.E.: *CO₂ capture technologies for cement industry.* Energy Procedia 2009; 1; 133-140.
- Bradshaw J., Boreham C., la Pedalina F.: *Storage retention time of CO₂ in sedimentary basins: Examples from petroleum systems.* Proceedings of the 7th International Conference on Greenhouse Gas Control Technologies (GHGT-7), September 5-9, 2004, Vancouver, Canada, v.I, 541-550.

Buhre B.J.P., Elliott L.K., Sheng C.D., Gupta R.P., Wall T.F.: *Oxy-fuel combustion technology for coal-fired power generation*. Progress in Energy and Combustion Science 2005; 31; 283-307.

C

Chandel M.K., Hoteit A., Delebarre A.: *Experimental investigation of some metal oxides for chemical looping combustion in a fluidized bed reactor*. Fuel 2009; 88; 898-908.

Charitos A., Hawthorne C., Bidwe A.R., Sivalingam S., Schuster A., Spliethoff H., Scheffknecht G.: *Parametric investigation of the calcium looping process for CO₂ capture in a 10 kW_{th} dual fluidized bed*. Int. J. Greenh. Gas Cont. 2010; 4; 776-84.

Chen Z., Song H.S., Portillo M., Lim C.J., Grace J.R., Anthony E.J.: *Long-term calcination/carbonation cycling and thermal pretreatment for CO₂ capture by limestone and dolomite*. Energy and Fuels 2009; 23; 1437-1444.

Chrissafis K., Dagounaki C., Paraskevopoulos K.M.: *The effects of procedural variables on the maximum capture efficiency of CO₂ using a carbonation/calcination cycle of carbonate rocks*. Thermochemica Acta 2005; 428; 193-198.

Curran G.P., Fink C.E., Gorin E.: *CO₂ acceptor gasification process*. Advances in Chemistry 1967; 69; 141-165.

D

Dam-Johansen K.; Østergaard K.: *High-temperature reaction between sulphur dioxide and limestone-I, II, III, IV*. Chemical Engineering Science 1991; 46; 827-859.

de Diego L.F., García-Labiano F., Adánez J., Gayán P., Abad A., Corbella B.M., Palacios J. M.: *Development of Cu-based oxygen carriers for chemical-looping combustion*. Fuel 2004; 83; 1749–1757.

Dean C.C., Blamey J., Florin N.H., Al-Jeboori M.J., Fennell P.S.: *The calcium looping cycle for CO₂ capture from power generation, cement manufacture and hydrogen production*. Chemical Engineering Research and Design 2011a; 89; 836-855.

Dean C.C., Dugwell D., Fennell P.S.: *Investigation into potential synergy between power generation, cement manufacture and CO₂ abatement using the calcium looping cycle*. Energy & Environmental Science 2011b; 4; 2050-2053.

Dunsmore H. E.: *A geological perspective on global warming and the possibility of carbon dioxide removal as calcium carbonate mineral*. Energy Convers. Mgmt. 1992; 33; 5-8, 565-72.

F

Fang F., Li Z.-S., Cai N.-S.: *Continuous CO₂ capture from flue gases using a dual fluidized bed reactor with calcium-based sorbent*. Industrial & Engineering Chemistry Research 2009; 48; 11140–11147.

Fennell P.S., Davidson J.F., Dennis J.S., Hayhurst A.N.: *Regeneration of sintered limestone sorbents for the sequestration of CO₂ from combustion and other systems*. Journal of the Energy Institute 2007a; 80; 116–119.

Fennell P.S., Pacciani R., Dennis J.S., Davidson J.F., Hayhurst A.N.: *The effects of repeated cycles of calcination and carbonation on a variety of different limestones, as measured in a hot fluidized bed of sand*. Energy & Fuels 2007b; 21; 2072–2081.

Figueroa J.D., Fout T., Plasynski S., McIlvried H., Srivastava R.D.: *Advances in CO₂ capture technology–The U.S. Department of Energy’s Carbon Sequestration Program*. International Journal of Greenhouse Gas Control 2008; 2; 9–20.

Florin N.H., Harris A.T.: *Mechanistic study of enhanced H₂ synthesis in biomass gasifiers with in-situ CO₂ capture using CaO*. AIChE Journal 2008; 54; 1096-1109.

G

German, R. *Surface area reduction during isothermal sintering*. Journal of the American Ceramic Society 1976; 59; 379-383.

González B., Alonso M., Abanades J.C.: *Sorbent attrition in a carbonation/calcination pilot plant for capturing CO₂ from flue gases*. Fuel 2010; 89; 2918-2924.

Grasa G.S., Abanades J.C.: *CO₂ capture capacity of CaO in long series of carbonation/calcination cycles*. Industrial and Engineering Chemistry Research 2006; 45; 8846-8851.

Grasa G.S., Alonso M., Abanades J.C.: *Sulfation of CaO particles in a carbonation/calcination loop to capture CO₂*. Industrial and Engineering Chemistry Research 2008; 47; 1630-1635.

Gupta H., Fan L.S.: *Carbonation–calcination cycle using high reactivity calcium oxide for carbon dioxide separation from flue gas*. Industrial & Engineering Chemistry Research 2002; 41; 4035–4042.

H

Harrison D.P.: *Sorption-enhanced hydrogen production: a review*. Ind. Eng. Chem. Res. 2008; 47; 6486–6501.

Hoffert M.I., Wey Y.-C., Callegari A.J., Broecker W.S.: *Atmospheric response to deep-sea injections of fossil-fuel carbon dioxide*. Climatic Change 1979; 2; 53-68.

Hughes R.W., Lu D., Anthony E.J., Wu Y.H.: *Improved long-term conversion of limestone-derived sorbents for in situ capture of CO₂ in a fluidized bed combustor*. *Industrial & Engineering Chemistry Research* 2004; 43; 5529–5539.

I

IEA. *World Energy Outlook 2008*. <http://www.iea.org> (2008)

IPCC. *Carbon Dioxide Capture and Storage*. <http://www.ipcc.ch/> (2005).

IPCC. *Climate Change 2007*. <http://www.ipcc.ch/> (2007).

IPCC. *Renewable Energy Sources and Climate Change Mitigation*. <http://www.ipcc.ch/> (2011).

Itskos G., Grammelis P., Scala F., Kruczek H., Coppola A., Salatino P., Kakaras E., *Comparative characterization of sorbents from Ca-looping investigations*. Proc. of 2nd Int. Conf. on Chemical Looping, Darmstadt 2012, Germany, paper 37.

Ives M., Mundy R.C., Fennell P.S., Davidson J.F., Dennis J.S., Hayhurst A.N.: *Comparison of different natural sorbents for removing CO₂ from combustion gases, as studied in a bench-scale fluidized bed*. *Energy & Fuels* 2008;22; 3852-3857.

Iyer M.V., Fan L.S.: *High temperature CO₂ capture using engineered eggshells: a route to carbon management*. World patent WO/2006/099599; 2006.

J

Jia L., Hughes R., Lu D., Anthony E.J., Lau I.: *Attrition of calcining limestones in circulating fluidized-bed systems*. *Industrial and Engineering Chemistry Research* 2007; 46; 5199-5209.

Johansson M.: *Screening of oxygen-carrier particles based on iron-, manganese-, copper- and nickel oxides for use in chemical-looping technologies*. Department of Chemical and Biological Engineering Environmental Inorganic Chemistry Chalmers University of Technology Göteborg, Sweden 2007.

K

Kanniche M., Gros-Bonnivard R., Jaud P., Valle-Marcos J., Amann J.M., Bouallou C.: *Pre-combustion, post-combustion and oxy-combustion in thermal power plant for CO₂ capture*. Applied Thermal Engineering 2010; 30; 53–62.

Kheshgi H.S., Flannery B.P., Hoffert M.I., Lapenis A.G.: *The effectiveness of marine CO₂ disposal*. Energy 1994; 19; 967-975.

Kremer J., Galloy A., Ströhle J., Epple B.: *Continuous CO₂ capture in a 1 MW_{th} carbonate looping pilot plant*. Proc. of 2nd Int. Conf. on Chemical Looping, Darmstadt 2012, Germany, paper 11.

Koppatz S., Pfeifer C., Rauch R., Hofbauer H., Marquard-Moellenstedt T., Specht M.: *H₂ rich product gas by steam gasification of biomass with in situ CO₂ absorption in a dual fluidized bed system of 8 MW fuel input*. Fuel Processing Technology 2009; 90; 914-921.

L

Lackner K. S., Wendt C. H., Butt D. P., Joyce E. L., Sharp D. H.: *Carbon dioxide disposal in carbonate minerals*. Energy 1995; 20; 1153-1170.

Larson, E. D.: *Technology for electricity and fuels from biomass*. Annual Review of Energy and Environment 1993; 18; 567–630.

Laursen K., Duo W.L., Grace J.R., Lim J.: *Sulfation and reactivation characteristics of nine limestones*. Fuel 2000; 79; 153-163.

- Li Z.-S., Cai N.-S., Huang Y.-Y., Han H.-J.: *Synthesis, experimental studies, and analysis of a new calcium-based carbon dioxide absorbent*. Energy & Fuels 2005a; 19; 1447–1452.
- Li Y., Buchi S., Grace J.R., Lim J.C.: *SO₂ removal and CO₂ capture by limestone resulting from calcination/sulfation/carbonation cycles*. Energy & Fuels 2005b; 19; 1927-1934.
- Li Z.-S., Cai N.-S., Huang Y.-Y.: *Effect of preparation temperature on cyclic CO₂ capture and multiple carbonation-calcination cycles for a new Ca-based CO₂ sorbent*. Industrial & Engineering Chemistry Research 2006; 45; 1911–1917.
- Li F., Fan L.S.: *Clean coal conversion processes – progress and challenges*. Energy & Environmental Science 2008; 1; 248-267.
- Li Y.-J., Zhao C.-S., Duan L.-B., Liang C., Li Q.-Z., Zhou W., et al.: *Cyclic calcination/carbonation looping of dolomite modified with acetic acid for CO₂ capture*. Fuel Processing Technology 2008a; 89; 1461–1469.
- Li Y., Zhao C.-S., Qu C., Duan L., Li Q., Liang C.: *CO₂ capture using CaO modified with ethanol/water solution during cyclic calcination/carbonation*. Chemical Engineering and Technology 2008b; 31; 237–244.
- Lisbona P., Martinez A., Lara Y., Romeo L.M.: *Integration of carbonate CO₂ capture cycle and coal-fired power plants. A comparative study for different sorbents*. Energy & Fuels 2010; 24; 728-736
- Lohmann U., Feichter J.: *Global indirect aerosol effects: A review*. Atmospheric Chemistry and Physics 2005; 5; 715–737.
- Lyngfelt A., Johansson M., Mattison T.: *Chemical-looping combustion-status of development*. 9th International Conference on Circulating Fluidized Beds (CFB-9), May 13-16, 2008, Hamburg, Germany.
- Lysikov A.I., Salanov A.N., Okunev A.G.: *Change of CO₂ carrying capacity of CaO in isothermal recarbonation–decomposition cycles*. Industrial & Engineering Chemistry Research 2007; 46; 4633–4638.

M

- MacKenzie A., Granatstein D.L., Anthony E.J., Abanades J.C.: *Economics of CO₂ capture using the calcium cycle with a pressurized fluidized bed combustor*. Energy & Fuels 2007; 21; 920-926.
- Magoon L.B., Dow W.G.: *The petroleum system*. American Association of Petroleum Geologists 1994, Memoir 60; 3-24.
- Manovic V., Anthony E.J.: *Steam reactivation of spent CaO-based sorbent for multiple CO₂ capture cycles*. Environmental Science & Technology 2007a; 41; 1420-1425.
- Manovic V., Anthony E.J.: *SO₂ retention by reactivated CaO-based sorbent from multiple CO₂ capture cycles*. Environmental Science and Technology 2007b; 41; 4435-4440.
- Manovic V., Anthony E.J.: *Thermal activation of CaO-based sorbent and selfreactivation during CO₂ capture looping cycles*. Environmental Science & Technology 2008a; 42; 4170-4174.
- Manovic V., Anthony E.J.: *Sequential SO₂/CO₂ capture enhanced by steam reactivation of a CaO-based sorbent*. Fuel 2008b; 87; 1564-1573.
- Manovic V., Anthony E.J., Lu D.Y.: *Sulphation and carbonation properties of hydrated sorbents from a fluidized bed CO₂ looping cycle reactor*. Fuel 2008a; 87; 2923-2931.
- Manovic V., Lu D.Y., Anthony E.J.: *Steam hydration of sorbents from a dual fluidized bed CO₂ looping cycle reactor*. Fuel 2008b; 87; 3344-3352.
- Manovic V., Anthony E.J.: *Improvement of CaO-based sorbent performance for CO₂ looping cycles*. Thermal Science 2009; 13; 89-104.
- Martínez I., Grasa G., Murillo R., Arias B., Abanades J.C.: *Evaluation of CO₂ carrying capacity of reactivated CaO by hydration*. Energy & Fuels 2011; 25; 1294-1301.

- Materić V., Edwards S., Smedley S.I., Holt R.: *Ca(OH)₂ Superheating as a low-attrition steam reactivation method for CaO in calcium looping applications*. Industrial and Engineering Chemistry Research 2010; 49; 12429-12434.
- Mattison T., Lyngfelt A.: *Capture of CO₂ using chemical-looping combustion*. In Scandinavian-Nordic Section of Combustion Institute 2001. Göteborg.
- McBride B.J., Zehe M.J., Gordon S.: *NASA Glenn coefficients for calculating thermodynamic properties of individual species*. NASA/TP-2002-211556; NASA Glenn Research Centre: September 2002.
- Montagnaro F., Salatino P., Scala F.: *Reactivation by water hydration of spent sorbent for fluidized-bed combustion application: influence of hydration time*. Industrial & Engineering Chemistry Research 2004; 43; 5692-5701.
- Montagnaro F., Pallonetto F., Salatino P., Scala F.: *Steam reactivation of a spent sorbent for enhanced SO₂ capture in FBC*. AIChE Journal 2006a; 52; 4090-4098.
- Montagnaro F., Scala F., Salatino P.: *Assessment of sorbent reactivation by water hydration for fluidized bed combustion application*. Journal of Energy Resources Technology 2006b; 128; 90-98.
- Montagnaro F., Salatino P., Scala F., Chirone R.: *An assessment of water and steam reactivation of a fluidized bed spent sorbent for enhanced SO₂ capture*. Powder Technology 2008 180; 129-134.
- Montagnaro F., Salatino P., Scala F.: *The influence of temperature on limestone sulfation and attrition under fluidized bed combustion conditions*. Experimental Thermal and Fluid Science 2010; 34; 352-358.

P

- Penner J.E., et al.: *Aerosols, their direct and indirect effects*. In: *Climate Change 2001: The Scientific Basis*. Contribution of Working Group I to the Third Assessment Report of the Intergovernmental Panel on Climate Change

[Houghton, J.T., et al. (eds.)]. Cambridge University Press, Cambridge, United Kingdom and New York, NY, USA, pp. 289–348.

Pörtner H.O., Langenbuch M., Reipschläger A.: *Biological impact of elevated ocean CO₂ concentrations: lessons from animal physiology and Earth history?* Journal of Oceanography 2004; 60; 705-718.

R

Ramaswamy V., et al.: *Radiative forcing of climate change. In: Climate Change 2001: The Scientific Basis. Contribution of Working Group I to the Third Assessment Report of the Intergovernmental Panel on Climate Change 2001* [Houghton, J.T., et al. (eds.)]. Cambridge University Press, Cambridge, United Kingdom and New York, NY, USA; 349–416.

Rochelle G.T.: *Amine scrubbing for CO₂ capture*. Science 2009; 325; 1652-1654.

Rodríguez N., Alonso M., Grasa G., Abanades J.C.: *Heat requirements in a calciner of CaCO₃ integrated in a CO₂ capture system using CaO*. Chemical Engineering Journal 2008 ; 138 ; 148-154.

Rodríguez N., Alonso M., Abanades J.C.: *Average activity of CaO particles in a calcium looping system*. Chemical Engineering Journal 2010; 156; 388–394.

Ryu H.J., Grace J.R., Lim C.J.: *Simultaneous CO₂/SO₂ capture characteristics of three limestones in a fluidized-bed reactor*. Energy & Fuels 2006; 20; 1621-1628.

S

Salatino P., Senneca O.: *Preliminary assessment of a concept of looping combustion of carbon*. Industrial & Engineering Chemistry Research 2009; 48; 102-109.

- Salvador C., Lu D., Anthony E.J., Abanades J.C.: *Enhancement of CaO for CO₂ capture in an FBC environment*. Chemical Engineering Journal 2003; 96; 187–195.
- Sánchez-Biezma A., Diaz L., López J., Arias B., Paniagua J., Lorenzo M., Álvarez J., Abanades J.C.: *CaOling Project - First experiences on the 1,7MW_{th} calcium looping pilot in La Pereda*. Presentation at 2nd International Workshop on Oxyfuel CFB technology, 28-29th June 2012, Stuttgart, Germany.
- Scala F., Cammarota A., Chirone R. and Salatino P.: *Comminution of limestone during batch fluidized-bed calcination and sulfation*. AIChE Journal 1997; 43; 363–373.
- Scala F., Salatino P., Boreefijn R., Ghadiri M.: *Attrition of sorbents during fluidized bed calcination and sulphation*. Powder Technol. 2000; 107:153-167.
- Scala F., Montagnaro F., Slatino P.: *Enhancement of sulfur uptake by hydration of spent limestone for fluidized-bed combustion application*. Industrial & Engineering Chemistry Research 2001; 40; 2495-2501.
- Scala F., Salatino P.: *Dolomite attrition during fluidized bed calcination and sulfation*. Combust. Sci. Technol. 2003; 175; 2201–2216.
- Scala F., Montagnaro F., Salatino P.: *Attrition of limestone by impact loading in fluidized beds*. Energy & Fuels 2007; 21; 2566-2572.
- Scala F., Montagnaro F., Salatino P.: *Sulphation of limestones in a fluidized bed combustor: The relationship between particle attrition and microstructure*. Canadian Journal of Chemical Engineering 2008; 86; 347-355.
- Seifritz, W.: *CO₂ disposal by means of silicates*. Nature 1990; 345; 486.
- Shimizu T., Hiramata T., Hosoda H., Kitano K., Inagaki M., Tejima K.: *A twin fluid-bed reactor for removal of CO₂ from combustion processes*. Chemical Engineering Research & Design 1999; 77; 62–68.
- Shimizu T., Hiramata T., Hosoda H., Kitano K.: *A new process for CO₂ recovery from flue gas using calcium oxide*. In: Proceedings of the 5th international symposium on CO₂ fixation and efficient utilization of energy. The 45th

international world energy system conference, Tokyo, Japan; March 4–6, 2002. 359–364.

Shulman A., Cleverstam E., Mattisson T., Lyngfelt A.: *Chemical-Looping with oxygen uncoupling using Mn/Mg-based oxygen carriers– Oxygen release and reactivity with methane*. Fuel 2011; 90; 941-950.

Silaban A., Harrison D.P.: *High temperature capture of carbon dioxide: characteristics of the reversible reaction between $\text{CaO}_{(s)}$ and $\text{CO}_{2(g)}$* . Chemical Engineering Communications 1995; 137; 177-190.

Silaban A., Narcida M., Harrison D.P.: *Characteristics of the reversible reaction between $\text{CO}_{2(g)}$ and calcined dolomite*. Chemical Engineering Communications 1996; 146; 149–162.

Silcox G. D., Kramlich J. C., Pershing D. W.: *A mathematical model for the flash calcinations of dispersed CaCO_3 and $\text{Ca}(\text{OH})_2$ particles*. Industrial & Engineering Chemistry Research 1989; 28; 155- 160.

Smith I.M.: *Properties and behaviour of SO_2 adsorbents for CFBC*.: IEA Clean Coal Centre 2007; London, UK.

Stanmore B.R., Gilot, P.: *Review-calcination and carbonation of limestone during thermal cycling for CO_2 sequestration*. Fuel Processing Technology 2005; 86; 1707–1743.

Stantan J.E.: *Sulphur retention in fluidized bed combustion*. In J.R. Howard 1983, (Ed.) Fluidized Beds: Combustion and Applications, Applied Science, United Kingdom; Chapter 5; 199-225.

Steenefeldt R., Berger B., Torp T.A.: *CO_2 capture and storage - closing the knowing-doing Gap*. Chemical Engineering Research and Design 2006; 84; 739-763.

Sun P., Grace J.R., Lim C.J., Anthony E.J.: *The effect of CaO sintering on cyclic CO_2 capture in energy systems (pages 2432–2442)*. AIChE Journal 2007a; 53; 2432-2442.

Sun P., Grace J.R., Lim C.J., Anthony E.J.: *Removal of CO₂ by calcium-based sorbents in the presence of SO₂*. *Energy & Fuels* 2007b; 21; 163-170.

Sun P., Grace J.R., Lim C.J., Anthony E.J.: *On the effect of CaO sintering on cyclic CO₂ capture in energy systems*. *AIChE Journal* 2007; 53; 2432-2442.

Sun P., Grace J.R., Lim C.J., Anthony E.J.: *Investigation of attempts to improve cyclic CO₂ capture by sorbent hydration and modification*. *Industrial & Engineering Chemistry Research* 2008; 47; 2024–2032.

T

Toftegaard M.B., Brix J., Jensen P.A., Glarborg P., Jensen A.D.: *Oxy-fuel combustion of solid fuels*. *Progress in Energy and Combustion Science* 2010; 36; 581-625.

Twomey, S.A.: *The influence of pollution on the shortwave albedo of clouds*. *Journal of the Atmospheric Sciences* 1977; 34; 1149–1152.

W

Wang J., Anthony E.J.: *Clean combustion of solid fuels*. *Applied Energy* 2007; 85; 73-79.

Werther J., Reppenhagen J.: *Chapter 8: Attrition*. *Handbook of Fluidization and Fluid-Particle Systems* (2003). Ed. Marcel Dekker Inc.

Wolf J., Anheden M., Yan J.: *Comparison of nickel- and iron-based oxygen carriers in chemical looping combustion for CO₂ capture in power generation*. *Fuel* 2005; 84; 993-1006.

Wu Y., Blamey J., Anthony E.J., Fennell P.S.: *Morphological changes of limestone sorbent particles during carbonation/calcination looping cycles in a thermogravimetric analyzer (TGA) and reactivation with steam*. *Energy & Fuels* 2010; 24; 2768-2776.

Z

Zeman F.: *Effect of steam hydration on performance of lime sorbent for CO₂ capture*. International Journal of Greenhouse Gas Control 2008; 2; 203–209.

Zsakó J., Hints M.J.: *Use of thermal analysis in the study of sodium carbonate causticization by means of dolomitic lime*. Journal of Thermal Analysis 1998; 53; 323-331.